②

AD-A225 704

NAVAL POSTGRADUATE SCHOOL
Monterey, California

THESIS

TERRAIN ANALYSIS
USING
LANDSAT THEMATIC MAPPER IMAGERY

by

Gerald T. Michael

March 1990

Thesis Advisor: Chin-Hwa Lee

Approved for public release; distribution is unlimited.

90 00 0   1045

REPORT DOCUMENTATION PAGE

Form Approved
OMB No. 0704-0188

1a. REPORT SECURITY CLASSIFICATION UNCLASSIFIED	1b. RESTRICTIVE MARKINGS
2a. SECURITY CLASSIFICATION AUTHORITY	3. DISTRIBUTION / AVAILABILITY OF REPORT Approved for public release;
2b. DECLASSIFICATION / DOWNGRADING SCHEDULE	distribution is unlimited

4. PERFORMING ORGANIZATION REPORT NUMBER(S)	5. MONITORING ORGANIZATION REPORT NUMBER(S)

6a. NAME OF PERFORMING ORGANIZATION Naval Postgraduate School	6b. OFFICE SYMBOL (If applicable)	7a. NAME OF MONITORING ORGANIZATION Naval Postgraduate School

6c. ADDRESS (City, State, and ZIP Code) Monterey, CA 93943-5000	7b. ADDRESS (City, State, and ZIP Code) Monterey, CA 93943-5000

8a. NAME OF FUNDING / SPONSORING ORGANIZATION	8b. OFFICE SYMBOL (If applicable)	9. PROCUREMENT INSTRUMENT IDENTIFICATION NUMBER

8c. ADDRESS (City, State, and ZIP Code)	10. SOURCE OF FUNDING NUMBERS			
	PROGRAM ELEMENT NO.	PROJECT NO.	TASK NO	WORK UNIT ACCESSION NO.

11. TITLE (Include Security Classification)

TERRAIN ANALYSIS USING LANDSAT THEMATIC MAPPER IMAGERY

12. PERSONAL AUTHOR(S)
Michael, Gerald T.

13a. TYPE OF REPORT Master's Thesis	13b. TIME COVERED FROM _____ TO _____	14. DATE OF REPORT (Year, Month, Day) March 1990	15. PAGE COUNT 176

16. SUPPLEMENTARY NOTATION The views expressed in this thesis are those of the author and do not reflect the official policy or position of the Department of Defense or the U.S. Government.

17.	COSATI CODES		18. SUBJECT TERMS (Continue on reverse if necessary and identify by block number)
FIELD	GROUP	SUB-GROUP	Terrain Analysis, Satellite Imagery, Landsat

19. ABSTRACT (Continue on reverse if necessary and identify by block number)

This study examined two sites from a Landsat scene of portions of Honduras and Nicaragua. One site was examined for potential water obstacles, and the other was examined for cover and concealment provided by vegetation. The results suggest that potential water obstacles can be detected. it is not clear if vegetative cover and concealment can be reliably detected. A study using better ground reference information than was available is necessary to answer that question. Several unsupervised classification algorithms were used and compared. A histogram clustering algorithm followed by a minimum distance classifier provided results comparable to the much slower K-means and isodata-type algorithms. Several methods to reduce the dimensionality of the classification problem were examined, including band subsets, between-band ratios, the principal component transformation, and the tasseled cap transformations. Band subsets provided adequate accuracy and is the easiest method to implement.

20. DISTRIBUTION / AVAILABILITY OF ABSTRACT ☒ UNCLASSIFIED/UNLIMITED ☐ SAME AS RPT ☐ DTIC USERS	21. ABSTRACT SECURITY CLASSIFICATION UNCLASSIFIED	
22a. NAME OF RESPONSIBLE INDIVIDUAL Chin-Hwa Lee	22b. TELEPHONE (Include Area Code) (408) 646-2910	22c. OFFICE SYMBOL EC/Le

DD Form 1473, JUN 86   Previous editions are obsolete.   SECURITY CLASSIFICATION OF THIS PAGE

Terrain Analysis
Using
Landsat Thematic Mapper Imagery

by

Gerald T. Michael
Captain, United States Army
B.S., Massachusetts Institute of Technology

Submitted in partial fulfillment
of the requirements for the degree of
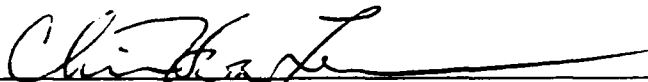

MASTER OF SCIENCE IN ELECTRICAL ENGINEERING

frcm the

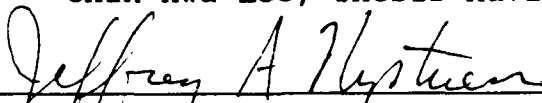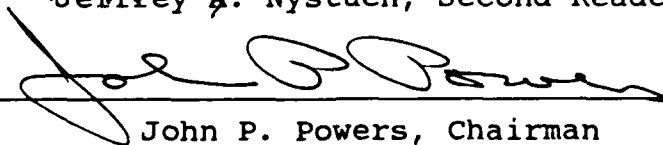NAVAL POSTGRADUATE SCHOOL
March 1990

Author: _____
Gerald T. Michael

Approved by: _____
Chin-Hwa Lee, Thesis Advisor

_____
Jeffrey A. Nystuen, Second Reader

_____
John P. Powers, Chairman
Department of Electrical and Computer Engineering

ABSTRACT

This study examined two sites from a Landsat scene of portions of Honduras and Nicaragua. One site was examined for potential water obstacles, and the other was examined for cover and concealment provided by vegetation. The results suggest that potential water obstacles can be detected. It is not clear if vegetative cover and concealment can be reliably detected. A study using better ground reference information than was available is necessary to answer that question. Several unsupervised classification algorithms were used and compared. A histogram clustering algorithm followed by a minimum distance classifier provided results comparable to the much slower K-means and isodata-type algorithms. Several methods to reduce the dimensionality of the classification problem were examined, including band subsets, between-band ratios, the principal component transformation, and the tasseled cap transformations. Band subsets provided adequate accuracy and is the easiest method to implement.

iii

TABLE OF CONTENTS

v

vi

LIST OF TABLES

x

LIST OF FIGURES

I. INTRODUCTION

A. MOTIVATION

The Armed Forces of the United States are responsible for being prepared to conduct military operations anywhere in the world on short notice. Accurate maps are essential to successful military operations, so a great deal of effort goes into creating, maintaining, and updating maps. In fact, an entire Department of Defense agency, the Defense Mapping Agency, exists for this purpose.

However, no matter how good a map was when it was created, it is a static entity. Once printed, it is difficult to update a map to reflect changed ground conditions. Also, seasonal variations (which can have significant effects on military operations) cannot always be completely included in a map.

For military operations, accurate information on current ground conditions is needed, since ground conditions significantly affect the ability of friendly and enemy forces to move, shoot, and communicate. The formal process of analyzing current ground conditions for their effects on military operations is called terrain analysis [Ref. 1:pp. 33-40].

In addition to maps, terrain analysis inputs include information from other sources: interrogation; ground and

aerial surveillance and reconnaissance; imagery interpretation; target acquisition and night observation devices; maps and charts; and studies on transportation, trafficability, cross-country movement, climate, and hydrography [Ref. 2:p. 2-2]. Many of these methods and sources rely on long-term information gathering (e.g., climate, hydrography, maps, and charts). The short-term information gathering methods (e.g., ground or aerial reconnaissance) can give the enemy information about planned operations simply because the reconnaissance effort is detected. Also, most intelligence collection methods are not really suited to rapid, large-scale data collection on current terrain conditions.

"Satellites can cover far more territory than an aircraft, and, of equal importance, they can photograph it all in the same day so that intelligence staffs can see the overall picture." [Ref. 3:p. 230] Though the quote in its original context referred more to special photographic reconnaissance satellites, the principle is clear: how to rapidly gather the most current information on terrain conditions.

Landsat thematic mapper (TM) imagery is used for a wide variety of applications, including crop yield estimation, forest inventory, urban land use mapping, and a variety of other land use/land cover and resource management applications [Ref. 4:p. 1-2]. Since some of these applications are related to items of interest in military terrain analysis,

2

Landsat TM imagery might be usable for part of military terrain analysis. It has been found that

> Landsat analyses usually cost less than 1 percent of the cost of comparable aerial surveys. They are therefore particularly useful for mapping inaccessible terrain. [Ref. 4:p. 1-2]

Since this is exactly the type of problem identified here, Landsat TM imagery may be useful in solving at least part of that problem.

Another advantage of Landsat imagery is that, because of its mission of earth resource observation, Landsat's orbit is both regular and periodic. Therefore, it covers the earth in a predictable pattern, so it gives no evidence of any particular interest in a given area. Because its orbital inclination is 96.22°, Landsat covers the entire globe between about 84° North and 84° South every 16 days [Ref. 4:p. 2-3].

B. OBJECTIVES

Using Landsat TM imagery it may be possible to develop a computer-assisted determination of the terrain analysis factors of concealment and cover and certain types of obstacles with an acceptable degree of accuracy. Not only would this save time in performing terrain analysis and provide more information than a paper map alone; it would also provide much more recent information about the area of interest.

3

The primary research question examined in this study is: can unsupervised pattern recognition algorithms be effectively used on Landsat thematic mapper imagery to perform parts of the terrain analysis step of the Intelligence Preparation of the Battlefield process? Specifically, the study will focus on the identification of obstacles and cover and concealment. Because of the 30 x 30 meter pixel size, relatively small obstacles will probably not be detectable, but obstacles with distinctive spectral characteristics or distinctive effects on the surrounding terrain (like streams and swamps) may be detectable. Heavy vegetation, especially woods and forests, are particularly good for providing concealment and some cover. Since forest inventory is already one of the uses of Landsat TM imagery [Ref. 4:p. 1-2], Landsat imagery may be useful in identifying forests with good military terrain properties.

The Landsat TM imagery was analyzed primarily by using the Land Analysis System (LAS), a software package optimized for earth resource evaluation of Landsat imagery. Some additional short computer programs were required where LAS routines either did not perform exactly the required function or were not convenient to use. The output of the above analyses was then used to produce a set of map overlays of the various terrain analysis factors. Producing the map overlays was the ultimate goal of this study.

C. LIMITATIONS

Due to the location and date of the Landsat TM imagery (Honduras and Nicaragua, 24 March 1986) available for this study, gathering ground reference information was impossible. Though 1:50,000 scale maps of the area were used for the ground reference, they may not be, in all cases, an adequate replacement for the on-the-ground verification of factors that are important in this study (e.g., density of a forest vs. the forest's spectral response pattern, identification of irrigated cropland and crop identification).

The pixel size in Landsat TM imagery is 30 x 30 meters. Many items of tactical interest, especially obstacles, may not be distinguishable at this resolution.

This study will only look at a subset of the items of interest in terrain analysis for a specific small area. The results will mainly be an indication of whether or not more research will be worthwhile on this subject rather than a definitive answer to the posed research question.

D. SUMMARY OF RESULTS

The results of this study seem to indicate that potential water obstacles can be identified using Landsat TM imagery. Several band sets and band combinations were evaluated for their relative usefulness in detecting potential water obstacles. Several unsupervised clustering

5

algorithms were also evaluated. The results are presented in Chapter IV.

A determination on the possibility of detecting vegetated areas providing cover or concealment could not be made. The results in this area were mixed. Better ground reference information is needed before a definite determination can be made. These results hold for all band combinations evaluated.

E. ORGANIZATION

Chapter II provides a background on the concepts and information that form the basis for this study. Chapter III provides details on how the study was conducted. Chapter IV presents an analysis of the results achieved in the study, and Chapter V draws some conclusions and recommends further research.

II. BACKGROUND

A. TERRAIN ANALYSIS

Terrain analysis is part of the U.S. Army's Intelligence
Preparation of the Battlefield (IPB) process, a formalized
situation and target development process that provides
commanders with the intelligence and targeting data needed
to plan and fight battles. [Ref. 1:pp. 33-40] Terrain
analysis focuses on the military aspects of terrain and
their effects on friendly and enemy capabilities to move,
shoot, and communicate (the basic tactical functions).
Terrain analysis includes the following five factors:
observation and fields of fire, concealment and cover,
obstacles, key terrain, and avenues of approach and mobility
corridors. While determination of key terrain and avenues
of approach are heavily dependent on a unit's size, mission,
and tactical situation, the other three factors are more
consistent.

Since weather can also have a significant effect on
terrain, and thus affect friendly and enemy capabilities,
weather analysis is also an important step in IPB [Ref. 1:p.
38].

An obstacle map overlay is created which combines all
terrain and weather induced obstacles identified in the

above analysis. [Ref. 1:p. 38] Next, avenues of approach and mobility corridors are identified, with emphasis on areas where the enemy can move. The most viable avenues of approach and mobility corridors are identified and overlays are prepared depicting each one. These overlays are then used in the final step of IPB, threat integration. Threat integration integrates enemy doctrine with terrain and weather information to determine how the enemy will fight as influenced by terrain and weather.

1. Observation and fire

Observation is the influence of terrain on the ability of a force to exercise surveillance over a given area either directly or through the use of sensors. [Ref. 2:p. 2-12] Characteristics of terrain which restrict observation include hills, cliffs, vegetation, and manmade features.

Fire is the influence of terrain on the effectiveness of direct and indirect fire weapons.

Indirect fire weapons such as mortars are affected primarily by terrain conditions within the target area which may influence the terminal effect of the projectile. Fields of fire for direct fire weapons such as machineguns and automatic rifles are primarily affected by terrain conditions between the weapon and the target. [Ref. 2:p. 2-12]

2. Concealment and cover

Concealment provides protection from observation. Cover provides protection from the effects of weapons fire.

[Ref. 2:p. 2-12] Concealment may be provided by terrain features such as woods, underbrush, tall grass, and cultivated vegetation.

> Concealment from ground observation does not necessarily provide concealment from air observation or from electronic or infrared devices. Concealment does not necessarily provide cover. [Ref. 2:p. 2-12]

Cover may be provided by trees, rocks, ditches, folds in the ground, buildings, embankments and similar features. [Ref. 2:p. 2-12] "Areas that provide cover from direct fires may or may not protect against the effects of indirect fire; however, most terrain features that afford cover also afford concealment." [Ref. 2:p. 2-13]

3. Obstacles

"An obstacle is any natural or artificial terrain feature which stops, impedes, or diverts military movement." [Ref. 2:p. B-3] Natural obstacles include rivers, streams, lakes, swamps, steep slopes, dense woods, deserts, mountains, cities, and certain types of unstable soil. Artificial obstacles are works of construction and destruction executed to stop, impede, or divert military movement. They include minefields, craters, antitank ditches, trenches, roadblocks, deliberately flooded areas, extensive rubble, and forest fires.

4. Key Terrain

A key terrain feature is any location or area whose seizure or control affords a marked advantage to either

opposing force. [Ref. 2:p. 2-13] Types of terrain features which are frequently selected as key terrain for tactical units include high ground that provides favorable observation and fire over a significant portion of the operation area and bridges over unfordable rivers.

5. Avenues of Approach and Mobility Corridors

An avenue of approach is a route for a force of a particular size to reach an objective. [Ref. 2:p. 2-14] The analysis of an avenue of approach at any level of command is based on the consideration of observation and fire, cover and concealment, obstacles, utilization of key terrain, adequate maneuver space, and ease of movement.

A mobility corridor is that part of an avenue of approach that allows a particular-sized unit to deploy in its doctrinal tactical formation [Ref. 1:p. 38].

This study focused on the military terrain classifications of water obstacles and cover and concealment as provided by vegetation.

B. LANDSAT

1. General Information

The Landsat series of satellites began with the Earth Resources Technology Satellite (ERTS), launched in July 1972. [Ref. 4:p. 1-1] ERTS was renamed Landsat 1 in 1975 to reflect its primary use as a land resources observatory.

10

The second generation of Landsat satellites (4 and 5) carried the thematic mapper (TM) in addition to the multispectral scanner (MSS) of the earlier Landsat satellites. [Ref. 4:p. 2-1] The TM improved on both the spectral (seven bands vs. three) and spatial (30 m vs. 82 m) resolution of the MSS.

Landsat 4, launched in July 1982, developed early communication and solar array problems that restricted it to use of the MSS only. [Ref. 4:p. 2-1] Landsat 5 was launched in March 1984 and is currently the only source of TM imagery.

As the earth turns below the orbiting Landsat spacecraft, the TM and MSS scan the ground directly beneath in a fixed width swathing pattern perpendicular to the direction of the orbit. [Ref. 4:pp. 2-2 to 2-3] Both sensors have a 185 kilometer east-to-west swathing pattern. Swaths are designed to overlap for complete surface coverage. Landsat 5 circles the earth in a sun-synchronous, near-polar orbit at an altitude of approximately 705 km. The ground track is repeated in a 16-day cycle totaling 233 orbits. Since the inclination of the orbit is 96.22°, Landsat can cover the entire globe between about 84° North and 84° South every 16 days. These characteristics were chosen to satisfy the need for near-constant resolution, periodic observations of the same site, and for moderately constant illumination. Land-

sat 5 crosses the equator on a north-to-south (daylight)
path at approximately 9:45 a.m. local time each morning.

At the equator, adjacent swaths overlap by approxi-
mately 7 percent. [Ref. 4:p. 2-3] This overlap increases
as the satellite moves toward either pole because the orbit
paths converge with increasing latitude.

2. Thematic Mapper

The thematic mapper (TM) is a scanning optical-
mechanical sensor operating in the visible and infrared
wavelengths. [Ref. 4:p. 3-1] It contains a scan mirror
assembly that projects reflected earth radiation onto detec-
tors arrayed in two focal planes. The TM uses the forward
motion of the spacecraft for along-track scan and uses a
moving mirror assembly for the cross-track (perpendicular to
the spacecraft) direction.

The seven TM spectral bands were selected for their
value in discriminating vegetation type and vigor, measuring
plant and soil moisture, differentiating clouds and snow,
and identifying hydrothermal alteration in certain types of
rock [Ref. 5:p. 32]. Table 1 [Ref. 5:p. 30] lists the
characteristics of the TM sensor and Table 2 [Ref. 4:p. 3-
2,6:p. 86] lists some of the applications of the TM spectral
bands.

The TM bands are numbered out of the order of the
wavelength intervals covered. [Ref. 6:p. 85] The wave-

12

TABLE 1.   THEMATIC MAPPER SENSOR SYSTEM CHARACTERISTICS. AFTER REF. 5:P. 30

Band Number	Micrometers	Radiometric Sensitivity (NEΔP)
1	0.45 - 0.52	0.8
2	0.52 - 0.60	0.5
3	0.63 - 0.69	0.5
4	0.76 - 0.90	0.5
5	1.55 - 1.75	1.0
7	2.08 - 2.35	2.4
6	10.4 - 12.50	0.5K (NEΔT)

Note: Radiometric sensitivities are the noise-equivalent radiance differences for the reflective bands expressed as a percentage and as a temperature difference for the thermal infrared band.

length interval for band 7 falls between the wavelength intervals covered by bands 5 and 6. This is because band 7 was added to the TM after the other six bands were defined, and a decision was made not to renumber the bands.

The instantaneous field of view (IFOV) for bands 1 through 5 and band 7 (the reflective bands) is equivalent to a 30 meter square when projected to the ground. [Ref. 4:p. 3-1] Band 6, the thermal infrared band, has an IFOV equivalent to a 120 meter square.   These data are resampled during geometric processing to produce 28.5 meter and 120 meter IFOVs for the reflective and thermal infrared bands, respectively.

Classification accuracy becomes acceptable for most remote sensing agriculture and forestry applications when field sizes are greater than 60 IFOVs.   [Ref. 5:p. 33]   This

TABLE 2. CHARACTERISTICS OF THE THEMATIC MAPPER BANDS. AFTER REF. 4:P. 3-2, 6:P. 86

Band	Wavelength, μm	Characteristics
1	0.45 - 0.52	Blue-green. Maximum penetration of water, which is useful for bathymetric mapping in shallow water. Useful for distinguishing soil from vegetation and deciduous from coniferous plants.
2	0.52 - 0.60	Green. Matches green reflectance peak of vegetation, which is useful for assessing plant vigor.
3	0.63 - 0.69	Red. Matches a chlorophyll absorption band that is important for discriminating vegetation types.
4	0.76 - 0.90	Reflected IR. Useful for determining biomass content and for water body mapping.
5	1.55 - 1.75	Reflected IR. Indicates moisture content of soil and vegetation. Penetrates thin clouds. Good contrast between vegetation types. Useful for snow/cloud differentiation.
6	10.40 - 12.50	Thermal IR. Nighttime images are useful for thermal mapping and for estimating soil moisture.
7	2.08 - 2.35	Reflected IR. Coincides with an absorption band caused by hydroxyl ions in minerals. Ratios of bands 5 and 7 are potentially useful for mapping hydrothermally altered rocks associated with mineral deposits.

corresponds to a square of about 8 IFOVs on a side. There-
fore, classification accuracy should be acceptable for
fields 240 x 240 m in size if a 30 x 30 m ground IFOV is
used. This should allow most of the field sizes in Canada,
the United States, and the Soviet Union to be adequately
sampled in the spatial domain. It should also provide some
information for fields in developing countries where field
sizes are less than 240 x 240 m.

There are some known limitations of the various TM
bands. At high sun angles, bands 5 and 7 saturate over
bright areas such as sandy beaches [Ref. 4:pp. 2-3 to 2-5].
The time of the Landsat overpass is too early in the day to

14

record maximum thermal contrast, which occurs in the early afternoon. Preliminary studies suggest that band 6 does not significantly enhance the accuracy of the usual land cover analysis [Ref. 7:p. 220].

3. Radiometric and Geometric Correction of Image Data

Landsat digital image data transmitted from the satellite have some degree of distortion because of characteristics of the sensing and recording systems as well as atmospheric and scene conditions. [Ref. 4:pp. 4-2 to 4-3] Radiometric distortion is caused by blurring effects of the sensor, transmission noise, atmospheric interference, variable surface illumination, and changes in surface radiance due to changes in the viewing angle. Geometric distortion results from spacecraft effects, such as attitude and altitude changes; earth effects caused by its curvature, rotation, and terrain relief; and temporary aberrations in the scanning system.

Radiometric corrections account for errors in the image pixel radiance values caused by changing sensor characteristics. [Ref. 4:p. 4-4] The sensors have internal calibration lamps, which were calibrated before launch. They are used to calibrate detector gains and biases. Data from these lamps can be used to track overall sensor response and identify drift away from nominal performance for each detector. Radiometric corrections are made on a band-

15

by-band basis. Different algorithms for estimating gain and bias are applied to the six reflective bands and to the thermal band.

Remotely sensed data usually contain both systematic and nonsystematic geometric errors. [Ref. 5:p. 102-103] Systematic errors can be corrected using data about the satellite's position and orientation and knowledge of the internal sensor distortion. Nonsystematic errors cannot be corrected with acceptable accuracy without a sufficient number of ground control points. A ground control point is a point on the surface of the earth where both image coordinates and map coordinates can be identified.

After the systematic errors have been corrected, some slight geometric distortion remains because of uncertainties in spacecraft position and orientation. [Ref. 4:p. 4-5] This distortion is normally acceptable, but the distortion can be removed through the use of ground control points.

C. ENERGY INTERACTIONS

When electromagnetic energy is incident on any earth surface feature, three fundamental energy interactions are possible. [Ref. 8:p. 11] The energy can be reflected, transmitted, or absorbed. Using the principle of conservation of energy, the relationship between these energy interactions is

$$E_I(\lambda) - E_R(\lambda) + E_A(\lambda) + E_T(\lambda) \qquad (1)$$

where E_I is the incident energy, E_R is the reflected energy, E_A is the absorbed energy, and E_T is the transmitted energy. All energy components are a function of the wavelength, λ.

It should be noted that the proportions of energy reflected, absorbed, and transmitted vary for different earth surface features, depending on the specific material type and condition. [Ref. 8:p. 12] Wavelength dependency means that, for a given surface feature, the proportions of energy reflected, absorbed, and transmitted will vary at different wavelengths.

An earth surface feature can be characterized by measuring the fraction of the incident energy that is reflected. [Ref. 8:p. 13] This quantity is called the spectral reflectance, ρ_λ, and is a function of wavelength. It is defined as

$$\rho_\lambda - \frac{E_R(\lambda)}{E_I(\lambda)} \times 100 \qquad (2)$$

where ρ_λ is expressed as a percentage.

A graph of the spectral reflectance of an earth surface material as a function of wavelength is called a spectral reflectance curve. [Ref. 8:p. 13] The spectral reflectance curve can give insight into the spectral characteristics of a surface material and has a strong influence on the choice

17

of wavelengths in which remote sensing data are acquired for a particular application.

Many earth surface features can be identified on the basis of their spectral characteristics [Ref. 8:p. 15]. Some features of interest cannot be spectrally separated. The success of multispectral image analysis depends on two factors: that any surface feature (e.g., a field of wheat) will have a different radiance at one wavelength than at another, providing that the difference between the two wavelengths is sufficiently large; and that no two dissimilar surface features will have the same radiance at both wavelengths [Ref. 9:p. 363].

Figure 1 shows typical spectral reflectance curves for three basic types of earth surface feature: healthy green vegetation, dry bare soil, and clear lake water. [Ref. 8:p. 15] The curves represent average values for these material types. The reflectance of individual features can vary considerably above and below the average.

D. PATTERN RECOGNITION

1. General

"The signals from a given sensor can be thought of as defining a multi-dimensional space where each sensor band corresponds to a dimension." [Ref. 10:p. 81] The boundaries of that space are then defined by the minimum and maximum possible values in each of the bands. The basic pattern
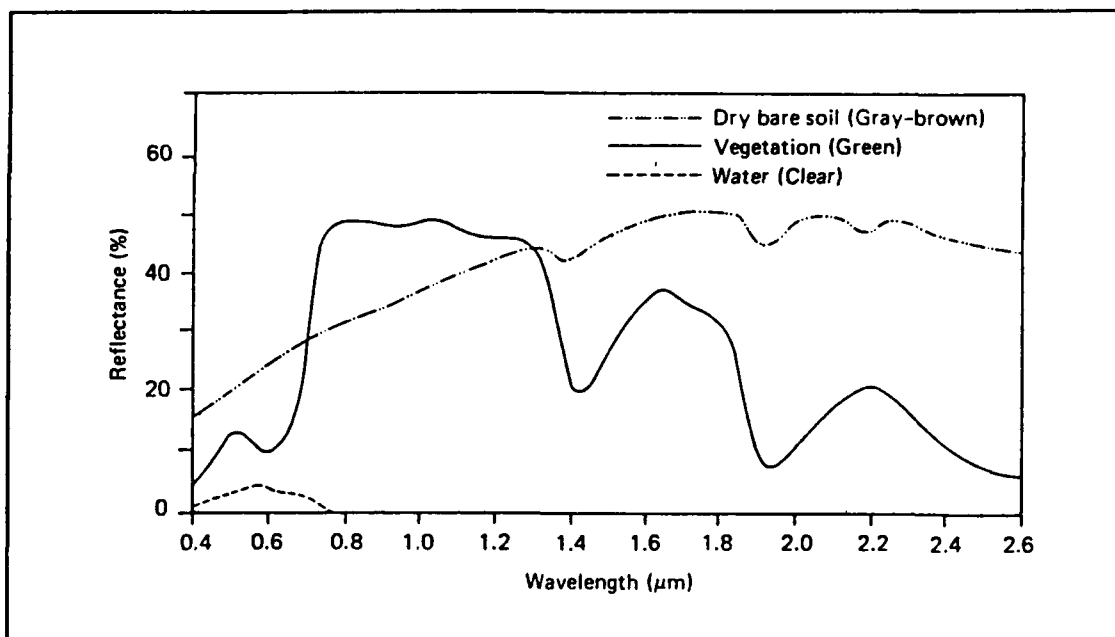
Figure 1. Typical Spectral Reflectance Curves for Vegetation, Soil, and Water. From Ref. 8:p. 15

recognition problem is to determine the information class or category of each distinct region on the ground using the set of sensor measurements and to estimate the error rate for the class assignments [Ref. 11:p. 793].

Information classes are those defined by man [Ref. 5:p. 179]. Information classes can be land use or land cover types which are of interest to the user of the final classification product. Conversely, spectral classes are those that are inherent in the remote sensor measurement space. Spectral classes are only of interest to the extent that they can be matched to one or more information classes [Ref. 7:p. 308]. Often spectral classes do not match directly to information classes because of the effect of mixed pixels (i.e., pixels containing more than one class) and

19

because of spectral diversity in nominally uniform information classes (i.e., one information class corresponds to several spectral classes) [Ref. 7:pp. 308-309].

The sensor may not gather sufficient information to allow discrimination to take place between the classes of interest. [Ref. 11:p. 795] In these cases one may be forced to define more discernable classes even though they may be of less interest to the user of the final product. To help determine the discernable classes, one can employ an unsupervised classification or clustering process which can identify what the naturally distinguishable classes are from the sensor's data.

If the individual classes of the patterns are already known, then one has a supervised pattern recognition problem. [Ref. 12:pp. 1-2] In supervised pattern recognition a portion of the set of known patterns is extracted and used to derive a pattern classification algorithm. These patterns are called the training set. The remaining known patterns are then used to test the classification algorithm. These patterns are referred to as the test set. Since the correct class of each of the patterns in the test set are known, one can evaluate the performance of the algorithm. Once a desired level of performance is achieved, which is normally measured in terms of the misclassification rate, the algorithm can be used on initially unlabeled patterns.

If the classes, and perhaps even the number of classes, of the available patterns are unknown, then one has an unsupervised pattern recognition or clustering problem [Ref. 12:p. 1-2]. In clustering problems, one attempts to find classes of patterns with similar properties [Ref. 12:p. 215]. Similarity is often defined as proximity of the points in multispectral space according to a distance measure [Ref. 12:p. 216].

There are many reasons why pattern recognition provides an ideal approach to the problem of dividing an image into its spectral or information classes. [Ref. 13:p. 136] Since pattern recognition is computer-oriented, it allows for rapid and repeatable analysis and a statistical treatment of multivariate data. It is easily tailored to a wide range of problems, and it produces quantitative results. Pattern recognition is most applicable when the goal is to categorize or classify each elementary observation into one of a limited number of discrete classes.

2. Supervised Classification

In a supervised classification, the identity and location of some of the land cover types, such as urban, agriculture, wetland, and forest, are already known through a combination of field work, analysis of aerial photography, maps, and personal experience. [Ref. 5:pp. 177-178] With this knowledge, one attempts to locate specific sites in the

image that represent homogeneous examples of the known land cover types. These areas are commonly referred to as training sites because the spectral characteristics of these known areas are used to "train" the classification algorithm. The classifier is then used to assign every pixel in the image to the class which it has the greatest likelihood of being a member.

"To yield acceptable classification results, training data must be both representative and complete." [Ref. 8:p. 678] This means that all spectral classes constituting each information class must be adequately represented in the training data for a supervised classification to produce acceptable results [Ref. 8:p. 679].

Since the information to develop complete training data was not available, this study used unsupervised classification methods.

3. Unsupervised Classification

In an unsupervised classification, the identities of the classes of land cover types within a scene are not known beforehand because adequate ground information is lacking or surface features within the scene are not well defined [Ref. 5:p. 178]. Clustering algorithms are used to search for "natural" groupings of the pixels in multispectral feature space [Ref. 5:p. 215]. Once the data are classified, one attempts to assign these "natural" or spectral classes to

22

the information classes of interest. It is usually neces-
sary to combine some of the clusters, since one information
class may be composed of more than one spectral class [Ref.
5:p. 219]. Also, some of the clusters may be less meaning-
ful because they represent mixed classes of earth surface
materials [Ref. 5:p. 215].

Clusters are generally defined as groups of points
that are "similar" according to some measurement criteria.
[Ref. 12:p. 216] Usually, "similarity" is defined as prox-
imity of the points in multispectral space according to a
distance measure.

There are several reasons for interest in using
unsupervised pattern recognition. [Ref. 14:p. 67] The
collection and labeling of a large set of sample patterns
can be very costly and time consuming. In many applica-
tions, the characteristics of the patterns can change slowly
with time. In the early stages of an investigation it may
be valuable to gain some insight into the nature or struc-
ture of the data.

One of the primary advantages of unsupervised clas-
sification is that the classifier identifies the distinct
spectral classes present in the image data. [Ref. 8:p. 685-
686] Many of these classes might not initially be apparent
to an analyst applying a supervised classifier. Also, the
spectral classes in a scene might be so numerous that it

would be difficult to train on all of them. In an unsupervised approach they are found automatically.

There are several other advantages of unsupervised pattern recognition. [Ref. 7:p. 299] The classes defined by unsupervised classification are often much more uniform with respect to spectral composition than are those generated by supervised classification. Unique classes are recognized as distinct units. No extensive prior knowledge of the region is required, and the opportunity for human error is minimized.

A serious disadvantage of unsupervised classification is that clear matches between spectral and information classes are not always possible. [Ref. 7:p. 309] Some information classes may not have direct spectral counterparts, and vice versa. Also, comparing the classification results from different regions or dates may require the same set of information categories. This is easily handled in supervised classification by appropriate selection of training sites. This may be difficult to do with unsupervised classification, however, since there is no provision in unsupervised pattern recognition to use information from outside of the image being classified or to define training sites.

E. FEATURE SELECTION

The LANDSAT thematic mapper (TM) acquires images in
seven spectral bands. Because of the amount of data and the
related processing time, subsets or transformations of the
seven bands are often used to reduce the dimensionality of
the data and thus reduce the computation time of the classi-
fication problem.

Generally, the more bands analyzed in a classification
problem, the greater the cost and perhaps the greater the
amount of redundant spectral information being used. [Ref.
5:p. 198] Therefore, a basic problem in multispectral
pattern recognition is to find a technique that will allow
separation of the major land cover classes with a minimum of
error and a minimum number of bands.

> A judgement must be made to determine those bands that
> are most effective in discriminating each class from all
> others. This process is commonly called feature selec-
> tion. The goal is to delete from the analysis those
> bands that provide only redundant spectral information.
> In this way the dimensionality (i.e., the number of
> bands to be processed) in the data set may be reduced.
> This process minimizes the cost of the digital image
> classification (but hopefully, not the accuracy). [Ref.
> 5:p. 189]

A feature or feature vector can be any mathematical
transformation of the band measurements. [Ref. 13:p. 175]
Transformations that are often used in remote sensing appli-
cations include band subsets, between band ratios, and
linear transformations. Though many linear transformations
are possible, attention was restricted to two of the more

25

common ones, the principal component transformation and the so-called tasseled cap transformation. All of these methods of reducing data dimensionality were used in this study, though the band ratio method was only used with the CORINTO site.

1. Band Subsets

The simplest method of reducing the dimensionality of the original multispectral data is to select only a subset of the available bands for use in pattern recognition. "Generally, the best three-band combinations include one of the visible bands (TM 1, 2, or 3) and one of the longer-wavelength infrared bands (TM 5 or 7) together with TM band 4." [Ref. 5:p. 91]

Studies frequently use one of the visible bands, one of the mid-IR bands, and the near-IR band, band 4, to reduce the dimensionality while retaining a "maximum" amount of information. Band 6 (the thermal IR band) is often not used because of its different spatial resolution.

Thompson and Henderson [Ref. 15] used the band set (4 5 7) to investigate soil properties under grassland vegetation. Crippen [Ref. 16] claims that the band set (1 4 7) is commonly the combination of choice based on qualitative evaluations for both barren and vegetated areas. Karaska et al. [Ref. 17] found the band set [(1, 2, or 3) 4 5] to be useful in distinguishing forest cover types.

2. Band Ratios

Sometimes differences in brightness from similar surface materials are caused by topographic conditions, shadows, or seasonal changes in sunlight illumination. [Ref. 5:p. 135] These conditions may hamper the ability of a classification algorithm to identify the surface materials in a remotely sensed image. Ratio transformations of the remotely sensed data can, in certain instances, be used to reduce the effects of such conditions. These ratios may also provide unique information not available in any single band that is useful in discriminating between soil and vegetation.

Ratios can also be useful in reducing a condition called the "topographic effect," which is manifested in Landsat images by the visual appearance of terrain ruggedness. [Ref. 18:p. 115] The topographic effect is caused by differential spectral radiance due to surface slope and aspect variations.

When using a simple ratio, division by zero is possible, and ratios less than one are common. [Ref. 8:p. 655] Rounding to the nearest integer will compress much of the ratio into gray levels 0 or 1. One means of solving this problem is to define a new gray scale value using the equation

$$G' = K \arctan\left(\frac{G_{band1}}{G_{band2}}\right) \qquad \text{(3)}$$

where G' is the new gray scale value and K is a scaling factor calculated to place the ratio values in the proper integer range. For positive values of G_1 and G_2, the ratio G_1/G_2 will range from 0 to infinity and the arc tangent will range from 0 to $\pi/2$. Therefore, for an eight-bit display, a value of 162.3 is appropriate for K. The value of G' will then range from 0 to 255.

The ratio image has several useful properties. Since the relationship holds for both shadowed and directly illuminated pixels, the ratio image shows pure reflectance information without the effects of topography. [Ref. 7:p. 454] This result allows one to examine the reflectance properties of surfaces without the confusing effects of mixed brightness of topography and material reflectance.

Ratioed images are often useful for discriminating subtle spectral variations in a scene that are masked by the brightness variations in the individual spectral bands. [Ref. 8:p. 650] Ratioed images portray variations in the slopes of the spectral reflectance curves between the two bands involved, regardless of the absolute reflectance values observed in the bands. However, since ratio images are intensity blind, dissimilar materials with different absolute radiances but having similar slopes of their spec-

tral reflectance curves may appear identical in the ratio image [Ref. 8:p. 654].

A problem with band ratios is that severe atmospheric effects, if present, can differ from one band to the other. [Ref 7:pp. 457-458] The value of the band ratio will no longer portray only the spectral properties of the ground surface. It will have values greatly altered by the varied atmospheric contributions to the separate bands.

3. Principal Component Transformation

Extensive interband correlation is often encountered in the analysis of multispectral image data. [Ref. 8:p. 655-656] The images generated from the various spectral bands appear similar and convey much of the same information. The purpose of the principal component transformation is to compress the information contained in the original set of n bands into a fewer number of bands or components. The components are then used instead of the original data.

The principal component transform (also known as the Hotelling, eigenvector, or discrete Karhunen-Loève transform [Ref. 19:p. 122]) transforms a correlated set of multispectral image data into an uncorrelated data set with certain ordered variance properties [Ref. 5:p. 151]. The choice of the basis vectors for the transform is made so that these vectors point in the direction of the maximum variance of the data, subject to the constraint that all of the vectors

be mutually orthogonal and the transformed components be uncorrelated [Ref. 19:p. 125-126].

The principal component vectors are computed at each pixel from the original set of n image bands by the transformation

$$y - T(x-m_x) \qquad (4)$$

where x is the (n x 1) vector of gray scale values for each pixel, m_x is the mean vector of the image, T is an (n x n) orthogonal transformation matrix, the rows of which are the normalized eigenvectors of the image covariance matrix arranged with the eigenvalues in descending order, and y is the vector of principal components, which is calculated independently for each pixel. [Ref. 20:pp. KARLOV-2 to KARLOV-3]

Since processing cost is dependent on the dimensionality of input to the pattern recognition algorithm, the usual procedure is to select a subset of the principal component vector for further processing [Ref. 19:p. 325]. Since the components are ranked so that each component has a variance less than the previous component, a reduction in the effective number of bands can occur, since the higher numbered components will contain less information [Ref. 21:p. 220].

The eigenvalues of the transformation also contain useful information. [Ref. 5:p. 154] It is possible to

determine the percent of total variance explained by each of the principal components, $\%_p$, using the equation

$$\%_p = \frac{\lambda_p \times 100}{\sum\limits_{k=1}^{n} \lambda_k} \tag{5}$$

where λ_p is the pth eigenvalue out of the possible n eigenvalues.

4. Tasseled Cap Transformation

A principal component transformation can fail to capture the complex structure of Landsat TM data and is extremely scene dependent [Ref. 22:p. 262].

> The TM tasseled cap transformation, on the other hand, specifically emphasizes the inherent data structures, and is intended to be an invariant transformation which can therefore be applied to any TM scene (although atmosphere and illumination geometry will affect results, as may substantial deviation from a mid-latitude, temperate environment). [Ref 22:p. 262]

The analysis of remotely sensed data can be thought of as a three-step process. [Ref. 22:p. 256] The first step is to understand the relationship among the sensor bands for the scene classes of interest. The second step is to compress the number of spectral bands into a manageable number of features, and the third step is to extract physical scene characteristics from the spectral features. The principal component transformation provides data volume reduction, but it presents significant obstacles with regard to physical interpretation of the derived features and

31

comparisons between dates or scenes. The tasseled cap transformation accomplishes all of these functions.

The TM tasseled cap transformation is a linear transformation that rotates the six TM reflective bands into TM tasseled cap coordinates. [Ref. 22:pp. 256-257] The components of the transformation matrix are given in Table 3.

TABLE 3. THEMATIC MAPPER TASSELED CAP COEFFICIENTS. FROM REF. 22:P. 257

Feature	Band 1	Band 2	Band 3	Band 4	Band 5	Band 7
Brightness	0.3037	0.2793	0.4743	0.5585	0.5082	0.1863
Greenness	-0.2848	-0.2435	-0.5436	0.7243	0.0840	-0.1800
Wetness	0.1509	0.1973	0.3279	0.3406	-0.7112	-0.4572
Fourth	-0.8242	0.0849	0.4392	-0.0580	0.2012	-0.2768
Fifth	-0.3280	0.0549	0.1075	0.1855	-0.4357	0.8085
Sixth	0.1084	-0.9022	0.4120	0.0573	-0.0251	0.0238

The data in the six TM reflective bands were found to primarily occupy a three-dimensional space defined by two perpendicular planes and a transition region between them. [Ref. 10:p. 84-85] One plane, the plane of vegetation, contains fully-vegetated samples, while the other plane, the plane of soils, contains bare soil samples. Samples that contain both soil and vegetation fall in the transition region between the two planes. These features typically capture 95 percent or more of the total variation in TM images.

32

The three basic features of the TM tasseled cap are called greenness, brightness, and wetness. "Brightness" is a weighted sum of all six reflective TM bands. [Ref. 22:p. 257-259] It is responsive to changes in total reflectance and to those physical properties that affect total reflectance. "Greenness" is a contrast between the sum of the visible bands and the near-infrared band. (The two mid-infrared bands essentially cancel each other.) "TM greenness responds to the combination of high absorption in the visible bands (due to plant pigments and particularly chlorophyll) and high reflectance in the near-infrared (due to internal leaf structure and the resultant scattering of near-infrared radiation) which is characteristic of green vegetation." [Ref. 22:p. 259] "Wetness" contrasts the sum of the visible and near-infrared bands with the sum of the mid-infrared bands. The name wetness was chosen because the mid-infrared bands have been suggested to be most sensitive to both soil and plant moisture.

Brightness defines the intersection between two perpendicular planes, the plane of vegetation and the plane of soils. [Ref. 22:p. 258-261] The plane of vegetation is defined by brightness and greenness, the plane of soils is defined by brightness and wetness, and the transition zone between the two planes is defined by greenness and wetness. The final three features contain the residual variation of the scene.

The tasseled cap transformation presents TM data in a more accessible fashion by changing the viewing perspective. [Ref. 22:p. 262] It reduces the data volume by concentrating the majority of data variability in three features. By making a direct link between the features and the physical scene characteristics it enhances both the interpretation of observed spectral variation and the prediction of the spectral effects of particular changes in scene characteristics.

An agricultural field can be used to provide an example of the uses of the tasseled cap transformation. [Ref. 5:p. 165] During a growing season, the field is expected to begin near the plane of soils, move through the transition zone as the crop grows, arrive at the plane of vegetation near the end of crop development, and then move back toward the plane of soils during harvest or senescence.

All of the methods of reducing data dimensionality mentioned above (band subsets, band ratios, the principal component transformation, and the tasseled cap transformation) were used in this study. The band-ratio method was only used with the CORINTO site.

III. METHODOLOGY

A. SELECTION OF STUDY SITES

1. Site Selection

The scene used in this study was acquired by the Landsat 5 thematic mapper on 24 March 1986 and covered the area shown in the large box in Figure 2 (path 17, row 51, scene identification 507531500). It was obtained on CCT-P computer-compatible tapes, which have been resampled to 28.5 x 28.5 m pixels in the reflective bands and 120 x 120 m pixels in the thermal-infrared band. [Ref 4:p. 4-5] The images were radiometrically and geometrically corrected, as far as available information allowed.

Since a Landsat scene covers an area of 185 x 185 km, a significant reduction in area was necessary to achieve a study site of a manageable size. First, a one-quarter scale photomosaic of the entire Landsat scene was made by photographing screen images of portions of the scene. Cloud-free areas of the scene were identified as potential sites for further study. Maps of 1:50,000 scale for portions of the scene were then obtained from the Defense Mapping Agency. These maps were examined for a variety of terrain types and for ease in registering the maps to the Landsat scene.

Figure 2.   Area Covered by Landsat Scene.   After Ref.
23:p. 61

Because of the variety of terrain types available in
a relatively small area, attention was focused on an area
covered by six map sheets. This area is approximately 72 x
36 km in size. It lies completely in Nicaragua and runs
roughly from Corinto on the Pacific coast to the western
shore of Lake Managua, including the cities of Leon and
Chinandega and part of the Cordillera de los Marrabios chain

36

of volcanoes, including the volcanoes Telica and Momotombo. The smaller box in Figure 2 shows the six-map area.

From the six-map area, two 512 x 512 pixel (14.6 x 14.6 km) sites were selected for detailed study. These two areas together contain a variety of terrain types. The first area, called CORINTO, contains the port city of Corinto, a river/estuary system with extensive mangrove swamps, some streams, and agricultural land. The second area, called MALP, lies east of the town of Malpaisillo and contains some smaller streams and a variety of vegetative cover types such as woodland, scrub, and agricultural land. The boxed areas in Figure 3 show the approximate site boundaries.

2. Geography of the Area

Nicaragua can be divided into three major regions: the drier, fertile Pacific region and Great Rift Valley; the wetter cooler Central Highlands; and the hot and humid Atlantic Coast region. [Ref. 24:p. 66] The six-map area lies completely in the first region.

Western Nicaragua is marked by a line of young volcanoes running between the Gulf of Fonseca and Lake Nicaragua. [Ref. 24:p. 66] Many of these volcanoes are still active. These volcanic peaks protrude from a large crustal fracture or rift that forms a long, narrow
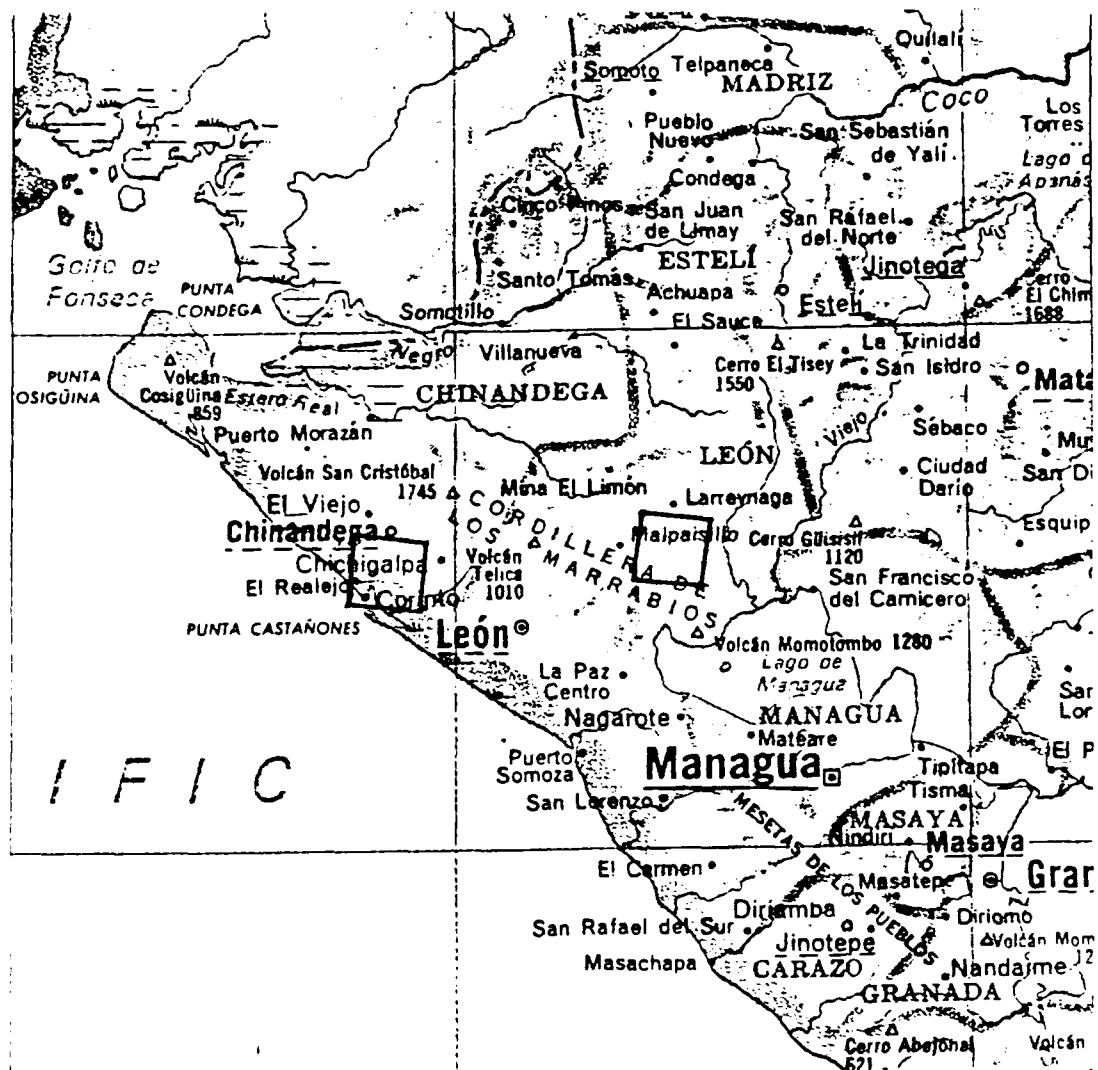
Figure 3. Approximate Study Site Boundaries. After Ref. 23:p. 61

depression running southeast from the Gulf of Fonseca to the Rio San Juan drainage.

Surrounding the lakes and extending northwest of them to the Gulf of Fonseca are fertile lowland plains highly enriched with volcanic ash. [Ref. 24:p. 66] These lowlands are densely populated and well cultivated. The

rivers in this area are short and carry a small volume of water. The soil is volcanic and 85% of the area is fertile.

Mean annual precipitation for these plains and the flanking uplands ranges from 100 to 150 centimeters. [Ref. 24 :p. 66] Rainfall is usually seasonal. May through October is the rainy season, and December through April is the driest period.

3. The CORINTO Site

The CORINTO site includes the city of Corinto and the area to the northeast. Figure 4 is a map of the site, with the dark rectangle marking the approximate site boundary. The dark areas around the rivers in the lower left part of the map represent mangrove swamp; the horizontal dashed lines at the edge of parts of the mangrove represent areas that are subject to inundation; and the pattern of lines in the right half of the map represent small irrigation works. The lower and upper portions of the map come from two different map sheets. The seven original TM band images of the site can be found in Appendix A.

The statistics of the CORINTO image are presented in Table 4. The three visible bands (1, 2, and 3) exhibit a considerable degree of redundancy; their correlations range from 0.89 to 0.94. There is also considerable redundancy between the mid-infrared bands (5 and 7), with a correlation of 0.91. There are redundancies between the visible bands

39

Figure 4. Map of the CORINTO Site. From Ref. 25,26

and the mid-infrared bands, The lowest correlations occur
between band 4, the near-infrared band, and the other bands,
so band 4 is the least redundant. Band 6, the thermal-
infrared band, is most correlated with band 7. It is prac-
tically uncorrelated with band 4, and it is moderately
correlated with the other bands. Band 5 has the greatest
variance, followed by bands 4 and 7.

40

TABLE 4. STATISTICS FOR THE CORINTO THEMATIC MAPPER IMAGE

Band number	1	2	3	4	5	6	7
Univariate statistics							
Mean	93.75	38.35	44.17	65.79	86.28	160.41	40.18
Std. dev.	8.75	6.56	12.53	22.70	33.43	12.03	20.11
Variance	76.65	43.08	157.06	515.24	1117.65	144.75	404.41
Minimum	71	21	15	4	0	134	0
Maximum	255	138	170	159	255	223	255
Variance-covariance matrix							
1	76.65						
2	52.46	43.08					
3	102.86	73.34	157.06				
4	64.95	89.56	88.54	515.24			
5	232.33	177.52	372.15	357.62	1117.65		
6	71.18	45.30	114.99	17.33	308.07	144.75	
7	136.59	89.46	220.56	64.47	611.42	216.26	404.41
Correlation matrix							
1	1.00						
2	0.91	1.00					
3	0.94	0.89	1.00				
4	0.33	0.60	0.30	1.00			
5	0.79	0.81	0.89	0.47	1.00		
6	0.67	0.57	0.76	0.06	0.76	1.00	
7	0.77	0.68	0.87	0.14	0.91	0.89	1.00

4. The MALP Site

The MALP site is a fairly flat area of mixed terrain east of the town of Malpaisillo, hence the site name. The site name was abbreviated due to restrictions on file name length on the computer used in the study. Figure 5 is a map of the site, with the dark rectangle marking the approximate site boundary. Since the scrub areas show only as slightly shaded areas and the woodland areas do not show up at all (a problem of copying multi-colored maps in black and white), Figure 6 was created, which is an overlay of the map in Figure 5 showing the missing woodland terrain feature. The white area to the upper right of the map is outside of the

41

Figure 5. Map of the MALP Site. From Ref. 27

six-map area and was not available during the study. The seven original TM band images of the site can be found in Appendix A.

The statistics of the MALP image are presented in Table 5. The three visible bands are all highly correlated with one another (correlation $\geq$ 0.95), indicating that there is substantial redundant information in these bands. There

Figure 6.   Overlay of the MALP Map Showing Woodland and Scrub

Woodland

Land subject to inundation

Scrub

43

TABLE 5. STATISTICS FOR THE MALP THEMATIC MAPPER IMAGE

Band number	1	2	3	4	5	6	7
Univariate statistics							
Mean	108.06	47.60	68.26	73.11	137.75	170.26	67.92
Std. dev.	12.05	8.31	16.45	13.44	24.93	5.95	14.02
Variance	145.14	69.12	270.65	180.79	621.77	35.40	196.49
Minimum	77	27	24	25	28	139	13
Maximum	187	91	147	144	224	198	244
Variance-covariance matrix							
1	145.14						
2	97.08	69.12					
3	189.17	134.06	270.65				
4	99.20	78.44	145.17	180.79			
5	259.04	178.40	358.80	218.43	621.77		
6	27.01	17.52	41.90	-7.34	54.61	35.40	
7	142.34	94.75	194.14	72.75	302.90	53.11	196.49
Correlation matrix							
1	1.00						
2	0.97	1.00					
3	0.95	0.98	1.00				
4	0.61	0.70	0.66	1.00			
5	0.86	0.86	0.87	0.65	1.00		
6	0.38	0.35	0.43	-0.09	0.37	1.00	
7	0.84	0.81	0.84	0.38	0.87	0.64	1.00

is also considerable redundancy between the visible and mid-infrared bands (5 and 7), as the correlations range from 0.81 to 0.87. Band 4 is not highly correlated with any of the other bands. Band 6 is also not highly correlated with any of the other bands. The range of pixel values in each band is less than that of the CORINTO image because there is less variety of terra types in this image and no open water.

B. BAND AND FEATURE SELECTION

The LANDSAT thematic mapper (TM) records images in seven spectral bands. Because of the amount of data and the related processing time, subsets or transformations of the

seven bands are often used to reduce the dimensionality of the data, and thus reduce the computation time of the classification problem.

1. Band Subsets

There are 35 possible combinations of the seven TM bands and 20 possible combinations of six bands (if the thermal IR band is not used). Clearly, one does not want to analyze every possible band combination, especially when some of the bands are highly correlated.

a. The Optimum Index Factor

Use of the optimum index factor (OIF) is one way to deal with the problem of evaluating the possible band combinations. [Ref. 5:pp. 90-91] This technique is based on the amount of total variance and correlation within and between various band combinations. The OIF for a three-band subset is

$$OIF = \frac{\sum_{k=1}^{3} s_k}{\sum_{j=1}^{3} Abs(r_j)} \qquad (1)$$

where s_k is the standard deviation of band k and r_j is the correlation coefficient between any two of the three bands being evaluated. The three-band combination with the largest OIF generally will have the most information (as measured by variance) with the least amount of duplication (as

45

measured by correlation). Combinations ranking close together may produce similar results.

The OIF rankings were calculated under two conditions: both including and excluding band 6, the thermal IR band. The OIF rankings for the CORINTO image are in Table 6 and the rankings for the MALP image are in Table 7.

TABLE 6. OPTIMUM INDEX FACTOR RANKINGS FOR THE CORINTO IMAGE

Rank	Combination (Using all bands)	OIF	Combination (Without Band 6)	OIF
1	4,5,6	52.501	4,5,7	50.094
2	4,5,7	50.094	3,4,7	42.019
3	4,6,7	50.030	1,4,7	41.454
4	3,4,6	42.054	3,4,5	41.358
5	3,4,7	42.019	1,4,5	40.760
6	1,4,7	41.454	2,4,7	34.765
7	3,4,5	41.358	2,4,5	33.321
8	1,4,6	40.904	1,3,4	28.105
9	1,4,5	40.760	1,5,7	25.129
10	2,4,7	34.765	2,5,7	25.083
11	2,4,6	33.448	3,5,7	24.721
12	2,4,5	33.321	2,3,4	23.304
13	1,3,4	28.105	1,3,5	20.889
14	5,6,7	25.570	1,2,4	20.650
15	1,5,7	25.129	2,3,5	20.290
16	2,5,7	25.083	1,2,5	19.377
17	3,5,7	24.721	2,3,7	16.038
18	1,5,6	24.308	1,3,7	15.993
19	2,5,6	24.272	1,2,7	14.970
20	3,5,6	24.048	1,2,3	10.157
21	2,3,4	23.304		
22	1,3,5	20.889		
23	1,2,4	20.650		
24	2,3,5	20.290		
25	1,2,5	19.377		
26	2,6,7	18.099		
27	2,6,7	17.695		
28	1,6,7	17.489		
29	2,3,7	16.039		
30	1,3,7	15.993		
31	1,2,7	14.970		
32	1,3,6	14.705		
33	2,3,6	14.027		
34	1,2,6	12.705		
35	1,2,3	10.157		

TABLE 7. OPTIMUM INDEX FACTOR RANKINGS FOR THE MALP IMAGE

Rank	Combination (Using all bands)	OIF	Combination (Without Band 6)	OIF
1	4,5,6	39.886	4,5,7	27.519
2	3,4,6	30.478	3,4,5	25.124
3	4,6,7	29.978	1,4,5	23.717
4	1,4,6	29.084	2,4,7	23.307
5	3,5,6	28.331	1,4,7	21.458
6	4,5,7	27.519	3,5,7	21.448
7	1,5,6	26.710	2,4,5	21.093
8	3,4,5	25.124	1,3,5	19.853
9	2,5,6	24.764	1,5,7	19.830
10	2,4,6	24.143	1,3,4	18.867
11	5,6,7	23.995	2,4,7	18.824
12	1,4,5	23.717	2,5,7	18.608
13	3,4,7	23.307	2,3,5	18.303
14	1,4,7	21.458	1,2,5	16.826
15	3,5,7	21.448	2,3,4	16.343
16	2,4,5	21.093	1,3,7	16.109
17	1,3,5	19.853	1,2,4	14.806
18	1,5,7	19.830	2,3,7	14.718
19	1,3,6	19.579	1,2,7	13.096
20	3,6,7	19.100	1,2,3	12.677
21	1,3,4	18.867		
22	2,4,7	18.824		
23	2,5,7	18.608		
24	2,3,5	18.303		
25	2,3,6	17.427		
26	1,6,7	17.244		
27	1,2,5	16.826		
28	2,3,4	16.343		
29	1,3,7	16.109		
30	2,6,7	15.676		
31	1,2,6	15.474		
32	1,2,4	14.806		
33	2,3,7	14.718		
34	1,2,7	13.096		
35	1,2,3	12.677		

When all seven bands are considered, the (4 5 6) band combination ranked first for both images. Band 6 also appears in many of the top-ranked band combinations. This would seem to indicate that band 6 contains information that is not duplicated by the other bands, even though its spatial resolution is poorer. Bands 4 and 5 also appear in many of the top-ranked band combinations.

When band 6 is not included, the top-ranked band combination was the (4 5 7) combination. This is somewhat

47

unexpected, as bands 5 and 7 tend to be correlated. Almost all of the other highly-ranked band combinations are of the form [(1, 2, or 3) 4 (5 or 7)], which is what one would expect, since the visible bands and the mid-IR bands tend to be correlated. The band combination (1 2 3), the three visible bands, consistently ranked last.

b. Physical Arguments

From the spectral reflectance curves in Figure 1, it is readily seen that the greatest differentiation between the general land cover types of soil, water, and vegetation occurs in the mid-infrared, followed closely by the near-infrared. The thermal-infrared is best at differentiating soil from water and vegetation. The smallest differentiation occurs in the visible bands.

In the CORINTO image, water and vegetation form the main areas of interest, so the best choice of a three band subset might be the three bands that appear individually to be the best for discriminating those surface materials. Looking at the TM band characteristics in Table 2, it appears that bands 1, 4, and 5 would be the best choice, instead of bands 4, 5, and 7. The set (1 4 5) ranked fifth by OIF, but the OIF calculations included the total scene statistics, not just the statistics from the distinguishable surface features of interest. There is not enough ground information to classify much of the land cover in this

image, so the OIF may not be the best means of selecting a three band set.

In the MALP image, there are no large areas of open water, so the main problem is to distinguish the vegetation of interest from soil and other vegetation. From Table 2, it appears that band sets (1 4 5) or (3 4 5) would be the best choices. These band sets also ranked second and third by OIF. In this case, there is less scene variability (the band variances are less) and the cover types of interest are similar to the cover types in areas where no information is available.

2. Image Transformations

Since there is substantial redundant information in both images, the transformations discussed in Chapter II may be able to reduce dimensionality while retaining more information than a simple three band subset.

a. The Principal Component Transformation

The principal component transformation was performed on both images using the appropriate routine (KARLOV) from the Land Analysis System [Ref. 20:pp. KARLOV-1 to KARLOV-5]. The routine performs the transformation as outlined in Chapter II. The eigenvalues for the transformation of the CORINTO image are shown in Table 8, and the eigenvalues for the MALP image are in Table 9. For both images, the first three principal component bands explain

49

more than 97 percent of the total scene variance, as calcu-
lated by equation 5. The first three principal component
band images for each site are in Appendix B.

TABLE 8.   EIGENVALUES OF THE CORINTO IMAGE COVARIANCE MATRIX

Component number	1	2	3	4	5	6	7
Eigenvalue	1874.62	473.44	54.98	39.07	10.77	4.39	1.57
Percent Variance	76.24	19.25	2.24	1.59	0.44	0.18	0.06
Cumulative Percent Variance	76.24	95.49	97.73	99.32	99.76	99.94	100.0

TABLE 9.   EIGENVALUES OF THE MALP IMAGE COVARIANCE MATRIX

Component number	1	2	3	4	5	6	7
Eigenvalue	1277.50	132.74	66.09	23.31	12.42	6.23	1.06
Percent Variance	84.08	8.74	4.35	1.53	0.82	0.41	0.07
Cumulative Percent Variance	84.08	92.82	97.17	98.70	99.52	99.93	100.0

b. The Tasseled Cap Transformation

The other linear transformation discussed in
Chapter II was the tasseled cap transformation. The coeffi-
cients in Table 3 were used to transform both the CORINTO
and MALP images into their greenness, brightness, and wet-
ness components. A short program was written to perform the
transformation and to scale the output images to the proper
range (0 to 255) for the available display. The tasseled

cap component images are in Appendix B. The short program
used for the transformation is listed in Appendix C.

c. Band Ratios

The other image transformation discussed in
Chapter II was band ratios. Band ratios have been found to
be useful both to reduce the topographic effect and to
enhance certain information in an image. For example, the
ratio of bands 3 and 4 provides vegetation information, and
the ratio of bands 2 and 5 is useful for identifying water
bodies and provides subtle wetland information [ref 5:pp.
137-138].

To test the usefulness of band ratios, a few
ratios of the CORINTO image were made and grouped together
as multiband images. Since water, wetland, and vegetation
are the categories of interest in this image, the three
ratios (band 1)/(band 5), (band 2)/(band 5), and (band
3)/(band 4) were calculated. All three ratios were grouped
together as one three-band image, and the three possible
two-band combinations were grouped together as two-band
images. The three ratio images are in Appendix B, and the
program used to create these ratio images is listed in
Appendix C.

3. Band Selection

After considering the possible band combinations,
the most promising ones, based on the above discussion, were

selected. Since time and processor usage were not always a critical constraint on this study, for completeness the full seven band set was included as one of the band choices. This set will have all of the information available, so it should give a good indication of what features are and are not detectable. Since reducing the dimensionality does significantly affect processing time and would make the results more transportable to other processing environments, a number of three-band subsets and transformations were also selected.

The band combinations selected for further study were:

- The seven TM bands. This set has all of the sensor information available.

- Bands 4, 5, and 6. This set ranked first by OIF.

- Bands 4, 5, and 7. This set ranked was highly ranked by OIF and ranked first when band 6 was not included. The spectral reflectance curves of soil, water, and vegetation have the greatest separation in this range. These bands respond to soil variability as manifested by vegetation [Ref. 15:p. 321].

- Bands 1, 4, and 7. Fairly high ranking by OIF (without band 6). A common combination of choice [Ref. 16:p. 141]. These bands are not highly correlated, and this set includes one band from each of the three major reflective spectral regions (visible, near-infrared, and mid-infrared).

- Bands 1, 4, and 5. Fairly high OIF ranking (without band 6). Useful for distinguishing forest cover types [Ref. 17]. Physical arguments also support the selection of this band combination.

- Bands 3, 4, and 5 (MALP site only). Fairly high OIF ranking (without band 6). Useful for distinguishing

52

forest cover types [Ref. 17]. Physical arguments also support the selection of this band combination.

- Bands 3, 4, and 6 (MALP site only). Ranked second by OIF.

- The first three principal component bands.

- The three tasseled cap transformation bands (greenness, brightness and wetness).

- Ratio images (CORINTO site only). Various combinations of the ratios (band 1)/(band 5), (band 2)/(band 5), and (band 3)/(band 4).

C. THE LAND ANALYSIS SYSTEM

The Land Analysis System (LAS) is an image analysis system designed for use with satellite imagery. [Ref. 20:p. 1] It provides the capability to manipulate and analyze digital image data and includes a wide range of functions and statistical tools for image analysis. It was the primary software used in this study. In addition to routines for extracting the study sites from a Landsat scene, image statistics calculation, and file management functions, LAS includes a variety of routines for both supervised and unsupervised classification. All three of the routines for unsupervised classification (HINDU, KMEANS, and ISOCLASS) were used, as well as one of the supervised classification routines (MINDIST). The classification routines used are summarized below. A more detailed description of each algorithm is in Appendix D.

1. The HINDU Classification Routine

HINDU classifies a multiband image based upon its multidimensional histogram. [Ref. 20:p. HINDU-1] Regions in the histogram with high density are regarded as pattern clusters. The user specifies the input image, the minimum and maximum acceptable number of clusters, and the number of gray levels per histogram bin.

2. The KMEANS Classification Routine

KMEANS performs an unsupervised classification using the K-means algorithm. The basic K-means algorithm operates as follows [Ref. 12:p. 218]:

- Step 1: Begin with an arbitrary set of cluster centers for the desired number of clusters.

- Step 2: Compute the sample mean of each cluster.

- Step 3: Reassign each sample to the cluster with the nearest mean.

- Step 4: If the classification of all samples has not changed, stop. If not, go to step 2.

3. The ISOCLASS Classification Routine

ISOCLASS performs the unsupervised classification of am image using an isodata-type clustering algorithm [Ref. 20:p. ISOCLASS-1]. The basic isodata clustering algorithm operates as follows [Ref. 12:p. 219]:

- Step 1: Cluster the data into C classes. Eliminate any classes with fewer than T members.

- **Step 2:** On every other iteration, if C < 2N then split any clusters whose samples form sufficiently disjoint groups. If any clusters have been split, go to step 1.

- **Step 3:** Merge any clusters whose means are sufficiently close.

- **Step 4:** Go to step 1.

In the algorithm description, C is the number of classes, T is the minimum number of pixels allowed in a cluster, and N is the approximate desired number of clusters.

4. The MINDIST Classification Routine

MINDIST performs a supervised classification of multiband images based on minimum distance from class means. [Ref. 20:p. MINDIST-1] It can also be used to attempt to improve the results of the unsupervised clustering algorithms, either by discarding pixels that are too far from cluster centroids or by reclassifying clusters based on cluster means and a distance rule.

D. FEATURES OF INTEREST

1. Identifiable Information Classes

Given that the only ground reference available was 1:50,000 scale maps, a key question is: what are the meaningful terrain classes that can potentially be identified? The symbols and color coding used on a map are identified in the map legend. Using the map legend, the following types of terrain can be identified in the two study sites: water, stream, mangrove, land subject to inundation, woodland,

scrub, city, and road. Grassland and cultivated land are other probable terrain types, but these two terrain types were not marked on the maps.

Landsat TM images are appropriate sources for Level I and many Level II categories in the U.S. Geological Survey (USGS) Land Use and Land Cover Classification System [Ref. 8:pp. 138-140] As can be seen in Table 10, almost all of the areas identifiable from the map match categories in the USGS classification system. So the prospects appear good that the terrain types identified above may indeed be spectrally distinguishable.

Some of the terrain features (e.g., streams and roads) will generally be linear features much less than a pixel (28.5 m) wide. Bernstein et al. [Ref. 21:p. 195], when examining a TM image of Dulles airport, found that linear features as small as about 7.6 m (about a quarter of a pixel) wide could easily be visually discerned because of a favorable contrast ratio between the linear feature and its background. Since streams tend to encourage vegetation to grow along their banks by providing a ready source of water, and since water and vegetation have greatly different reflectivities in the infrared wavelengths, streams (at least the larger ones, which also have a greater potential for being obstacles) should also be detectable as linear features of subpixel width.

TABLE 10.   U.S. GEOLOGICAL SURVEY LAND USE/LAND COVER CLASSIFICATION SYSTEM FOR USE WITH REMOTE SENSOR DATA. FROM REF 8:P. 139

Level I		Level II
1 Urban or built-up land	11	Residential
	12	Commercial and services
	13	Industrial
	14	Transportation, communications, and services
	15	Industrial and commercial complexes
	16	Mixed urban or built-up land
	17	Other urban or built-up land
2 Agricultural land	21	Cropland and pasture
	22	Orchards, groves, vineyards, nurseries, and ornamental horticultural areas
	23	Confined feeding operations
	24	Other agricultural land
3 Rangeland	31	Herbaceous rangeland
	32	Shrub and brush rangeland
	33	Mixed rangeland
4 Forest land	41	Deciduous forest land
	42	Evergreen forest land
	43	Mixed forest land
5 Water	51	Streams and canals
	52	Lakes
	53	Reservoirs
	54	Bays and estuaries
6 Wetland	61	Forested wetland
	62	Nonforested wetland
7 Barren land	71	Dry salt flats
	72	Beaches
	73	Sandy areas other than beaches
	74	Bare exposed rocks
	75	Strip mines, quarries, and gravel pits
	76	Transitional areas
	77	Mixed barren land
8 Tundra	81	Shrub and brush tundra
	82	Herbaceous tundra
	83	Bare ground
	84	Mixed tundra
9 Perennial snow and ice	91	Perennial snowfields
	92	Glaciers

2. Information Classes of Interest

At TM pixel size, cities are not a distinct spectral class, but are made up of a number of sub-classes (e.g., residential, commercial/industrial, parks, mixed pixels), some of which may not be spectrally distinguishable from other terrain classes of interest. Since the locations of cities are generally known and normal weather variations

57

have much less impact on cities, identification of cities was not be pursued in this study.

Roads, since they do not generally fall under the categories of obstacles or cover and concealment, were also not addressed.

A pixel is considered to be a water pixel when it contains only water, i.e., when the pixel does not also contain some other terrain type. Stream pixels, on the other hand, will generally contain some other terrain type or types in addition to water, i.e., they will be mixed pixels. It is hoped that streams, at least the ones large enough to be potential obstacles, will be detectable by the influence of their water content on the spectral response of the pixel. It is also possible that streams may be detectable by their effect on the vegetation lining the stream banks, creating a contrast between the vegetation lining the stream and the other local vegetation.

Land subject to inundation may be inundated, have a specific type of vegetative cover (such as reeds or swamp grass), be barren soil, or have mixed cover types that do not permit them to be identified as a separate class. The question of separability can only be answered by examining the classified images. The question of exact cover type can not be answered here. The value of these areas as either obstacles or concealment will depend on the exact cover type or whether the area is inundated.

Woodland and scrub are very broad categories, but a finer distinction is not possible with the available ground information. The size, health, density, and type of woods or scrub can affect the spectral response and thus the classification of a given pixel, but any further subdivision of these classes would be speculation. More detailed information about subclasses would, of course, be important for making judgements about the quality of cover and concealment they may provide. If these land cover types are separable from the rest of the image, the value of using Landsat TM imagery for finding the correct state of these military terrain classes would be demonstrated.

a. The CORINTO Site

The CORINTO site was used to attempt to identify water obstacles. Figure 7 is an overlay of the map of the CORINTO site showing the information classes of interest. There are significant areas of open water and mangrove. There are numerous streams in the site, which may be detectable as subpixel-width linear features.

Along the streams in the eastern part of the site are three potential water obstacles. These potential water obstacles were identified on the map as being wider than the normal stream markings (see Figure 4). Two of these areas are above dams ("Presa" is Spanish for dam). Other
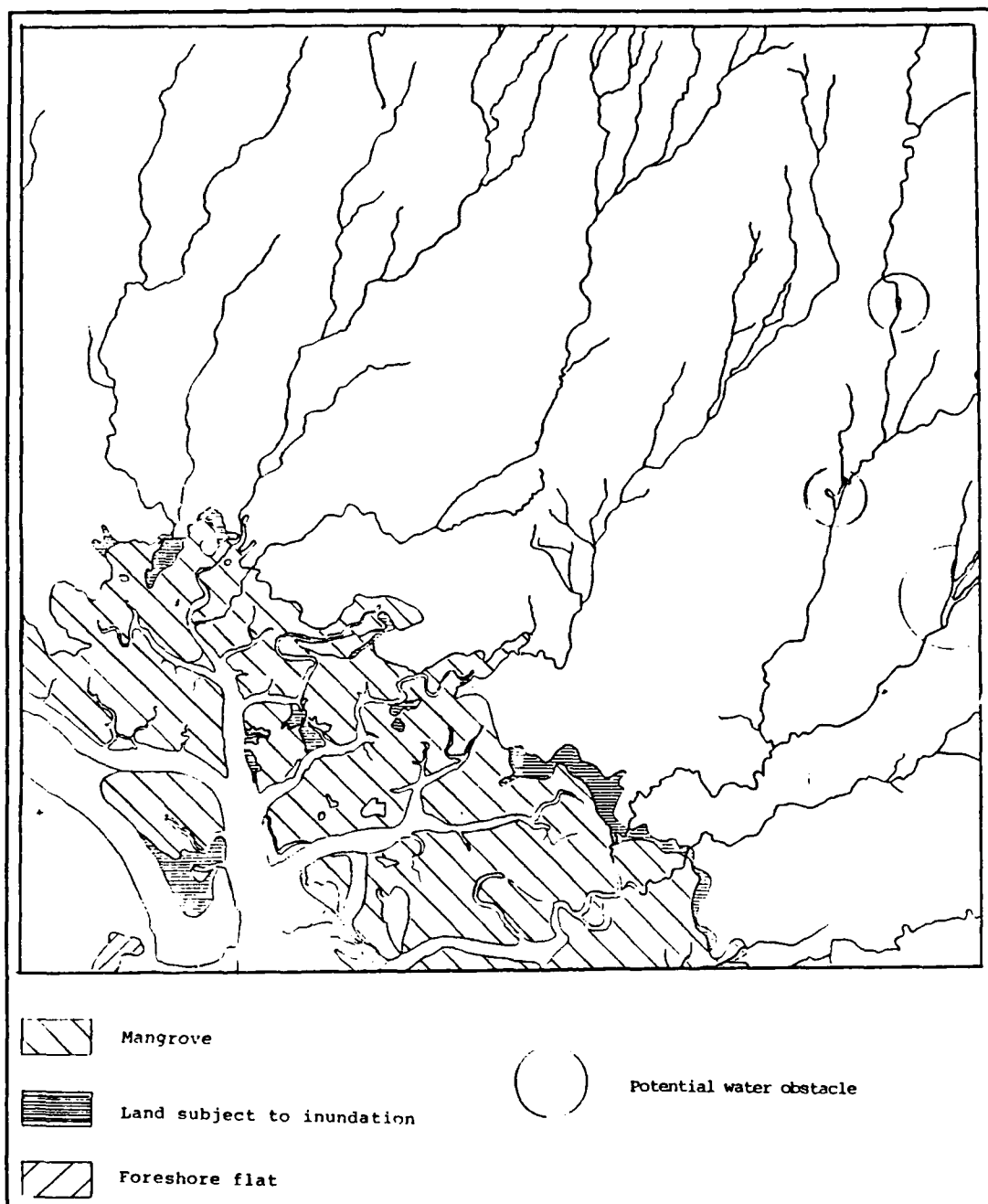
Figure 7.   Overlay of the CORINTO Map Showing Water Features, Mangrove, and Land Subject to Inundation

Legend:
- Mangrove
- Land subject to inundation
- Foreshore flat
- Potential water obstacle

portions of the streams could also be water obstacles, but no other candidates are obvious from the map reference.

As mentioned above, the land subject to inundation may or may not be identifiable as a separate class. There were no special markings on the rest of the site, so those areas were not considered in the rest of the study.

b. The MALP Site

The MALP site was used to attempt to identify vegetative cover and concealment. Figure 6 is a map overlay of the MALP site showing the information classes of interest. The only information classes of interest in this site are woodland and scrub. These are very broad categories, so it was expected that more than one or two spectral classes would map to each of these information classes. However, if portions of these classes can be separated from the rest of the site by the classification algorithms, that would indicate that further study with better ground information would be worthwhile.

Human activity could complicate the evaluation of vegetative cover and concealment in this site. This site is in the more populous part of Nicaragua. Human activity, eve over short periods of time, can have a significant effect on the woodland and scrub areas through such activities as logging, land clearing, and firewood collection. This could

61

render the map reference used here out-of-date and lead to poor results.

3. Assigning Spectral Classes to Information Classes

Clusters were manually assigned to information classes. This task was made much easier by means of a few simple procedures and one fortunate circumstance. When the map overlays of Figures 6 and 7 were copied at a 74 percent scale factor (available on local copying machines), they were almost the same size as the images produced by one of the available printers. The difference was about one percent, adequate for the task given the limited ground information. By making transparencies of the reduced overlays, the appropriate transparency could be laid on top of the printed classification image. This made the cluster identification process much easier.

The maps of Figures 4 and 5 were the ground reference used to identify the information classes of interest in this study. The map overlays of Figures 6 and 7 were the references used to assign spectral classes in the classified images to the information classes of interest.

E. CLASSIFICATION ACCURACY ASSESSMENT

If a remote sensing-derived land cover map is to be useful, there must be some method for assessing classification accuracy. [Ref. 5:p. 225] This normally requires the collection of information about some parts of the terrain

which can then be compared with the remote sensing-derived classification map. This means that to assess classification accuracy it is necessary to compare two classification maps, the remote sensing-derived map and a reference map that is assumed to be accurate. The reference map may be derived from on site investigation or, as is often done, from the interpretation of remotely sensed data obtained at a larger scale or higher resolution. For example, researchers often compare a Landsat-supervised classification map with a reference map produced by interpreting large-scale (e.g., 1:20,000) aerial photographs.

"The overall accuracy of land-use maps for earth resource management should generally be 85% and the accuracy must be approximately equal for most categories." [Ref. 5:pp. 225-226] Since the only ground reference available for this study was the 1:50,000 scale maps, the accuracy for the identifiable classes may not reach that goal, and not all of the area in each site will be classifiable. However, since the goal of this study is to demonstrate the feasibility of using Landsat satellite imagery for terrain analysis and not to manage earth resources, a lower level of accuracy is acceptable.

IV. ANALYSIS OF RESULTS

A. PRESENTATION OF CLASSIFICATION RESULTS

The results of the unsupervised classifications are best presented in image form. The different clusters in the classified image are assigned different colors or gray scale values to depict the spatial relationship of the various classes. Generally, spectral classes that do not contain information of interest are all assigned the same gray scale value. Here, a value of 255 (white) was used for the classes not shown in a classified image. These classes were usually the "unknown" parts of the site. The spectral classes corresponding to the information classes of interest are the only colored or gray areas in the classified image.

All of the spectral classes corresponding to one information class can be assigned the same gray scale value. This would be done to create a classified image containing only the information classes of interest. This was not done here. Each spectral class was assigned a different gray scale value so that the spectral structure of the image data could be clearly seen.

Some comments accompany each classified image to assist the reader in interpreting the results of the classification

and to call attention to points of interest in the classification result.

B. STATISTICAL SEPARABILITY OF CLUSTERS

It is relatively easy to run a large number of classifications. All that is required are computer time and patience. It is much more difficult and time consuming to analyze all of the results. One method of selecting the results for further analysis is to use a statistical measure of class separability.

Since class separability is a function not only of the distance between class means but also of the class probability distributions [Ref. 28:p. 335], a measure that includes both factors is needed. A measure called the divergence meets these criteria. A separability measure derived from the divergence, called the transformed divergence may also provide an indirect method of estimating the likelihood of correct classification [Ref. 29:p. 689].

The divergence is calculated from the mean and covariance of each spectral class and is a measure of the statistical distance between class pairs [Ref. 29:p. 688]. The divergence is derived from the logarithmic-likelihood ratio [Ref. 13:pp. 167-168]. The pairwise divergence between classes i and j is defined as [Ref. 29:p. 688]:

$$D_{ij} = \int \ln \frac{p(x|i)}{p(x|j)} [p(x|i) - p(x|j)]\, dx \qquad (1)$$

where p(x|i) is the probability density function of x for class i.

When the classes are assumed to have normal probability functions, the expression for divergence simplifies to [Ref. 13:p. 168]:

$$Dij = 0.5tr((C_i-C_j)(C_i^{-1}-C_j^{-1})) + 0.5tr((C_i^{-1}+C_j^{-1})(m_i-m_j)(m_i-m_j)') \quad (2)$$

where C_i is the covariance matrix for class i, m_i is the mean vector for class i, and tr(A) denotes the trace, or sum of the diagonal elements, of the matrix A.

A problem with divergence is that, as two classes are more widely separated in feature space, the probability of correct classification has an upper bound of 100 percent, but the divergence will continue to increase. [Ref. 28:p. 340] One solution is to use the transformed divergence, a saturating function of their divergence.

The transformed divergence is defined as [Ref. 20:p. DIVERGE-2]:

$$D^T_{ij} = 100(1-e^{-\frac{D_{ij}}{8}}) \quad (3)$$

where D^T_{ij} is the transformed divergence between classes i and j. The transformed divergence is extended to cover all of the class pairs by calculating the average transformed divergence D^T_{AVE}, which is simply the numerical average of

the transformed divergence D^T_{ij} over all class pairs [Ref 20:pp. DIVERGE-2 to DIVERGE-3].

One method of using the transformed divergence is to select the feature set having the greatest average transformed divergence [Ref. 13:p. 169]. This is similar to maximizing the probability of correct classification. Another method is to select the feature set having the largest minimum value of transformed divergence [Ref. 13:p. 173]. This would be the feature set with the best performance in separating the most difficult pair of classes to separate.

According to Jensen [Ref. 5:p. 201], a transformed divergence value of 100 suggests excellent class separation; a transformed divergence above 95 suggests good separation; and a value below 85 suggests poor class separation. Haack [Ref. 30:p. 269], on the other hand, states that a transformed divergence value of 75 or greater generally indicates an acceptable separability of classes. An exact threshold value for "acceptable" separability is not as important here as a feel for what the value of the transformed divergence means, i.e., a larger value is better, and a value below the range of 75 to 85 means that the two clusters are not well separated by this measure.

C. SUMMARY OF CLASSIFICATION RESULTS

A summary of selected classifications for the CORINTO site is presented in Table 11. A summary for the MALP site is in Table 12. Both summaries include the classified image name, the number of clusters, and the average and minimum transformed divergence. The number of iterations required

Table 11. SUMMARY OF SELECTED CLASSIFICATIONS FOR THE CORINTO SITE

Classified Image name	Number of clusters	D^T_{AVE}	D^T_{MIN}	Execution time	Number of iterations
CORINTO.CLASS1	29	97.94	33.93	27:54	60
CORINTO.CLASS1.MINDIST	29	97.99	40.09		
CORINTO.CLASS2	48			42:13	80
CORINTO.CLASS2.MINDIST	48				
CORINTO.KMEANS1	23	97.43	41.95	12:11	20
CORPCA.CLASS1	10	86.43	2.34	4:09	20
CORPCA.KMEANS3	20	85.35	5.00	4:11	14
COR457.KMEANS1	23	94.86	34.40		26
COR145.KMEANS2	23	86.84	3.13	8:34	25
COR145.CLASS1	13	84.93	5.50	9:57	40
COR456.KMEANS1	23	86.59	6.92		25
CORTC.KMEANS1	23	91.50	5.00		26
RATIO.KMEANS1	23	98.00	69.25	6·07	18
RATIO.KMEANS8	8	98.57	82.22		9
RATIO12.KMEANS8	8	95.86	65.73	0:55	?
RATIO13.KMEANS8	8	76.20	5.28		
RATIO23.KMEAAND8	8	70.20	4.47		9
COR147.KMEANS1	23	84.58	1.56		21
CORINTO.HINDU3	23	98.48	58.90	0:C5	
CORINTO.HINDU3.MINDIST	23	97.56	56.09	0:55	

for each iterative classification algorithm is also listed.
For some of the classifications, the time required for the
classification (in hours and minutes on a MicroVax II) is
included. This gives a relative measure of the speed of
each algorithm.

Table 12. SUMMARY OF SELECTED CLASSIFICATIONS FOR THE MALP SITE

Classified Image name	Number of clusters	D^T_{AVE}	D^T_{MIN}	Execution time	Number of iterations
MALP.CLASS4	17	98.01	61.18		60
MALP.CLASS4.MINDIST	17	98.28	72.00		
MALP.KMEANS2	23	97.96	17.35	17:39	29
MALP.KMEANS8	8	99.34	94.57		19
MALPPCA.CLASS2	11	89.23	31.49		40
MALPPCA.KMEANS1	23	91.26	5.90		28
MALPPCA.KMEANS8	8	90.41	43.28		25
MALP457.KMEANS1	23	90.08	21.90		33
MALP457.KMEANS8	8	88.15	39.15		39
MALP145.CLASS1	11	86.46	14.05	4:52	40
MALP145.KMEANS1	23	90.00	11.84	9:51	33
MALP.KMEANS8	8	89.88	33.30		19
MALP456.KMEANS1	23	80.23	1.83		38
MALP456.KMEANS8	8	80.23	14.78		23
MALP345.KMEANS8	8	90.22	40.69		19
MALPTC.KMENAS1	23	74.94	3.16		24
MALP346.KMEANS8	8	85.75	5.35		16
MALP147.KMEANS1	23	86.41	4.29		25
MALP.HINDU2.MINDIST	23	96.82	30.49		
MALP.HINDU3.MINDIST	13	98.44	81.94		

Most of the classified images have many more clusters
than there were information classes of interest. This was
done because the spectral structure of the data was unknown.
With more spectral classes than information classes, the
additional spectral classes are either subclasses of the
information classes of interest and can be combined, or they

can be ignored as classes not of interest. Classifying the images into too few spectral classes can result in spectral classes that are mixtures of information classes. Mixed spectral classes are of little or no use to this study.

1. Classified Image Naming Conventions

The naming convention used in Tables 11 and 12 provide information about the feature set and classification algorithm for each classified image. The classified image name is composed of two or three parts: the first part is the feature set identifier, the second is the classification algorithm identifier, and the third part, if there is one, indicates that the MINDIST algorithm was used as a post-processing step.

The feature set identifier part of the classified image name is constructed as follows:

- CORINTO or MALP indicates that all seven of the original thematic mapper bands were used.

- CORxyz or MALPxyz indicates that the three bands x, y, and z of the original seven thematic mapper bands were used.

- CORPCA or MALPPCA indicates that the first three bands of the principal component transformation were used.

- CORTC or MALPTC indicates that the three tasseled cap transformation components (greenness, brightness, and wetness) were used.

- RATIO indicates that the three ratio bands, (band 1)/(band 5), (band 2)/(band 5), and (band 3)/(band 4), were used.

70

- RATIOxy indicates that two of the three ratio bands were used, where a 1 indicates that the ratio (band 1)/(band 5) was included, a 2 indicates that the ratio (band 2)/(band 5) was included, and a 3 indicates that the ratio (band 3)/(band 4) was included.

The classification algorithm identifier was constructed as follows:

- CLASS indicates that the ISOCLASS algorithm was used

- KMEANS indicates that the KMEANS algorithm was used

- HINDU indicates that the HINDU algorithm was used

The number following the algorithm identifier is a reference number used to keep track of different results from using the same algorithm on the same feature set.

The presence of MINDIST in the classified image name indicated that the MINDIST algorithm was used on the image as a post-processing step to reclassify the image using the Euclidean distance rule. KMEANS already uses that distance rule, so MINDIST was not used on any of the KMEANS classifications.

2. Input Parameters for ISOCLASS

The ISOCLASS routine requires a number of input parameters. The parameters used are shown in Table 13. The meaning of these parameters is listed below [Ref. 20:pp. ISOCLASS-1 to ISOCLASS-2]:

- Any two clusters whose means are closer than DLMIN are combined.

- NMIN is the minimum number of members desired in any cluster. Clusters that have less than NMIN members are deleted.

- Any cluster whose standard deviation is greater than STDMAX and has more than 2(NMIN + 1) members is split.

- CHNTHS is the threshold for chaining clusters.

- MAXCLS is the maximum number of clusters.

Recommended ranges on the values of DLMIN and CHNTHS are given in the LAS User's Manual [Ref. 20:pp. ISOCLASS-1 to ISOCLASS-5]. The value of STDMAX was selected by a trial-and-error process based on the number of clusters produced by different values of this parameter. As long as the value of NMIN was small, it did not have much effect on the classification results.

The maximum allowable value of 64 for MAXCLS was used. This was done because the spectral structure of the data was unknown. With more spectral classes than information classes, the additional spectral classes are either subclasses of the information classes of interest and can be combined, or they can be ignored as classes not of interest. Classifying the images into too few spectral classes can result in spectral classes that are mixtures of information classes. Mixed spectral classes are of little or no use to this study.

A more detailed description of the ISOCLASS algorithm is given in Appendix D.

Table 13. INPUT PARAMETERS FOR THE ISOCLASS UNSUPERVISED CLASSIFICATION ALGORITHM

Image name	DLMIN	STDMAX	NMIN	CHNTHS
MALP.CLASS4	3.9	10.0	300	3.9
MALPPCA.CLASS2	3.2	4.5	150	3.2
MALP145.CLASS1	3.9	10.5	300	3.9
CORINTO.CLASS1	5.0	10.5	300	5.0
CORINTO.CLASS2	5.0	10.5	20	5.0
CORPCA.CLASS1	3.2	4.5	30	3.2
COR145.CLASS1	3.9	11.0	200	3.9

3. General Observations

From Tables 11 and 12, it can be seen that the classified imaged with the larger minimum values cf transformed divergence, D^T_{MIN}, tend to have the larger average values of transformed divergence, D^T_{AVE}. Since larger values of D^T_{MIN} indicate a better ability to separate hard-to-separate classes, the value of D^T_{MIN} was used to select classified images for analysis. The band sets with the largest values of both D^T_{MIN} and D^T_{AVE} are the original seven-band set, the (4 5 7) band set, the ratio images that include both the (band 1)/(band 5) and the (band 2)/(band 5) ratios, and many of the MALP site classifications with eight classes.

As can be seen in Tables 11 and 12, processing time increased both as the number of bands in the input image increased and as the number of output clusters increased. The processing time required by the various clustering algorithms for classifying the same input band set with similar numbers of clusters varied widely. Since all of the

73

seven-band-set results for the CORINTO site had fairly large values of D^T_{MIN} with all of the clustering algorithm combinations used in the study, this permits a comparison of the clustering algorithms. An evaluation of the ability of this band set to separate the classes of interest for this site is also possible.

D. COMPARISON OF CLUSTERING ALGORITHMS

1. The HINDU Algorithm

The HINDU algorithm runs very quickly, taking about five minutes to classify a seven-band, 512 x 512 pixel image. The one classification listed in Table 11 using this algorithm, called CORINTO.HINDU3, had a relatively high value of transformed divergence (58.90). However, the spectral classes in this classified image do not match very well to the information classes of interest, based on manual comparison with Figure 7.

Figure 8 shows the classes of interest extracted from the CORINTO.HINDU3 classified image. Comparing Figure 8 with the map overlay of Figure 7, it can be seen that this classification did detect one class of water and two of "mangrove." ("Vegetation and water" might be a more accurate description of the mangrove class. Other, clearly non-mangrove, areas were classified as belonging to this class, and it is not clear that mangrove can be spectrally separated from the other vegetation present.) It also detected the

74
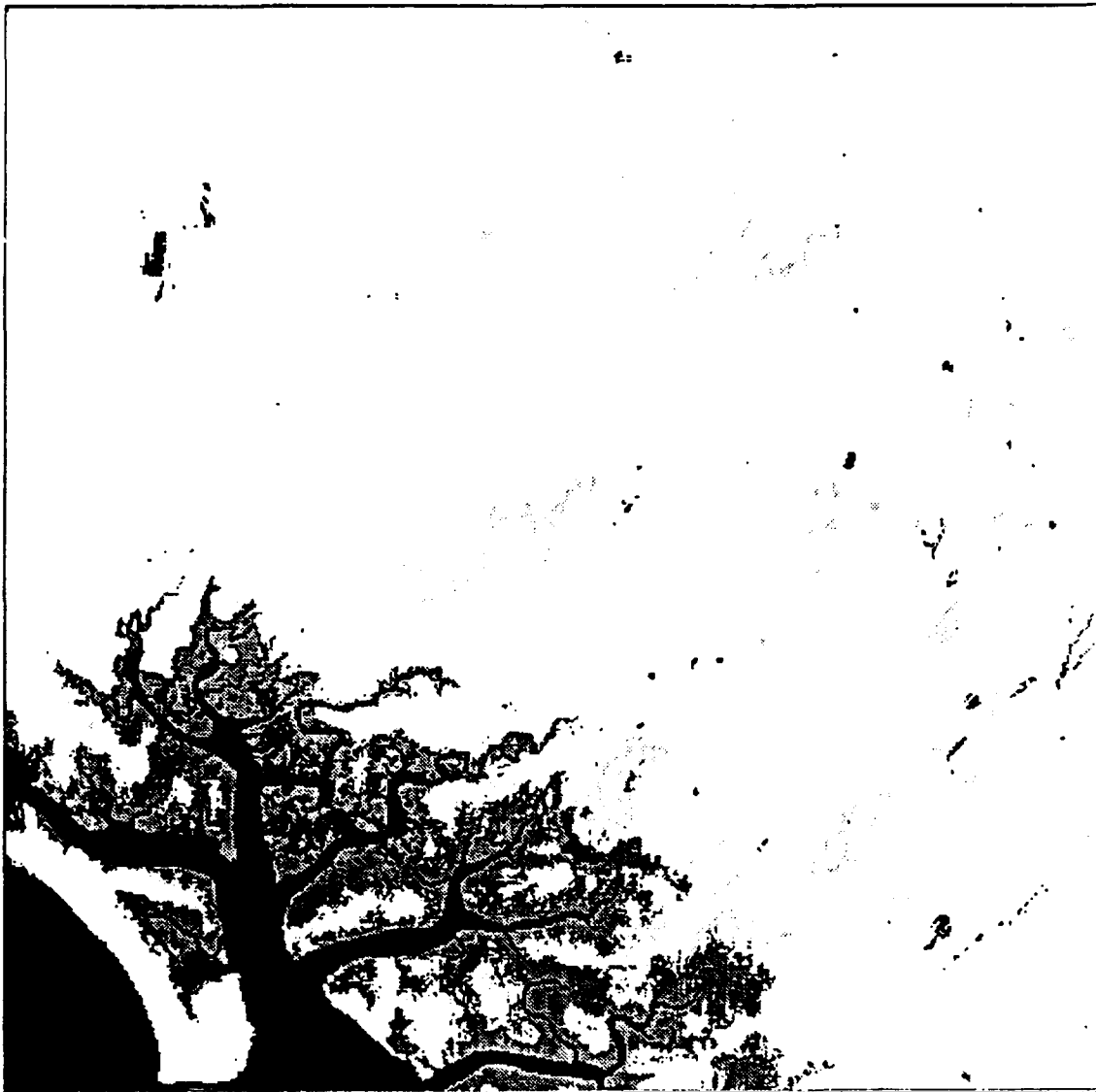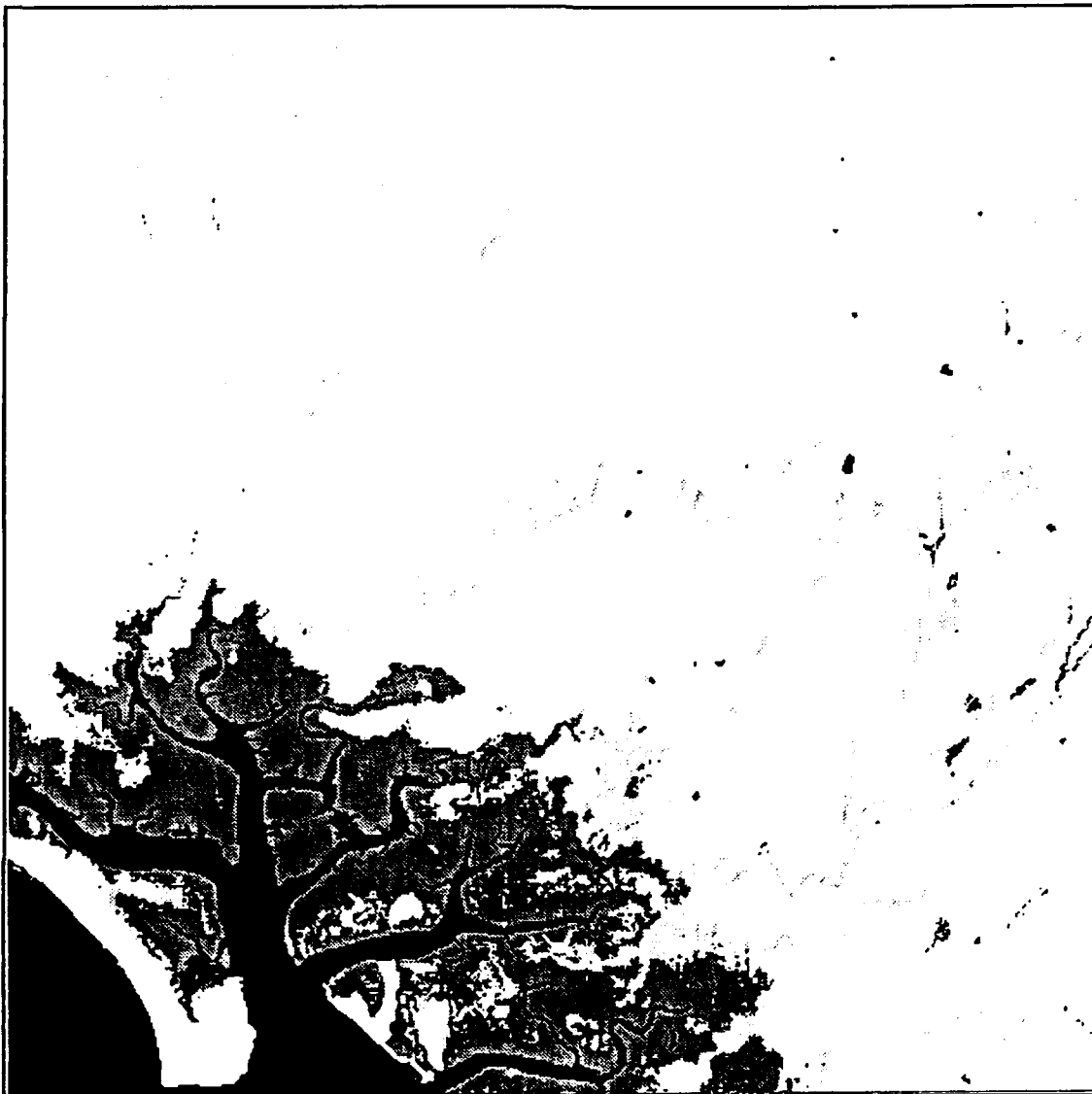
Figure 8. The CORINTO.HINDU3 Classified Image

three potential water obstacles on the streams in the eastern part of the CORINTO site. However, the water and mangrove do not have clear boundaries like those shown in the map overlay, but are mixed together in the northern part of the mangrove. There also seems to be a small amount of misclassification in the rest of the image.

75

The minimum value of the pairwise transformed divergence between the three classes was 96.3. Yool et al. found no clear relationship between divergence values and classification accuracy for individual classes, possibly because the assumption of Gaussian class distributions is not always accurate [Ref. 28:p. 689]. However, the transformed divergence will still be used here as a measure of the statistical separability of classes. It is the best measure of statistical separability available in the Land Analysis System.

2. HINDU Followed by MINDIST

As shown in Figure 9, using the MINDIST algorithm on the CORINTO.HINDU3 classification result still yields one class of water and two of mangrove, but the separation of classes appears to be much more accurate. Water was better separated from the mangrove, more of the streams in the area were detected, and there were fewer pixels in these classes in the "unknown" parts of the site. The minimum value of the pairwise transformed divergence between the three classes was 91.7.

It takes MINDIST about 50 minutes to reclassify a seven-band image using the cluster centers calculated using a different classification algorithm. MINDIST uses the input cluster centers and the selected distance measure to

Figure 9. **The CORINTO.HINDU3.MINDIST Classified Image**

reassign all of the pixels in the image to the various

classes.

3. The KMEANS Algorithm

The KMEANS algorithm runs at a moderate speed,

normally four to eight hours for a three-band image and six

to 12 hours for a seven-band image. Run times are somewhat

higher for a greater number of clusters and for a smaller value of the execution cutoff threshold, PCTCNG. Control over the number of clusters is very good, and the accuracy appears to be good also. However, the clusters may not all be significantly different if the analyst has specified incorrectly the number of clusters desired versus the number of clusters actually occurring in the image.

The classification results of CORINTO.KMEANS1 are similar to the CORINTO.HINDU3.MINDIST results, but two water classes were detected instead of one, and three mangrove classes were detected instead of two (see Figure 10). These additional spectral classes appear to be transition classes: one between water and mangrove, and the other between mangrove and the rest of the image. The information contained in these additional spectral classes might distinguish between terrain of significantly different obstacle value. Without better ground information, no definite conclusion can be made.

The minimum value of the pairwise transformed divergence between the five classes was 41.9 between the two mangrove classes. Between the remaining class pairs the minimum value was 94.0. This indicates that, according to the transformed divergence measure, the two mangrove classes are not well separated spectrally, but that the remaining class pairs are spectrally well separated.
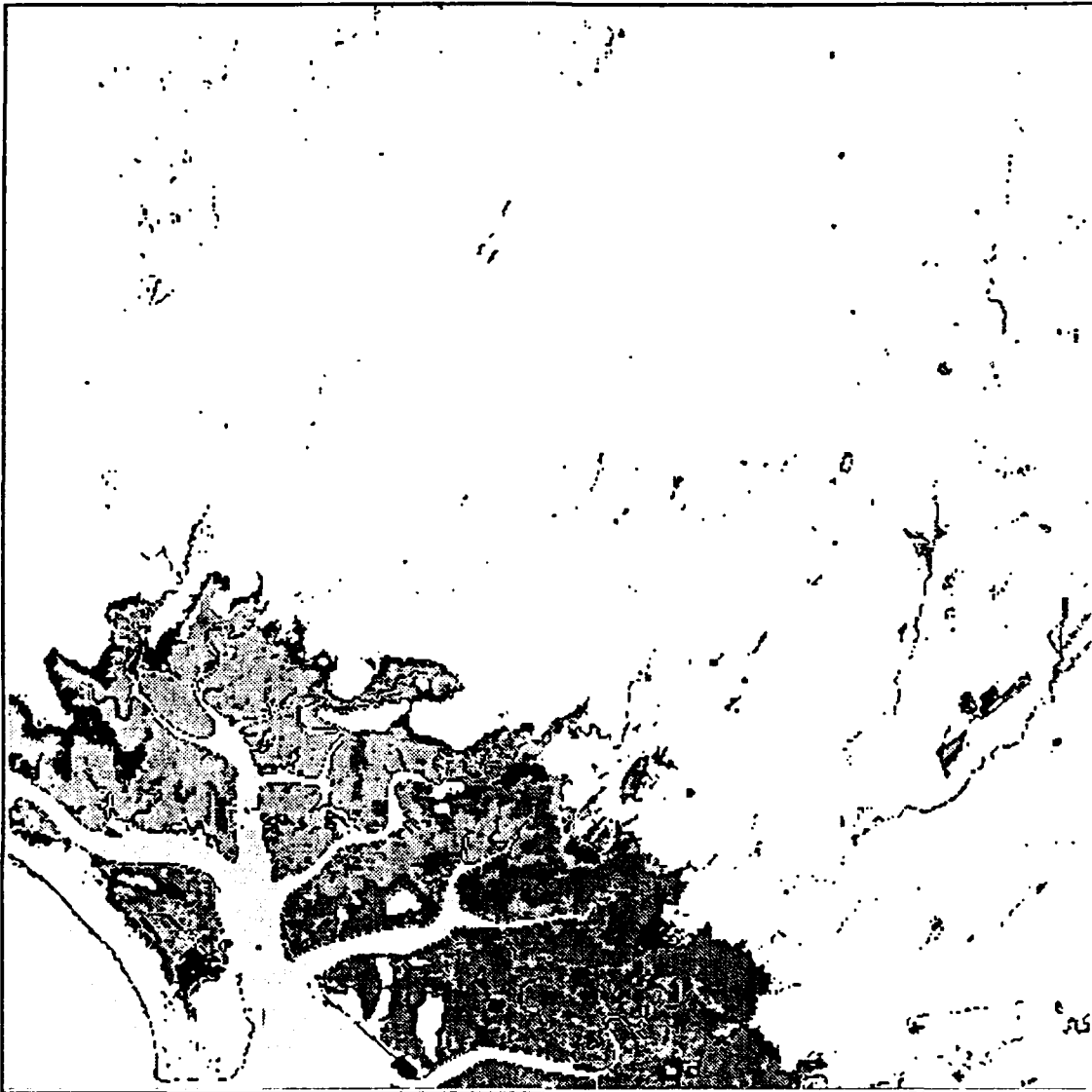
Figure 10. The CORINTO.KMEANS1 Classified Image

It took 12 hours and 11 minutes to reach the a termination threshold of one percent of the pixels changing clusters in an iteration for this classification.

4. The ISOCLASS Algorithm

ISOCLASS generally takes longer to produce results than the other two unsupervised classification algorithms.

ISOCLASS gives the user the most control over cluster statistics, but there is no direct way to estimate the number of clusters which a given set of input parameters is likely to produce. Each new run of the algorithm is, in part, a trial to see if the resulting number of clusters is in the desired range. Experience helps in the selection of input values, but still this only provides a starting point for a trial and error process. Of course, this process also gives the researcher some insight into the spectral structure of the natural clusters present in the image. There is also no completely unambiguous sign of convergence, though there are normally some fairly strong indications.

As seen in Figure 11, the CORINTO.CLASS1 classification result is almost the same as the CORINTO.KMEANS1 classification result, except for the assignment of gray scale values to classes. The same five classes were detected, with the same meanings and most of the same member pixels. There are fewer stream and "unknown" pixels in CORINTO.CLASS1 than in CORINTO.KMEANS1, especially in the northern part of the site.

The minimum value of the pairwise transformed divergence between the five classes was 44.4 between the two mangrove classes. Between the remaining class pairs the minimum value was 95.7.

The time of 27 hours and 52 minutes does not include the time required by several previous attempts. These

Figure 11. The CORINTO.CLASS1 Classified Image

previous attempts were necessary to find appropriate values
for the input parameters and to gain experience in better
estimating "good" input parameters for the ISOCLASS algo-
rithm.

The CORINTO.CLASS2 classification was a continuation
of CORINTO.CLASS1 with a smaller value for the minimum

81

number of pixels allowed in a cluster. The change was from 300 to 20. Although the number of clusters increased from 29 to 48, most of the additional clusters were small. Twelve of the additional 19 clusters had fewer than 300 pixels. Of interest to this study is that the "water boundary" class was split into two classes. One class appears to be the same as described above, a transition from water to mangrove. The other seems to be a transition from water to classes other than mangrove. The water obstacles were still classified as mangrove and water boundary. The other water transition class mainly consisted of coastal pixels that were not near any mangrove.

5. ISOCLASS Followed by MINDIST

Using the MINDIST algorithm on an image that has been classified using ISOCLASS slightly increases the average and minimum values of the transformed divergence, but the classification results for the classes of interest do not appear to be much different. As shown in Figure 12, the CORINTO.CLASS1.MINDIST image has slightly fewer stream and unknown pixels than the CORINTO.CLASS1 image, but there do not appear to be any other differences.

The minimum value of the pairwise transformed divergence for the five classes was 44.0 between the two mangrove classes. Between the remaining class pairs the minimum
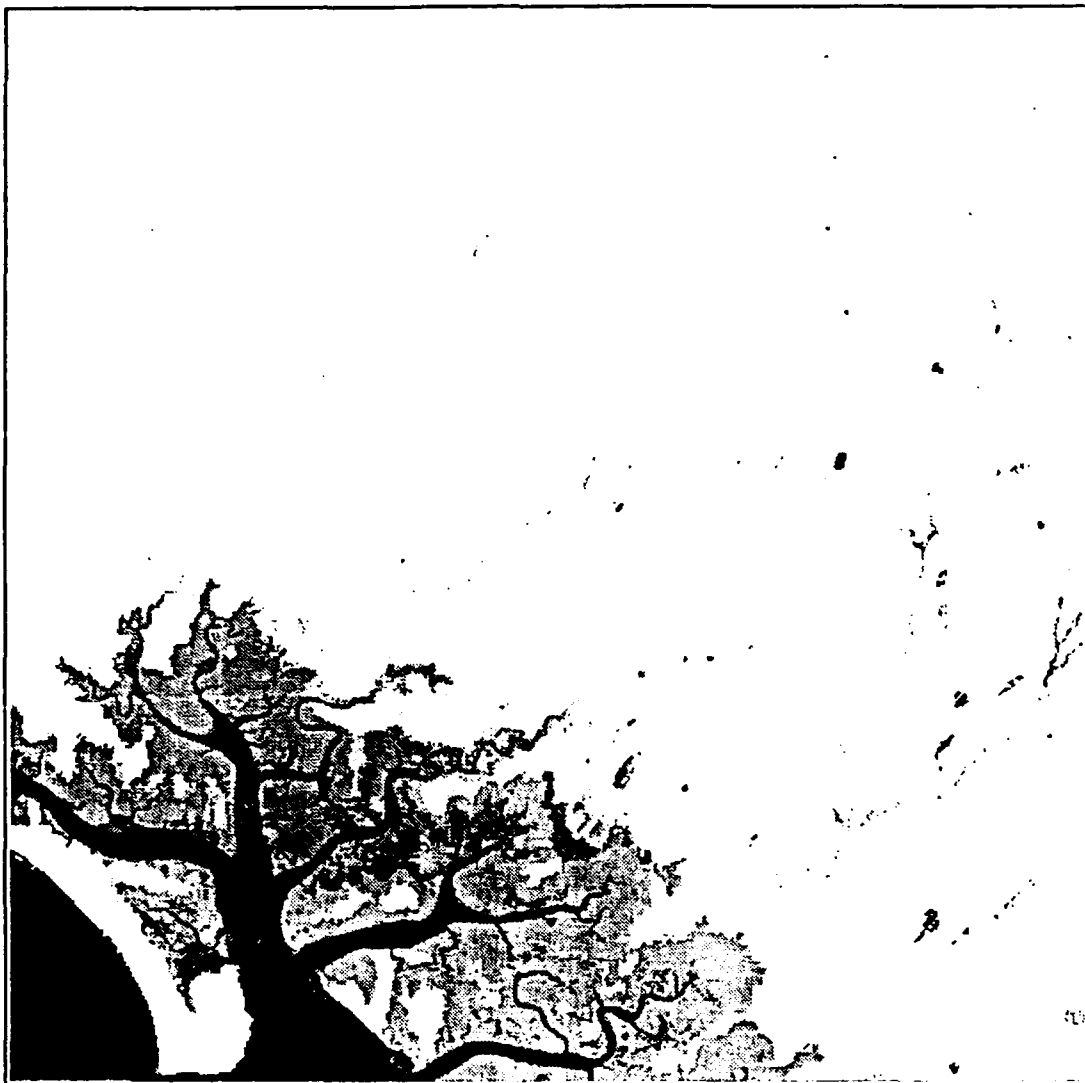
82

Figure 12.   The CORINTO.CLASS1.MINDIST Classified Image

minimum value was 94.6, indicating excellent between-class
statistical separability.

E. CORINTO SITE CLASSIFICATION RESULTS

1. Comments on Class Names

Most of the spectral clusters or classes fall into
one of two general categories: water or mangrove. These two
categories have one or more sub-categories in the various
classification images. Some of these sub-categories appear
to be the result of spectral differences in a single infor-
mation class, while others seem to be transitions between
information classes, since they predominantly occur at the
boundaries between the information classes. The transition
class between water and mangrove has been called "water
boundary," and the transition class between mangrove and the
rest of the image has been called "land boundary."

There was, in most images, no separate "stream"
class. Pixels for the potential water obstacles were clas-
sified as being water, mangrove, or one of the transition
classes. Other portions of streams detected were usually
classified as mangrove or the land boundary class. "Stream
pixel" has been used as a descriptive term identifying
pixels along streams and normally does not identify a sepa-
rate spectral class.

2. Use of the KMEANS Algorithm

The KMEANS algorithm was used for most of the clas-
sifications made during this study. From the comparison of
clustering algorithms above, KMEANS was more accurate than

84

HINDU, even when post-processed using MINDIST. It was also faster than ISOCLASS with about the same accuracy.

3. The COR457.KMEANS1 Classification Results

Shown in Figure 13, the COR457.KMEANS1 classification had a fairly high minimum value of transformed divergence, 34.40. This classification resulted in five spectral classes for the information classes of interest. In addition to one water and two mangrove classes, there was one class that appeared to be a mixed class containing both mangrove and the entire water boundary class. The other class was a mixed class of land boundary and streams, with streams making up about half of this class. This classification detected by far the most streams, and was the only classification with streams making up such a large percentage of the total number of pixels in any one class.

The three potential water obstacles were assigned to the water boundary/mangrove and the northernmost (black) mangrove classes.

The minimum value of the pairwise transformed divergence for the five classes was 69.8 between the two mangrove classes. Between the remaining class pairs the minimum value was 95.7.

4. The RATIO.KMEANS1 Classification Results

The RATIO.KMEANS1 classification has a very high minimum value for the transformed divergence, 69.25. This
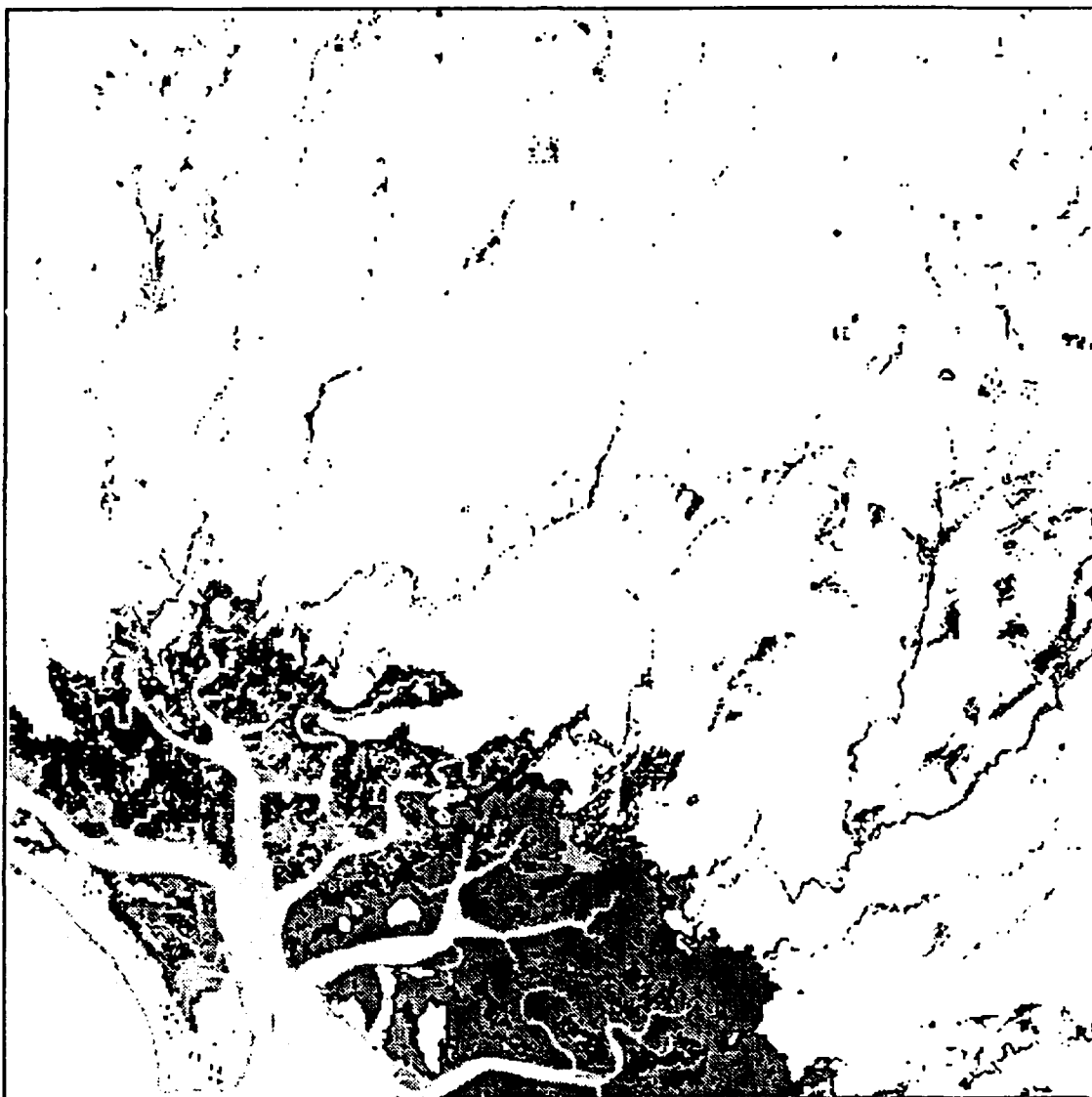
Figure 13. The COR457.KMEANS1 Classified Image

classification, shown in Figure 14, resulted in eight spec-
tral classes for the information classes of interest. This
was the greatest number of spectral classes for any classi-
fication of the CORINTO site. There was one water class,
three water boundary classes, three mangrove classes, and
one land boundary class.

The three potential water obstacles had pixels that
were assigned to two of the water boundary classes and to
all three of the mangrove classes.

Figure 14.   The RATIO.KMEANS1 Classified Image

For some reason, the streams detected in most of the other classifications were not detected here, but the stream in the northeast (upper right) part of the site was detected here and not shown in most of the other classifications.

The minimum value of the pairwise transformed divergence for the five classes was 71.1 between the two larger mangrove classes. Between the remaining class pairs, the minimum value was 91.1.

5. The RATIO.KMEANS8 Classification Results

To test if the information classes identified in the above classifications were spectrally homogeneous enough to classify the broad information classes with fewer spectral classes, the RATIO band set was classified with the KMEANS algorithm into eight spectral classes. The resulting classified image, shown in Figure 15, had three spectral classes of interest: one water class, one mangrove class, and one water boundary class.

The potential water obstacles were classified into the water boundary and mangrove classes.

The main difference between this classification result and the previous one, other than the different number of classes, is that here almost no stream pixels were detected.

Figure 15.   The RATIO.KMEANS8 Classified Image

The minimum value of the pairwise transformed diver-
gence between the three classes was 99.99, indicating excel-
lent spectral separability.

6.   The RATIO12.KMEANS8 Classification Results

To test the possible utility of a two-band-ratio set
for detecting water obstacles, the three two-band combina-

tions of the available ratios were classified using the KMEANS algorithm. Shown in Figure 16, the two-band set containing the (band 1)/(band 5) and (band 2)/(band 5) ratios was the only one with a large minimum value of transformed divergence. Again, there are three spectral classes of interest: one water class, one mangrove class, and one water boundary class.

The potential water obstacles were classified into the water boundary and mangrove classes. There were also more pixels of unknown information classes assigned to one of the three spectral classes.

The minimum value of the pairwise transformed divergence between the three classes was 99.99, indicating excellent spectral separability.

7. The CORPCA.KMEANS3 Classification Results

Since the desired number of classes is an input to KMEANS, it is possible that the number of clusters created is greater than the number of spectrally distinct classes. This could result in a low minimum value of the transformed divergence. With this possibility in mind, the principal component transformation classification results and the tasseled cap transformation classification results were examined.

The CORPCA.KMEANS3 classification, shown in Figure 17, had a low minimum value of transformed divergence, 5.00.

90

Figure 16. The RATIO12.KMEANS8 Classified Image

This classification resulted in four spectral classes of interest: one water class, two manjrove classes, and one land boundary class.

The classified image is very similar to the CORINTO.KMEANS1 and the CORINTO.CLASS1 results.

91

Figure 17. The CORPCA.KMEANS3 Classified Image

The three potential water obstacles were assigned primarily to the two mangrove classes, though a few pixels were assigned to the water class.

The minimum value of the pairwise transformed divergence for the four classes was 60.2 between the two mangrove classes. For the remaining class pairs, the minimum value

was 67.3 between the lighter (more southernmost) mangrove class and the land boundary class.

8. The CORTC.KMEANS1 Classification Results

The CORTC.KMEANS1 classification had a low minimum value of transformed divergence, 5.00. This classification, shown in Figure 18, resulted in six spectral classes for the information classes of interest: one water class, one water boundary class, three mangrove classes, and one land boundary class.

The three potential water obstacles were assigned primarily to the water boundary and two of the mangrove classes.

The minimum value of the pairwise transformed divergence between the six classes was 52.9. Several of the other class pairs had values of transformed divergence below 75.0. In spite of the low values of transformed divergence, these results are similar to the other classifications examined here.

9. Summary of CORINTO Site Classification Results

All of the algorithm and band combinations examined were able to detect the three potential water obstacles identified on the map of the CORINTO site. Most of the band and algorithm combinations used detected more than one mangrove class and a transition or boundary class between water and mangrove and between mangrove and the rest of the
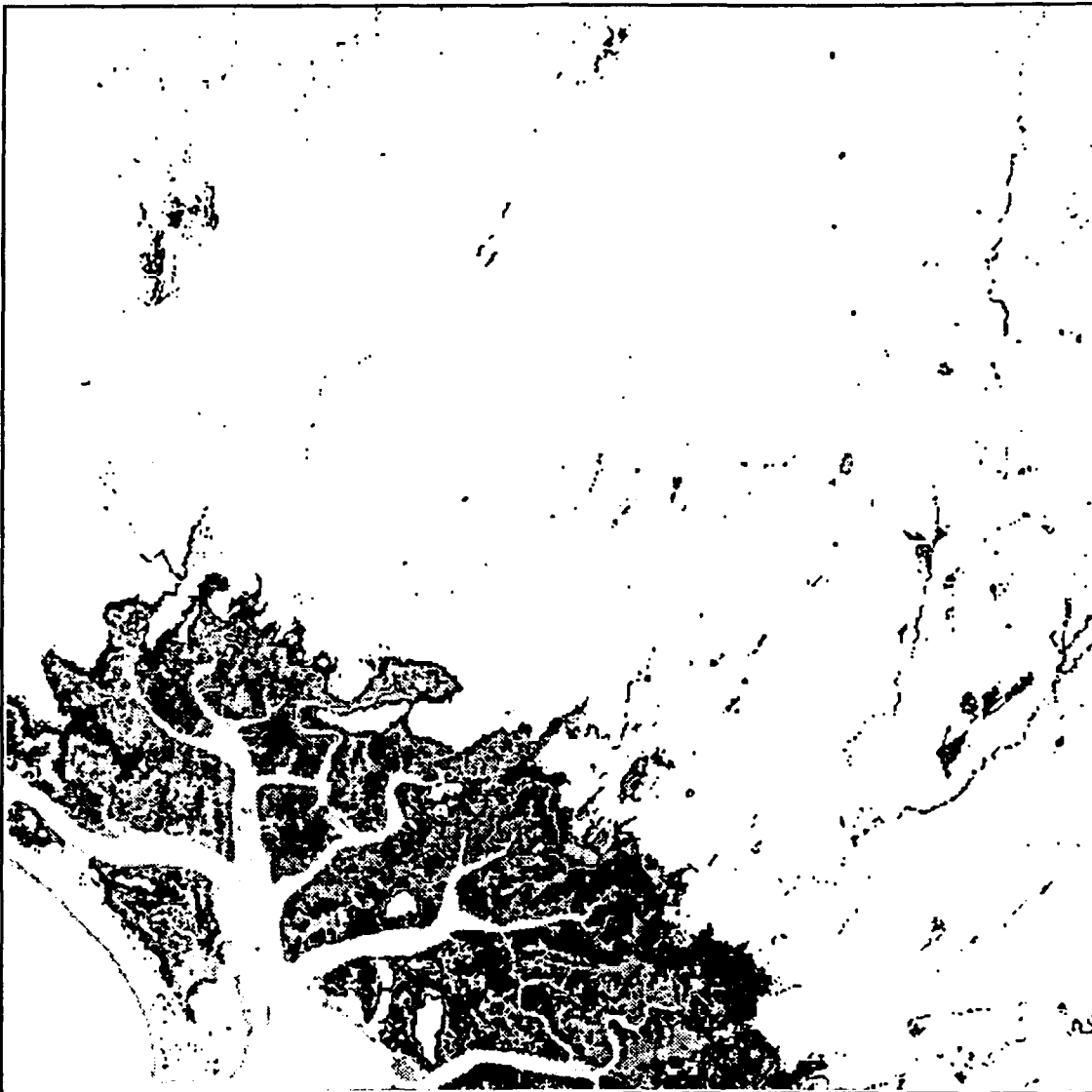
Figure 18.   The CORTC.KMEANS1 Classified Image

site.   Because of the limited ground information available,
it is not known if these additional spectral classes corre-
spond to terrain of significantly different obstacle value.

All of the band subsets and band transformations
detected the potential water obstacles, so a reduction in
the dimensionality of the classification problem is possi-

94

ble. Portions of the water obstacles were classified in the water boundary class and, in a few classifications, in the water class. It is likely that there was enough open water in these areas to affect the sensor readings.

Most of the classifications also detected portions of the streams in the study site, with the (4 5 7) band combination performing best at stream detection. Since most of the streams (other than the water obstacles) were classified in the mangrove or the land boundary classes, it is likely that this classification was due to the effect of the stream's water on the sensor response.

The minimum value of the transformed divergence does not appear to be a valid criteria for selecting band sets here. Since most of the spectral classes in the classified images were not used, separation of the hardest-to-separate spectral class may be of no consequence to the analysis. Two classified images were examined that had low minimum values of transformed divergence (CORPCA.KMEANS3 and CORTC. KMEANS1). However, the lowest value of transformed divergence between spectral classes of interest in these images was greater than in many of the classified images with much greater minimum values of transformed divergence. This is shown in Table 14, which shows both the minimum value of transformed divergence for the entire image and the minimum value of transformed divergence for the information classes of interest.

Table 14.   MINIMUM VALUES OF TRANSFORMED DIVERGENCE

Classified Image name	D^T_{MIN} Overall	D^T_{MIN} Between classes of interest
CORINTO.CLASS1	33.93	44.4
CORINTO.CLASS1.MINDIST	40.09	44.0
CORINTO.KMEANS1	41.95	41.95
CORPCA.KMEANS3	5.00	60.2
COR457.KMEANS1	34.40	69.8
CORTC.KMEANS1	5.00	52.9
RATIO.KMEANS1	69.25	71.1
RATIO.KMEANS8	82.22	99.99
RATIO12.KMEANS8	65.73	99.99
CORINTO.HINDU3	58.90	96.3
CORINTO.HINDU3.MINDIST	56.09	91.7

F.   MALP SITE CLASSIFICATION RESULTS

The results for the MALP site were mixed. Since the results for all of the classifications were similar, only a few will be examined here.

1. The MALP.KMEANS8 Classification Results

The MALP.KMEANS8 classification had the greatest values of both the minimum and average transformed divergence of all of the classifications in Table 12, 94.57 and 99.34, respectively.

Figure 19 shows all eight classes of the MALP.KMEANS8 classified image. Comparing Figure 19 to Figure 6, the map overlay of the MALP site, one finds that the woodland area in the center of the site and extending to the northeast (upper right) is well defined, as are portions of the woodland in the southern part of the site. The rest of the vegetation classes of interest are confused with the

96

rest of the site. This confusion of classes holds for all of the other classification results for this site. Woodland and scrub were generally not distinguishable as distinct classes, either.

Figure 19. The MALP.KMEANS8 Classified Image

Figure 20 shows the two classes that make up most of
the central woodland. The darker class also makes up a
portion of the woodland in the southern part of the site, in
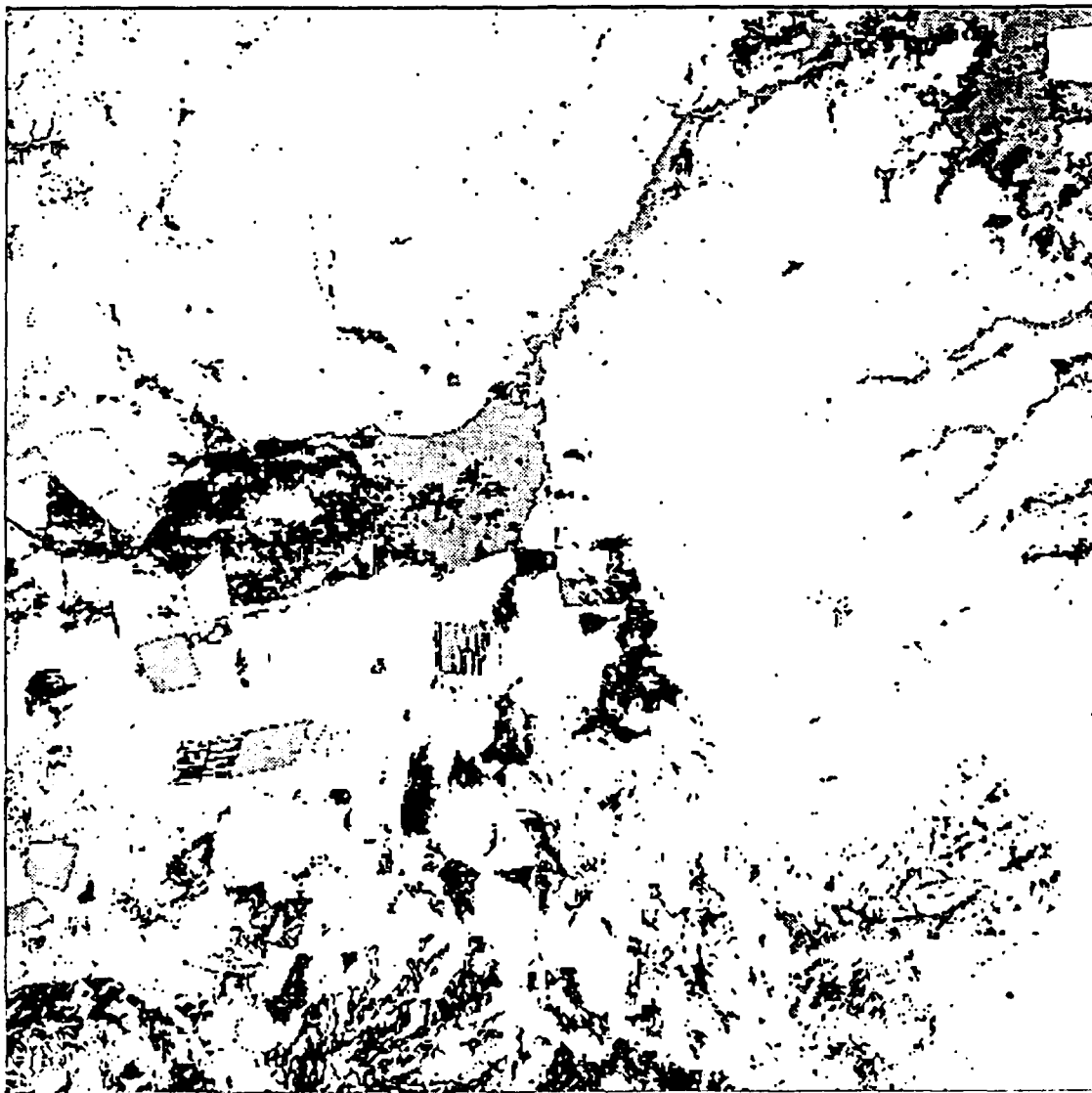addition to some of the scrub in that part of the site. The

Figure 20.   Woodland/Scrub Classes in the MALP.KMEANS8
Classified Image

lighter class contains some areas to the southwest of the central woodland as well as much of the central woodland. To some extent, this occurred in all of the classification results for this site. From the ground information available, there is no clear explanation for this.

2. The MALP.KMEANS2 Classification Results

Figure 21 shows the six classes that predominantly fell within the boundaries of woodland or scrub for the MALP.KMEANS2 classification. These two information classes were not spectrally distinguishable in this classification, so they were treated as one category.

In Figure 21, it can be seen that the central woodland area is again well-distinguished, as are the woodland and scrub in the southern part of the site. More of the scrub in the northwest part of the site was included in these spectral classes than in MALP.KMEANS8. There is still a significant amount of misclassification in these spectral classes, based on a manual comparison with the 1:50,000 scale maps.

Figure 22 shows the five mixed spectral classes, i.e., that contained large portions of both the woodland/scrub and the unknown parts of the site. The same mixed classes are also consistently mixed in the other classifications.
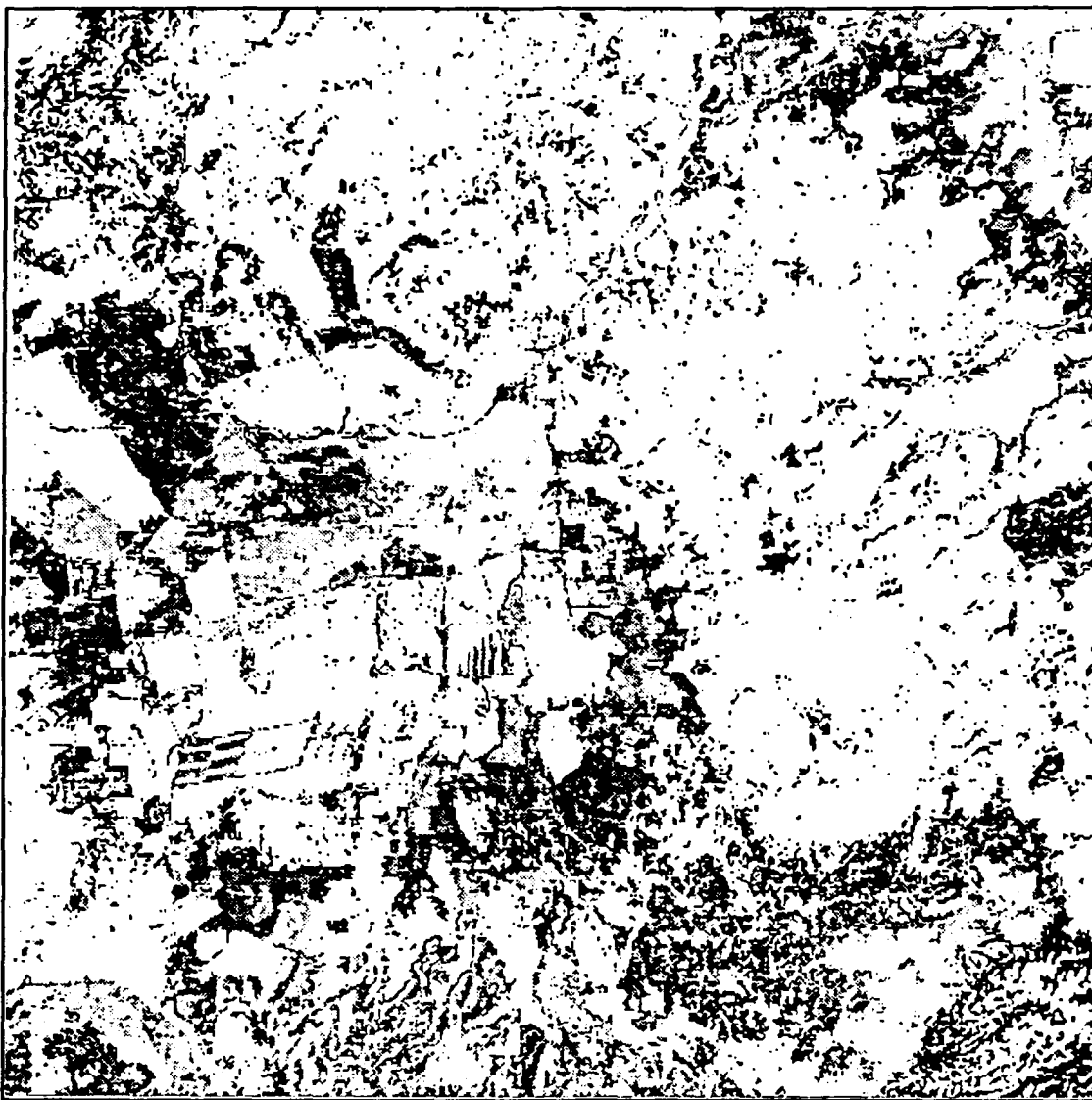
Figure 21.   Woodland/Scrub Classes in the MALP.KMEANS2
Classified Image

3. The MALP.CLASS4 Classification Results

Figures 23 and 24 show the five woodland/scrub and
the six mixed classes of the MALP.CLASS4 classification,
respectively. Again, the central woodland area and much of
the southern woodlands were in the woodland/scrub classes,
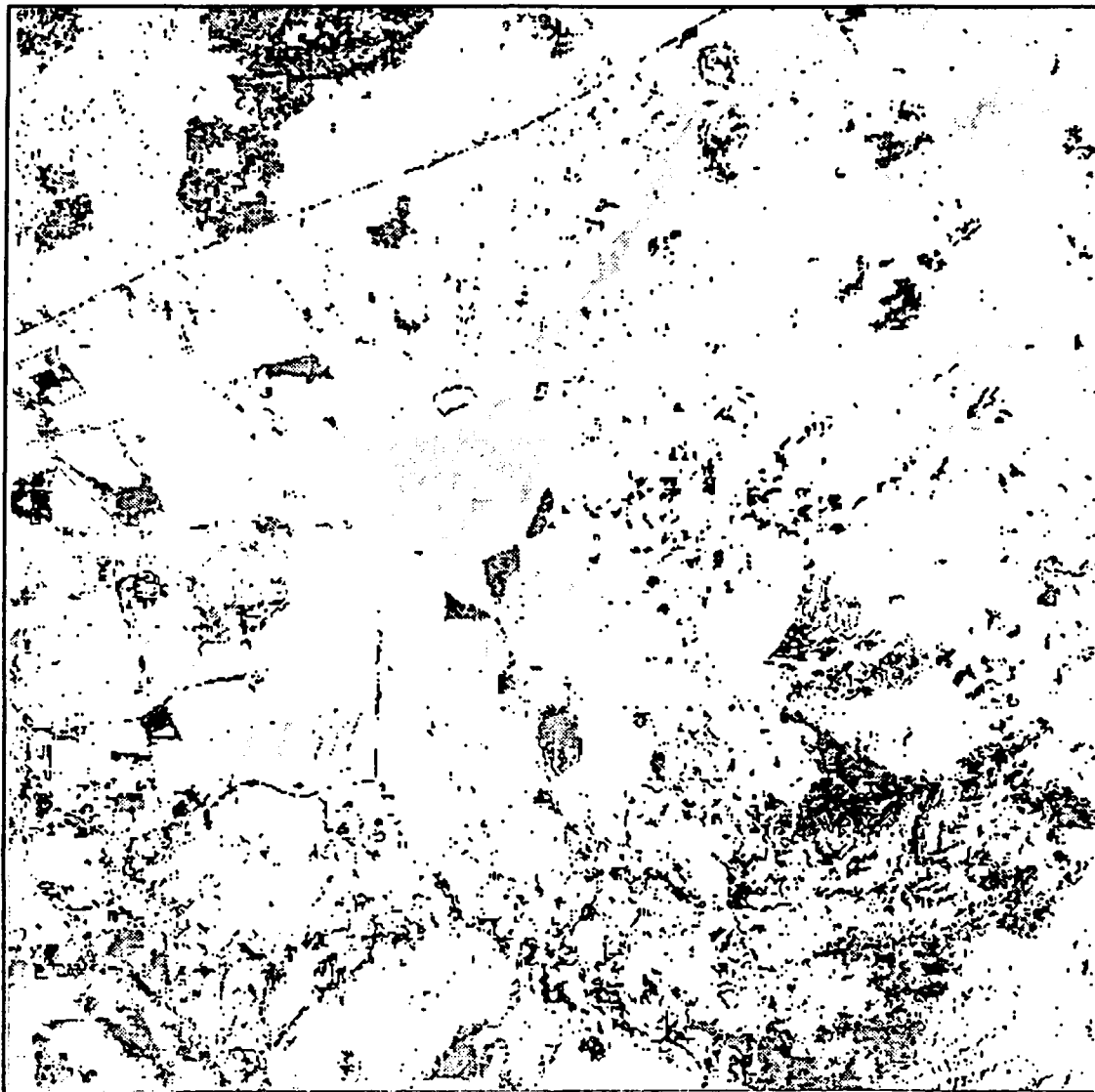
Figure 22.   Mixed Classes in the MALP.KMEANS2 Classified Image

along with some of the southern scrub areas.   Though a small

amount of the northwestern scrub was in these classes, most

of the scrub in that area shows in Figure 24, where it is

mixed with unknown parts of the site.

The spectral differences within the woodland and

scrub classes in this site may be due to differences in the

Figure 23.   Woodland/Scrub in the MALP.CLASS4 Classified Image

value of the cover and concealment afforded by the different

spectral classes.   The classes shown in Figure 23, for

example, could provide good cover and concealment, while the

classes in Figure 24 could be useless as cover or conceal-

ment.   The differences could also be due to some other

reason.   The difficulty in separating woodland from scrub

102

Figure 24. Mixed Classes in the MALP.CLASS4 Classified Image

and scrub from the rest of the site indicate that better

ground information is necessary before any definite conclu-

sions can be drawn about the ability of Landsat TM imagery

to identify suitable vegetated areas of cover and conceal-

ment.

V. CONCLUSIONS

A. EVALUATION OF THE ALGORITHMS USED

Of the classification algorithms examined in this study, only the HINDU algorithm produced a highly inaccurate result. After post-processing with the MINDIST algorithm, the HINDU classification results were comparable to the results of the other classification algorithms.

Both the KMEANS and the ISOCLASS algorithms found more spectral classes in the mangrove area than did the HINDU algorithm. They also found what appear to be transition regions between information classes. The "land boundary" transition class was useful for identifying streams. If these additional spectral classes provide more or better information about terrain conditions, then KMEANS and ISO-CLASS would be superior to HINDU. If not, the speed of the HINDU-MINDIST combination would clearly be superior because of the much faster processing time.

Post-processing the results of the ISOCLASS algorithm with the MINDIST algorithm was shown not to be worthwhile.

B. DETECTION OF POTENTIAL WATER OBSTACLES

All of the algorithm and band combinations examined were able to detect the three potential water obstacles identified on the map of the CORINTO site. Most of the band and

104

algorithm combinations used detected more than one mangrove class and a transition or boundary class between water and mangrove and between mangrove and the rest of the site. Because of the limited ground information available, it is not clear if these additional spectral classes correspond to terrain of significantly different obstacle value.

All of the band subsets and band transformations detected the potential water obstacles, so a reduction in the dimensionality of the classification problem is possible. Portions of the water obstacles were classified in the water boundary class and, in a few classifications, in the water class. It is likely that there was enough open water in these areas to affect the sensor readings.

Most of the classifications also detected portions of the streams in the study site, with the (4 5 7) band combination performing best at stream detection. Since most of the streams (other than the water obstacles) were classified in the mangrove or the land boundary classes, it is likely that this classification was due the effect of the stream's water on the sensor response.

The minimum value of the transformed divergence does not appear to be a valid criteria for selecting band sets here. Since most of the spectral classes in the classified images were not used, separation of the hardest-to-separate spectral class may be of no consequence to the analysis. Two classified images with low minimum values of transformed

105

divergence (CORPCA.KMEANS3 and CORTC.KMEANS1) were examined. As shown in Table 14, the minimum value of the transformed divergence between "spectral classes of interest" in these two images was greater than it was for many of the other classified images examined in this study.

C. DETECTION OF VEGETATION PROVIDING COVER AND CONCEALMENT

Some portions of the MALP site were spectrally separable as belonging to the vegetation classes identified from the map of the site (see Figures 5 and 6). However, much of the two information classes of woodland and scrub belonged to mixed spectral classes. These mixed spectral classes also included large areas outside of the woodland and scrub boundaries, according to the map reference.

These mixed spectral classes could be the result of different species or mixes of species of vegetation in the different parts of the site. They could also be the result of different inaccuracy in the reference map, effects of the dry season on different species or parts of the site, or they could be the result of other reasons.

Given the above possibilities, it is apparent that the information classes, woodland and scrub, are very broad. The likelihood of a homogeneous woodland or scrub class, even over the small area of the site (14.6 x 14.6 km) is not large. This is especially true when human activity is present and when it is related to the cover and concealment

value of the vegetation in the area. Better ground information is necessary before any firm conclusions can be made about evaluating vegetative cover and concealment with Landsat TM imagery.

Most of the classified images with eight clusters had significantly greater minimum values of transformed divergence than the corresponding classified image with more (normally 23) clusters. However, the images with more clusters appear to better separate the classes of interest. This is probably because the classes of interest are not spectrally well-separated, so it is not appropriate to use the transformed divergence measure under these circumstances (i.e., to rank unsupervised classification results).

D. SUMMARY

1. Primary Research Question

The primary research question examined in this study was: can unsupervised pattern recognition algorithms be effectively used on Landsat thematic mapper imagery to perform parts of the terrain analysis step of the Intelligence Preparation of the Battlefield process? Specifically, the study focused on water obstacles and cover and concealment provided by vegetation.

It appears that some aspects of terrain analysis can be performed using the methods examined in this study. Though further research is needed to validate and extend the

results, these methods may make possible rapid, current, large area terrain analysis, at least for certain terrain features.

2. CORINTO Site Summary of Results

All of the unsupervised pattern recognition algorithms and all of the band combinations examined were able to detect all three of the potential water obstacles identified from the map of the CORINTO site, so it appears that water obstacles can indeed be detected using these methods. The HINDU algorithm followed by the MINDIST algorithm provided the fastest acceptable classification of the CORINTO site, where "acceptable" is a qualitative judgment based on comparing the classified image with the map overlay of Figure 7. This assumes that there is no significant obstacle information added by the additional spectral classes in the other classified images, an assumption which could be wrong. Better ground reference information is necessary to determine if these additional spectral classes add information about obstacles, and thus to determine which is the "best" classification algorithm.

The simplest method of data reduction examined, band subsets, provided acceptable classification results based on a manual comparison with the map overlay of Figure 7. Therefore, it is probably not necessary to use any of the other more complicated and time-consuming methods of reduc-

tion of dimensionality examined in this study to detect water obstacles. Band subsets, using the (4 5 7) band combination, also provided the best classification of the streams in the site.

3. MALP Site Summary of Results

All of the band combinations examined had similar, mixed results. Much of the two information classes of interest, woodland and scrub, belonged to mixed spectral classes. Since the cover and concealment value of the vegetation in these two information classes was not known, better ground information is necessary before any firm conclusions can be made about evaluating vegetative cover and concealment with Landsat TM imagery.

4. Evaluation of Statistical Separability

The minimum value of the transformed divergence does not appear to be a valid criteria for selecting band sets here. Since most of the spectral classes in the classified images were not used, separation of the hardest-to-separate spectral class in an image is of no consequence to the analysis.

Most of the spectral classes of interest did have high values of transformed divergence, so the transformed divergence may be of some value in deciding which spectral classes add unique information to the classification re-sults.

E.   DIRECTIONS FOR FURTHER RESEARCH

The greatest limitation on this study was the limited availability of ground reference information. Further study with better ground information is necessary to validate or refute these results, as well as to discover the reason for the mixed results of the attempt to separate vegetative cover and concealment. Also, with better ground information, a better evaluation of the clustering algorithms and band combinations would be possible.

Ideally, one would like to discover and catalog characteristic spectral response patterns for features of interest (e.g., water obstacles) for use with a supervised classification algorithm such as MINDIST. That would eliminate the requirement that the 'water obstacle' class be large enough to be considered to be a separate class by an unsupervised classification algorithm. Supervised clustering algorithms tend to be faster than unsupervised ones, and the post-processing requirement for assigning spectral classes to information classes is reduced or eliminated. More study is necessary to determine if such a spectral response pattern can be identified and applied with an acceptable classification rate.

Militarily 'interesting' areas are often those areas that are different from other areas. For example, military excavations or camouflaged areas will not normally cover a significant portion of a scene, but these areas would be of

110

great military interest. Since these areas may be spectral-
ly different from the remainder of a scene, they may be
'outlier' pixels to the normal scene clusters. Using a
reverse of the MINDIST algorithm's option to eliminate
pixels far from cluster means, one can search for these
outlier pixels. This has the potential to reduce the time
required for an image analyst to identify areas of enemy
activity, especially if it is coupled with some method of
change detection. It could also be useful in identifying
features such as water obstacles in scenes where there is no
large, similar class present in the image.

Figure 25. CORINTO Site, Thematic Mapper Band 1 Image
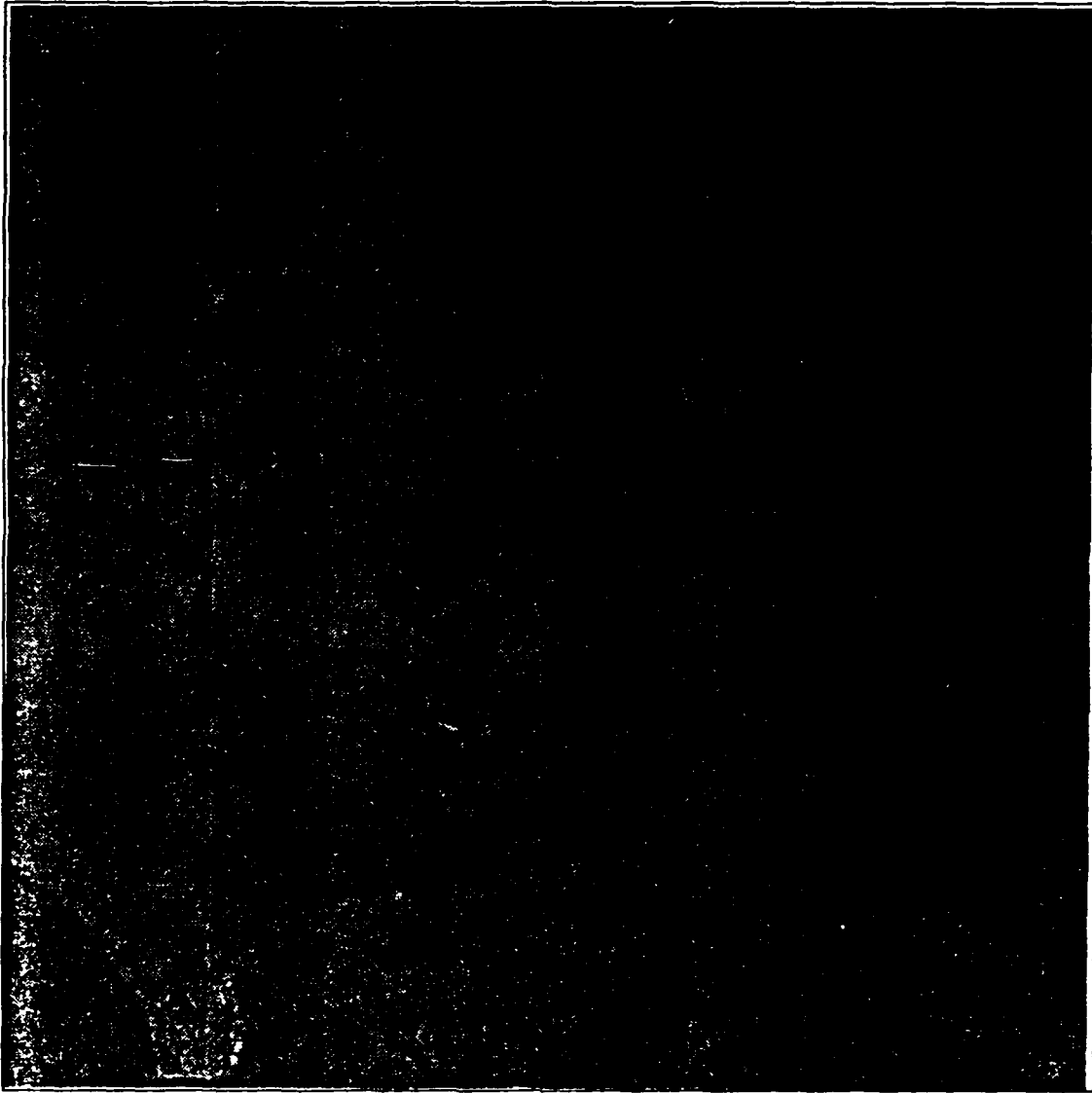
Figure 26.   CORINTO Site, Thematic Mapper Band 2 Image
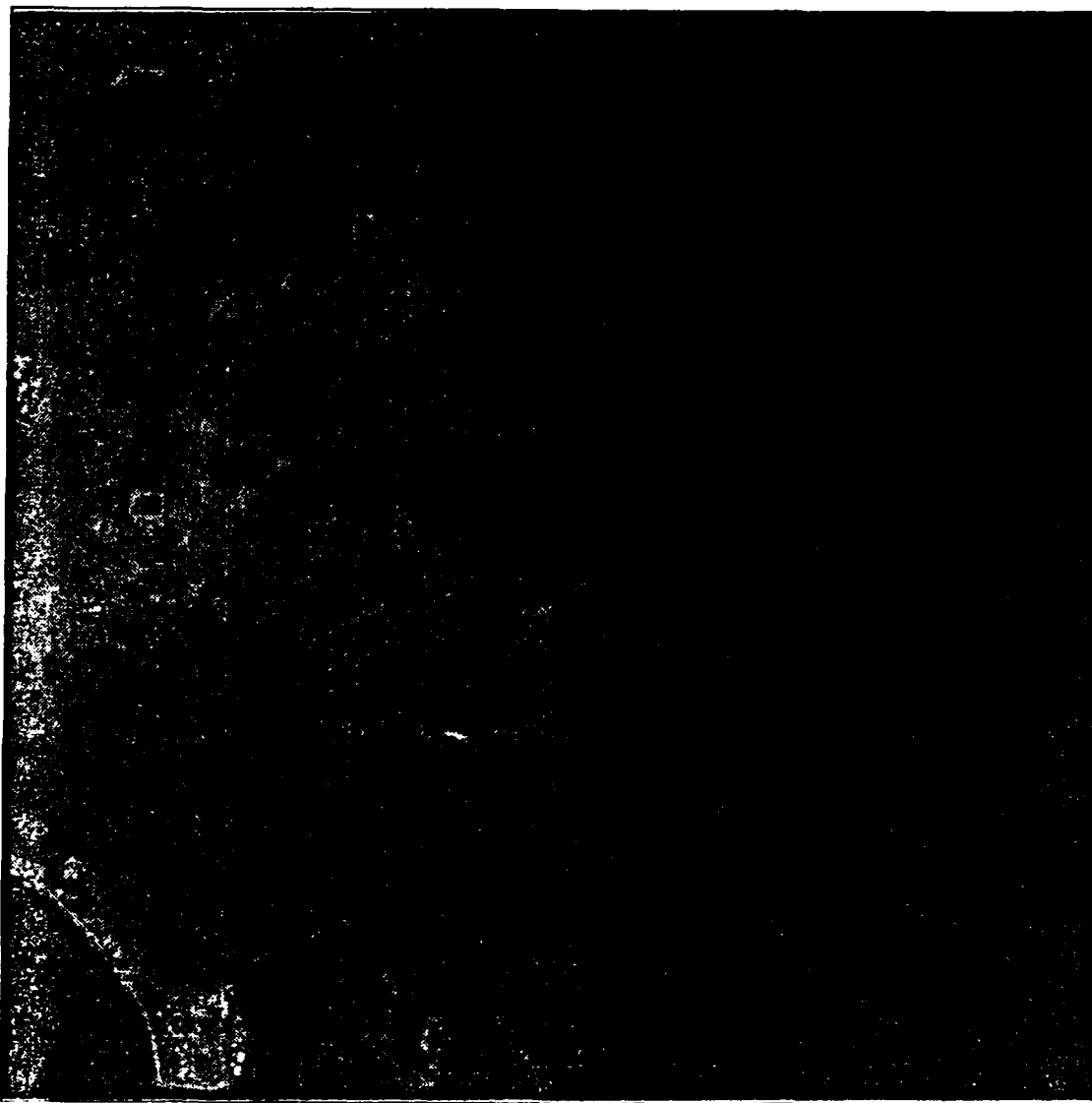
Figure 27. CORINTO Site, Thematic Mapper Band 3 Image
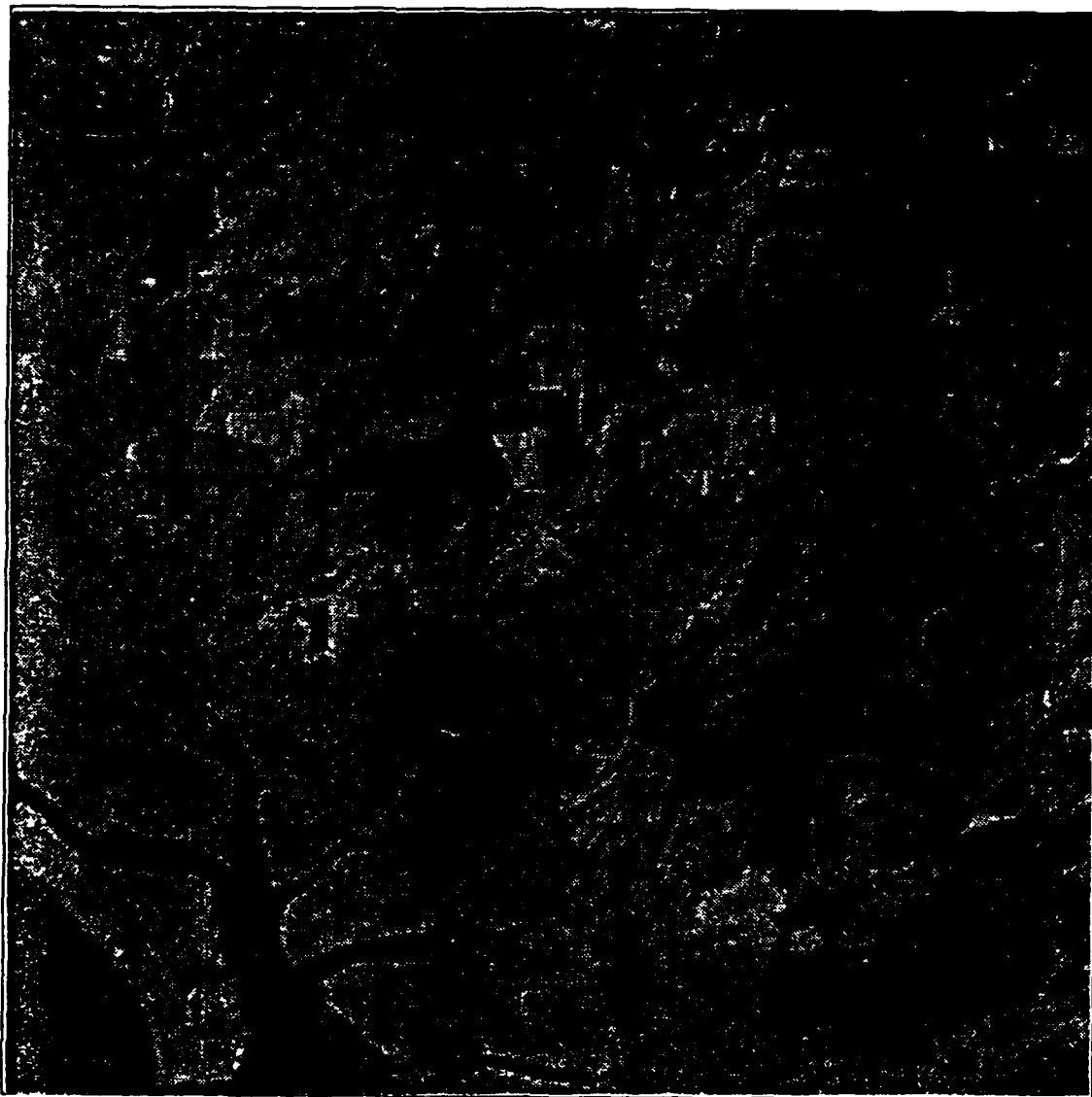
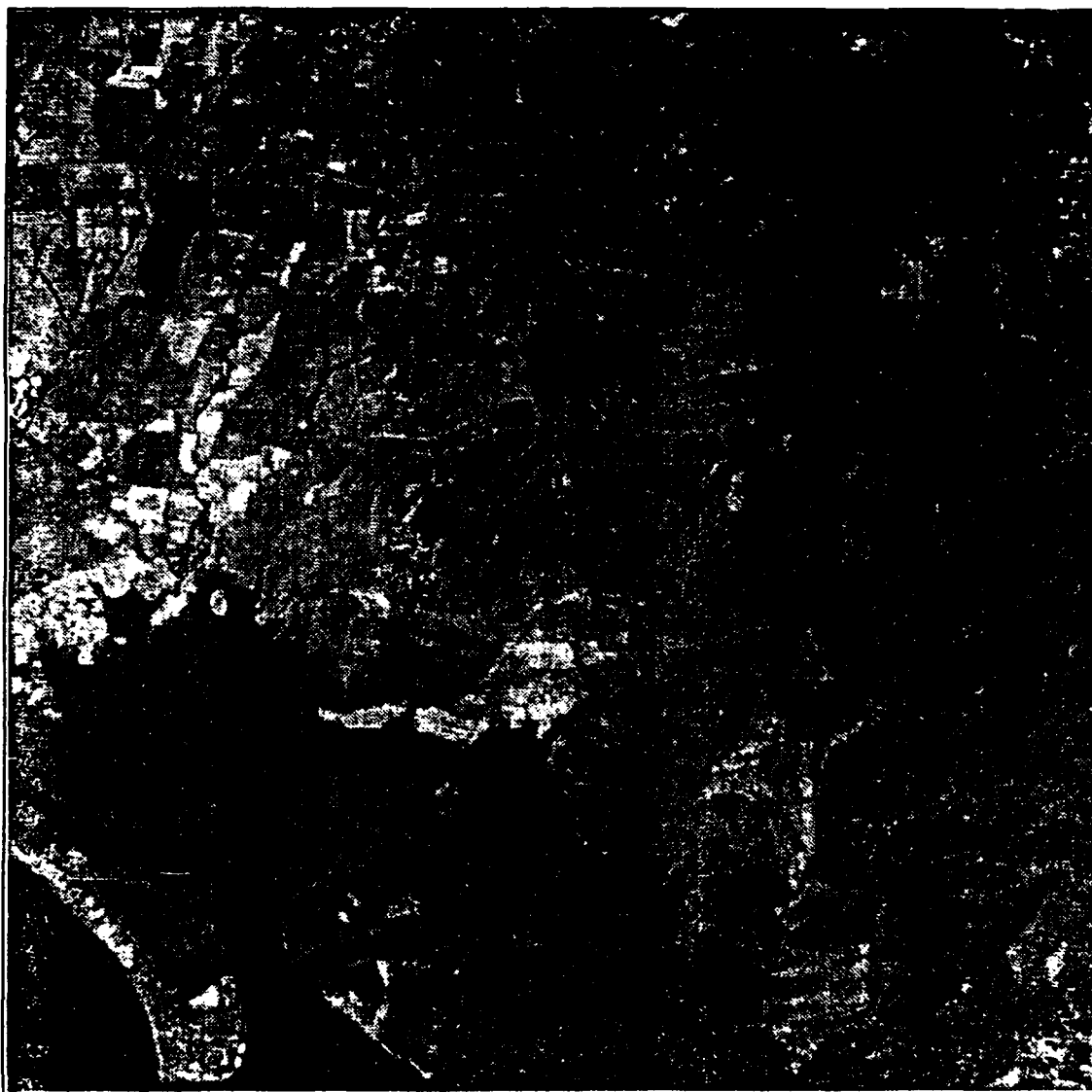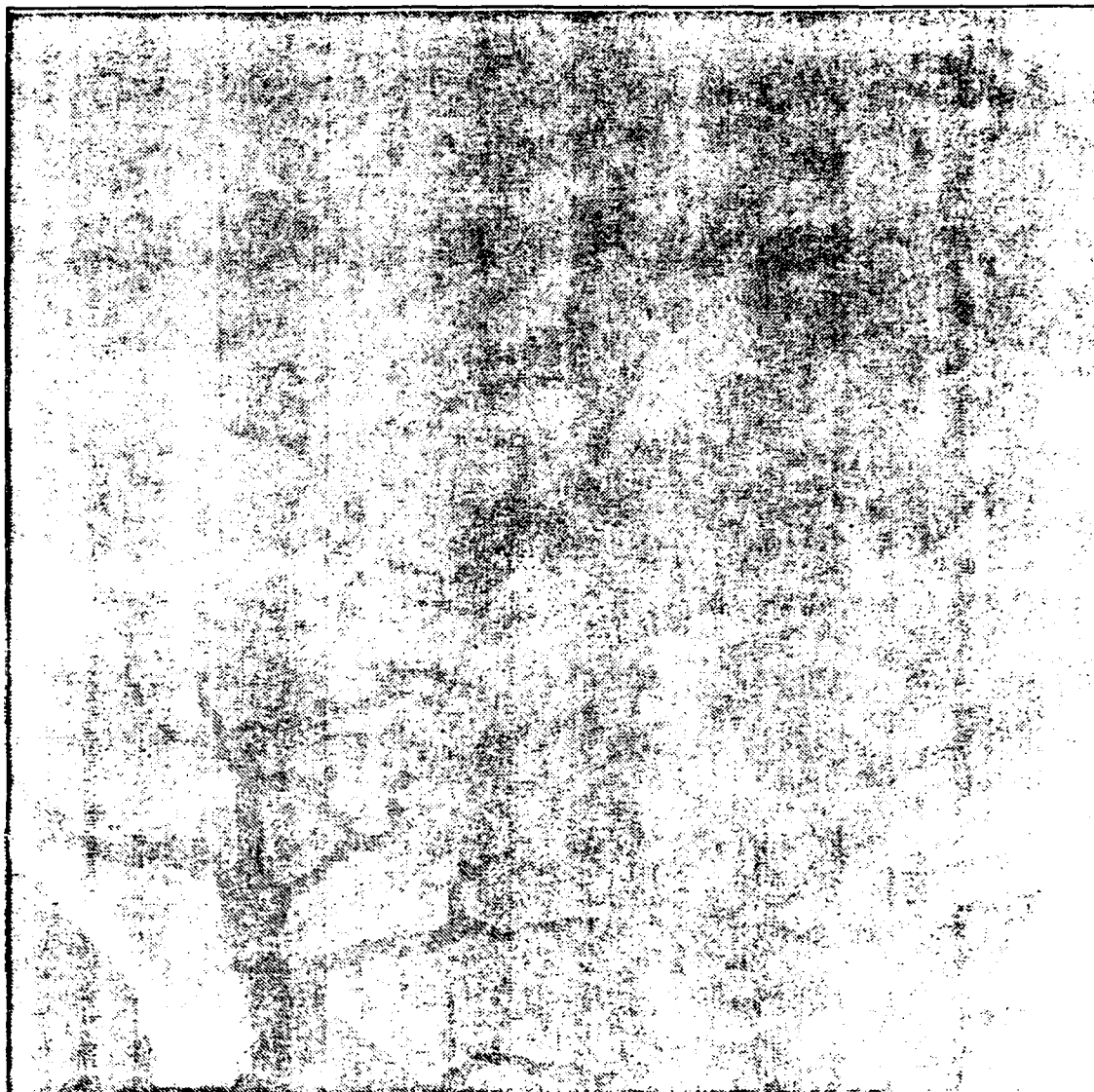Figure 28.   CORINTO Site, Thematic Mapper Band 4 Image

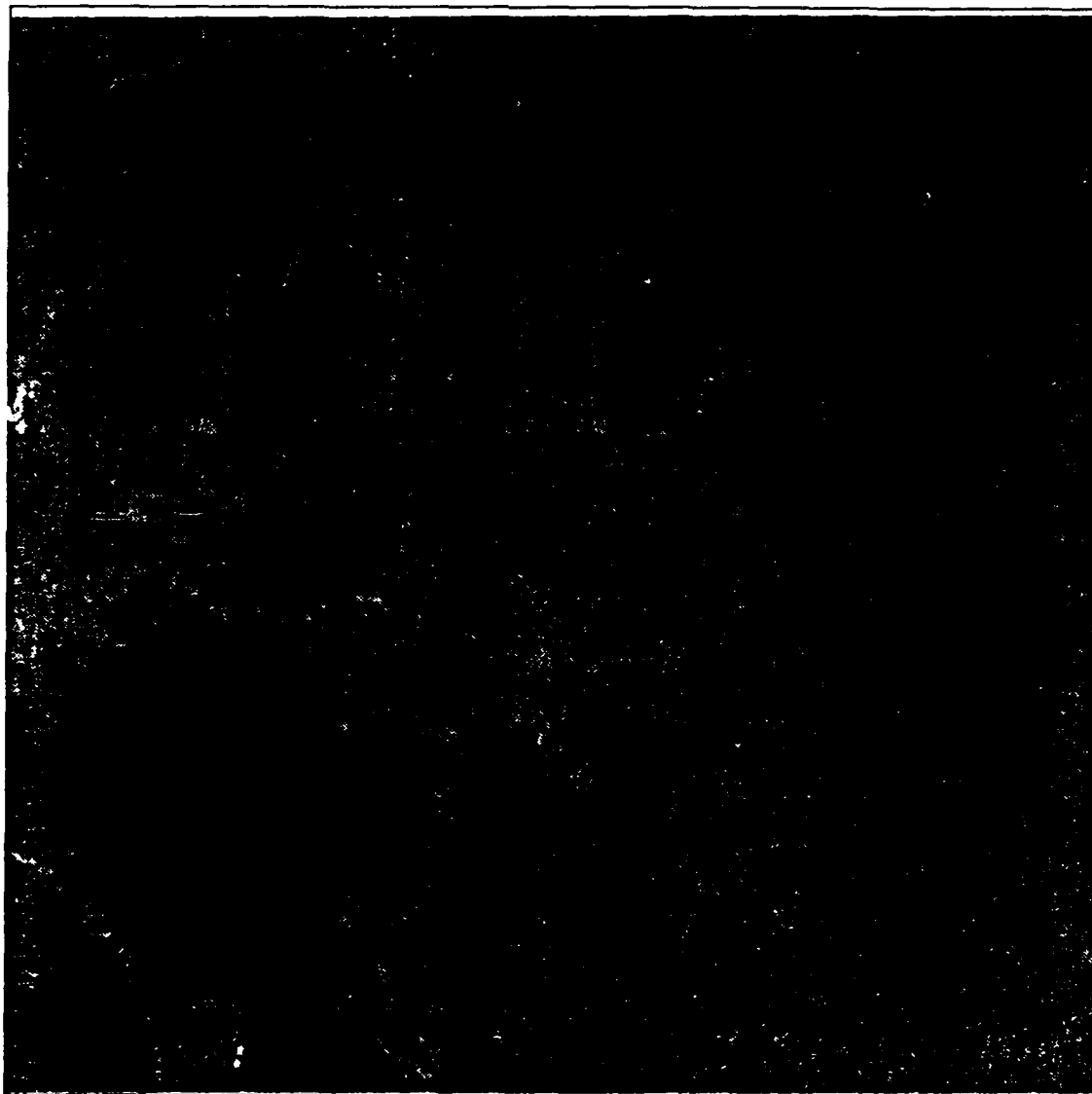**Figure 29.   CORINTO Site, Thematic Mapper Band 5 Image**

Figure 30. CORINTO Site, Thematic Mapper Band 6 Image

117

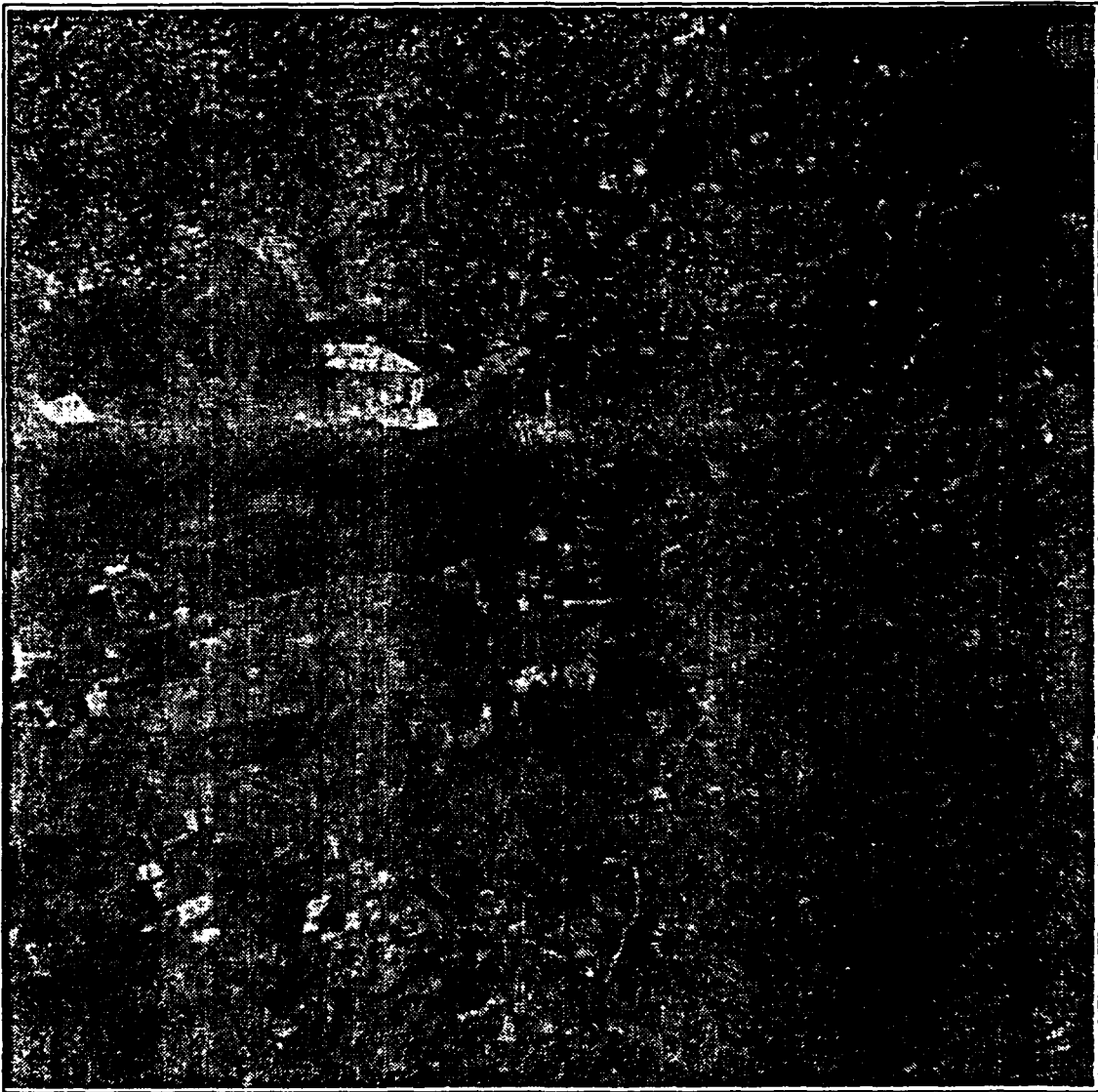Figure 31. CORINTO Site, Thematic Mapper Band 7 Image

118

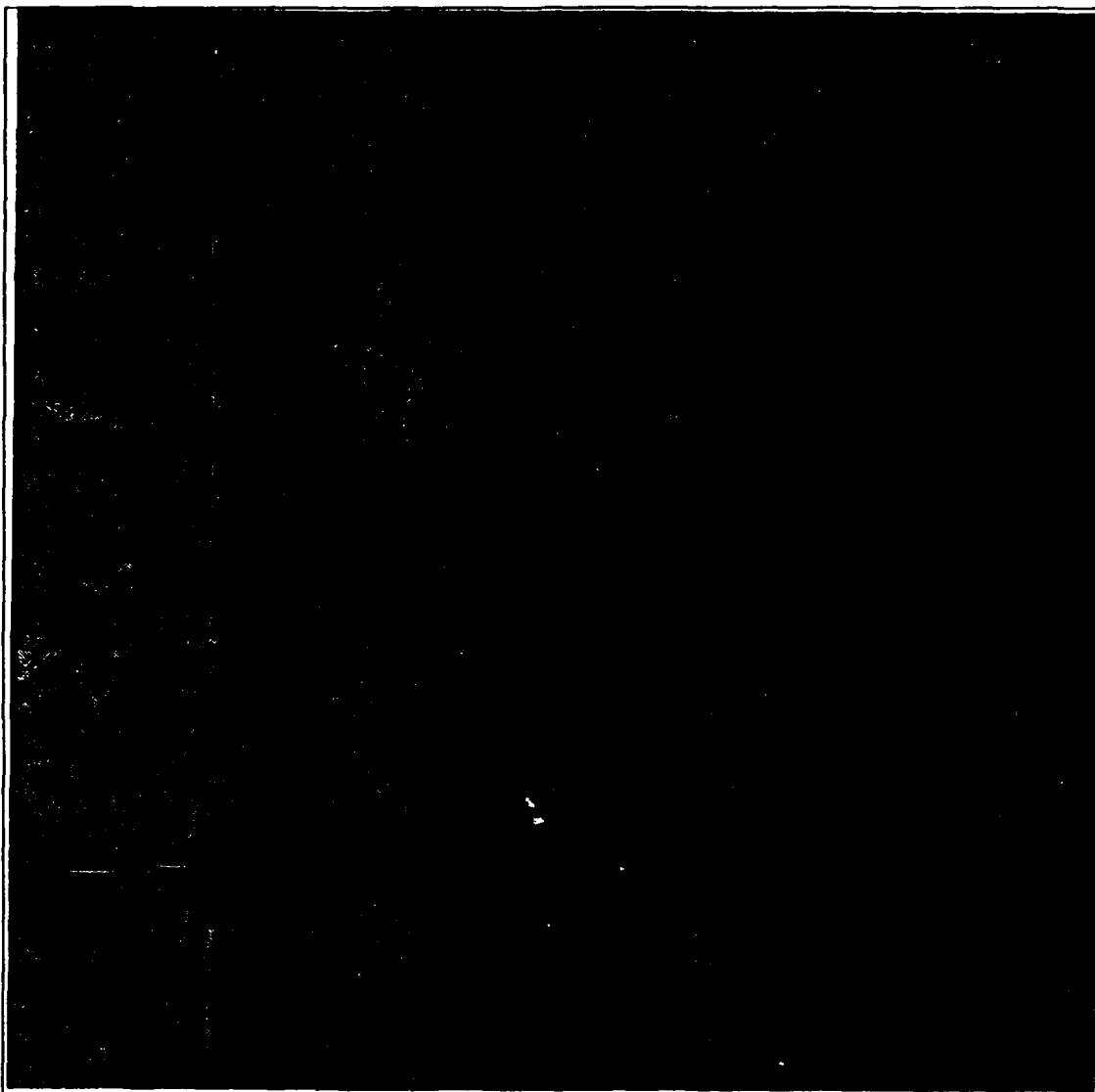Figure 32.   MALP Site, Thematic Mapper Band 1 Image

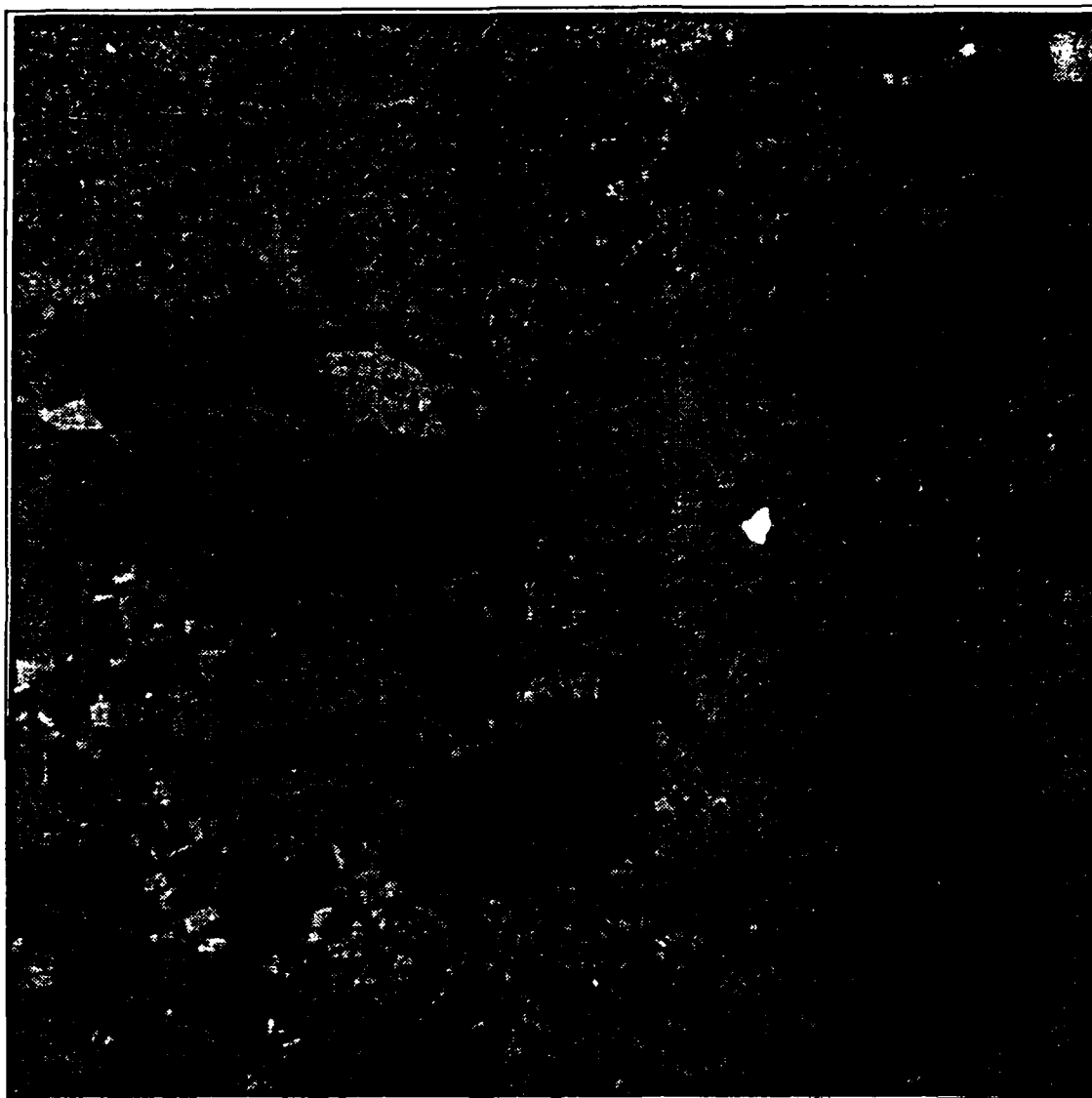Figure 33.   MALP Site, Thematic Mapper Band 2 Image

120

Figure 34. MALP Site, Thematic Mapper Band 3 Image
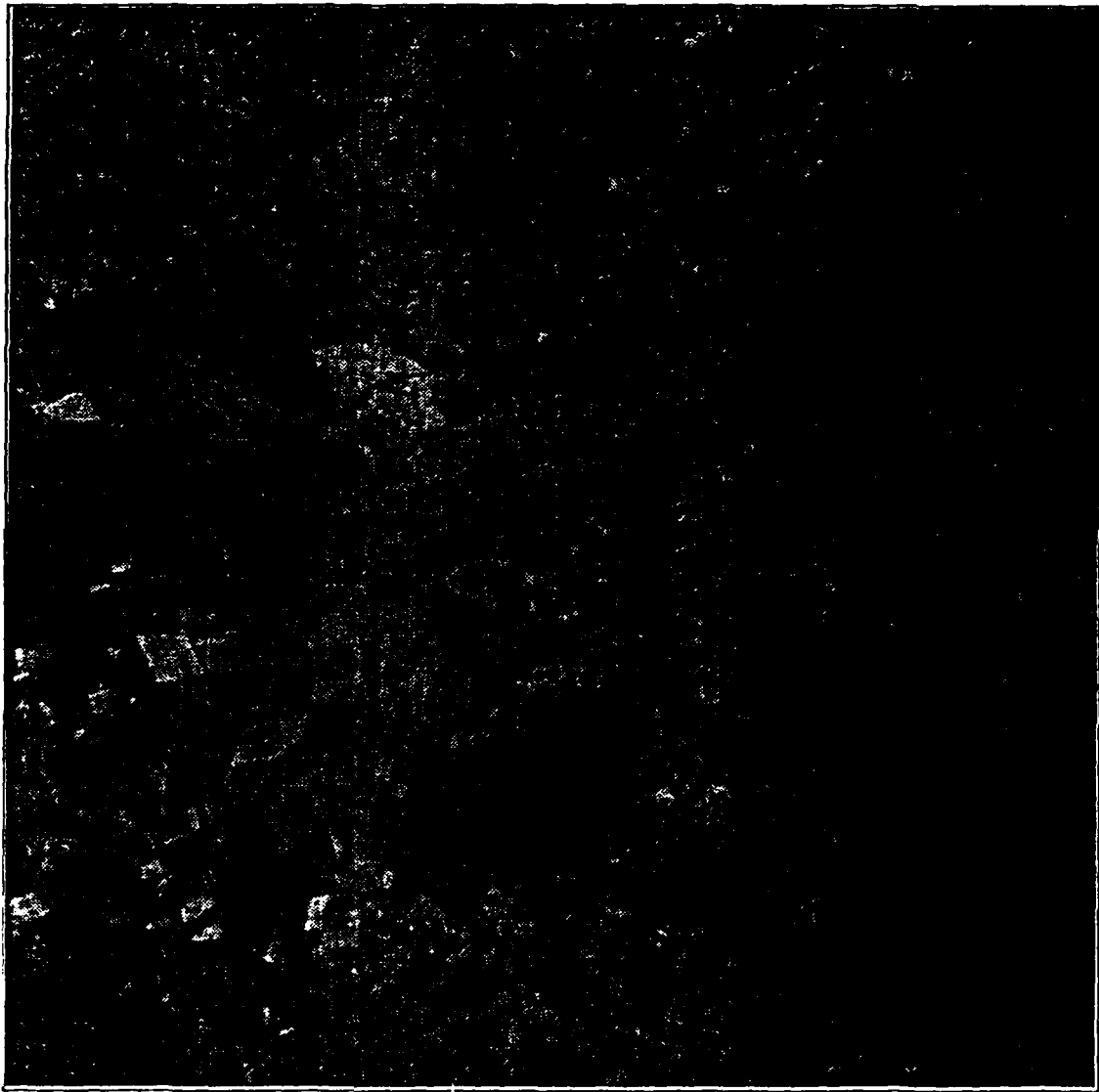
121

Figure 35. MALP Site, Thematic Mapper Band 4 Image

Figure 36. MALP Site, Thematic Mapper Band 5 Image

Figure 37.   MALP Site, Thematic Mapper Band 6 Image
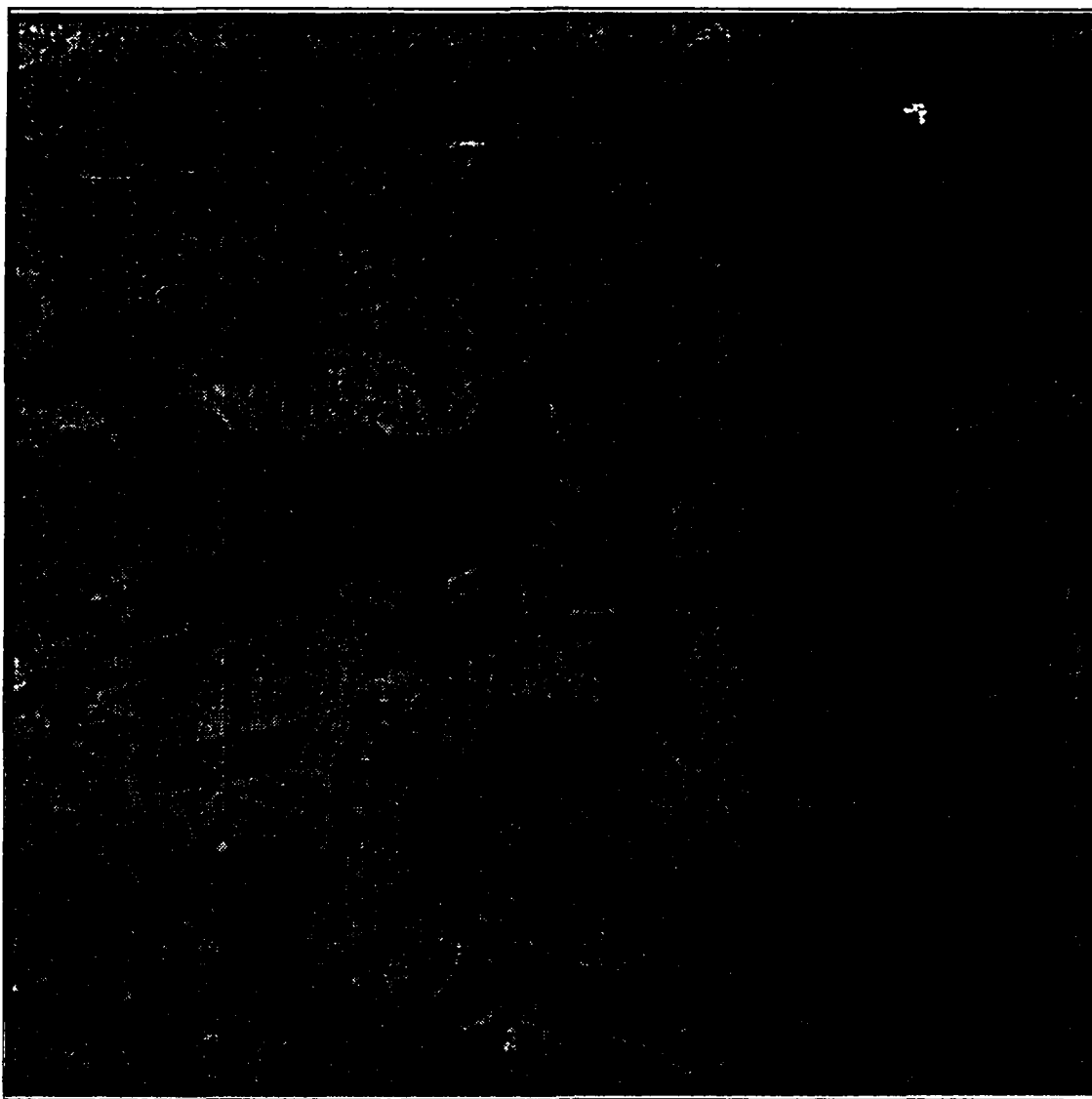
Figure 38.   MALP Site, Thematic Mapper Band 7 Image
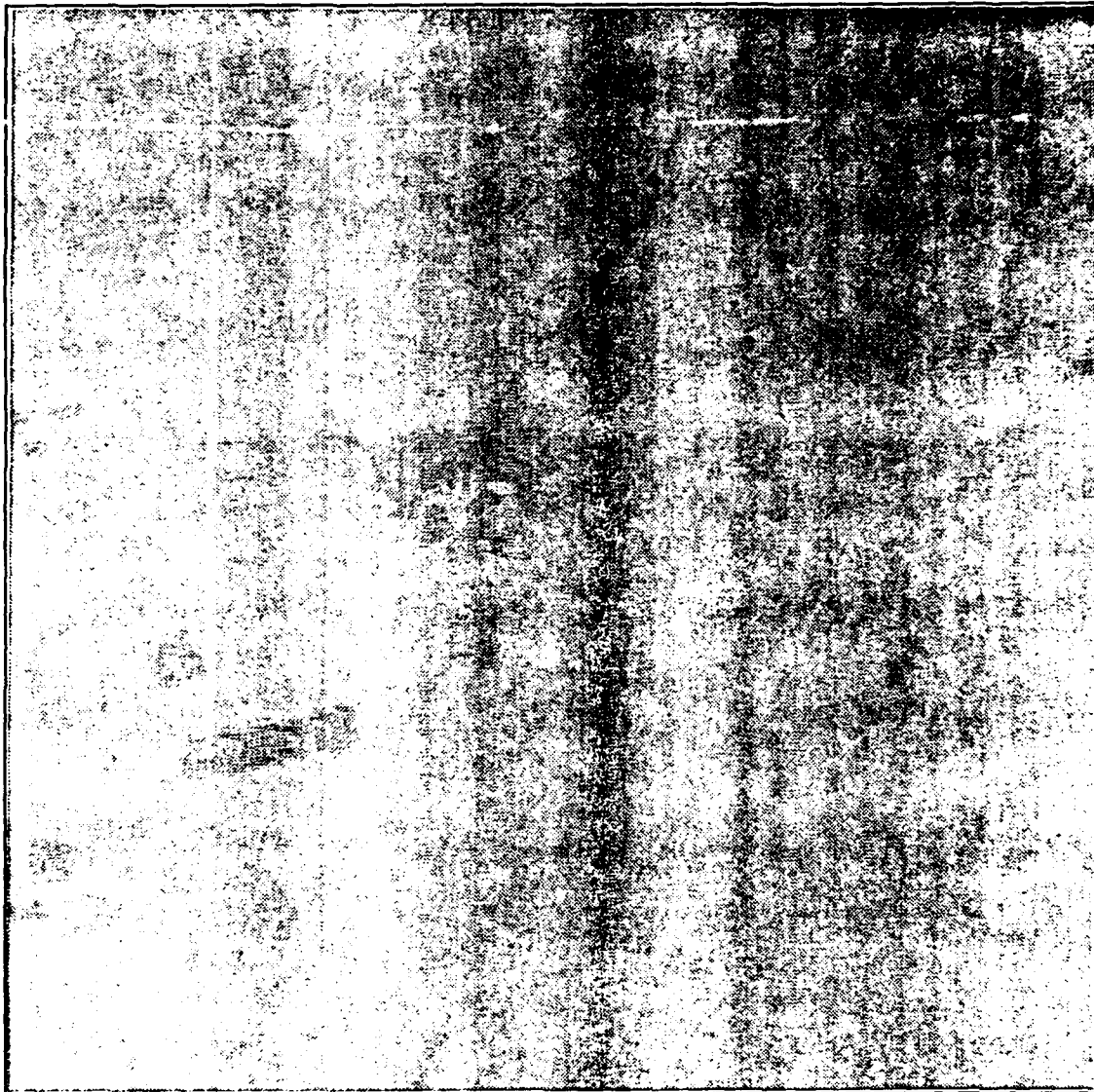
125

Figure 39.   CORINTO Site, Principal Component 1 Image
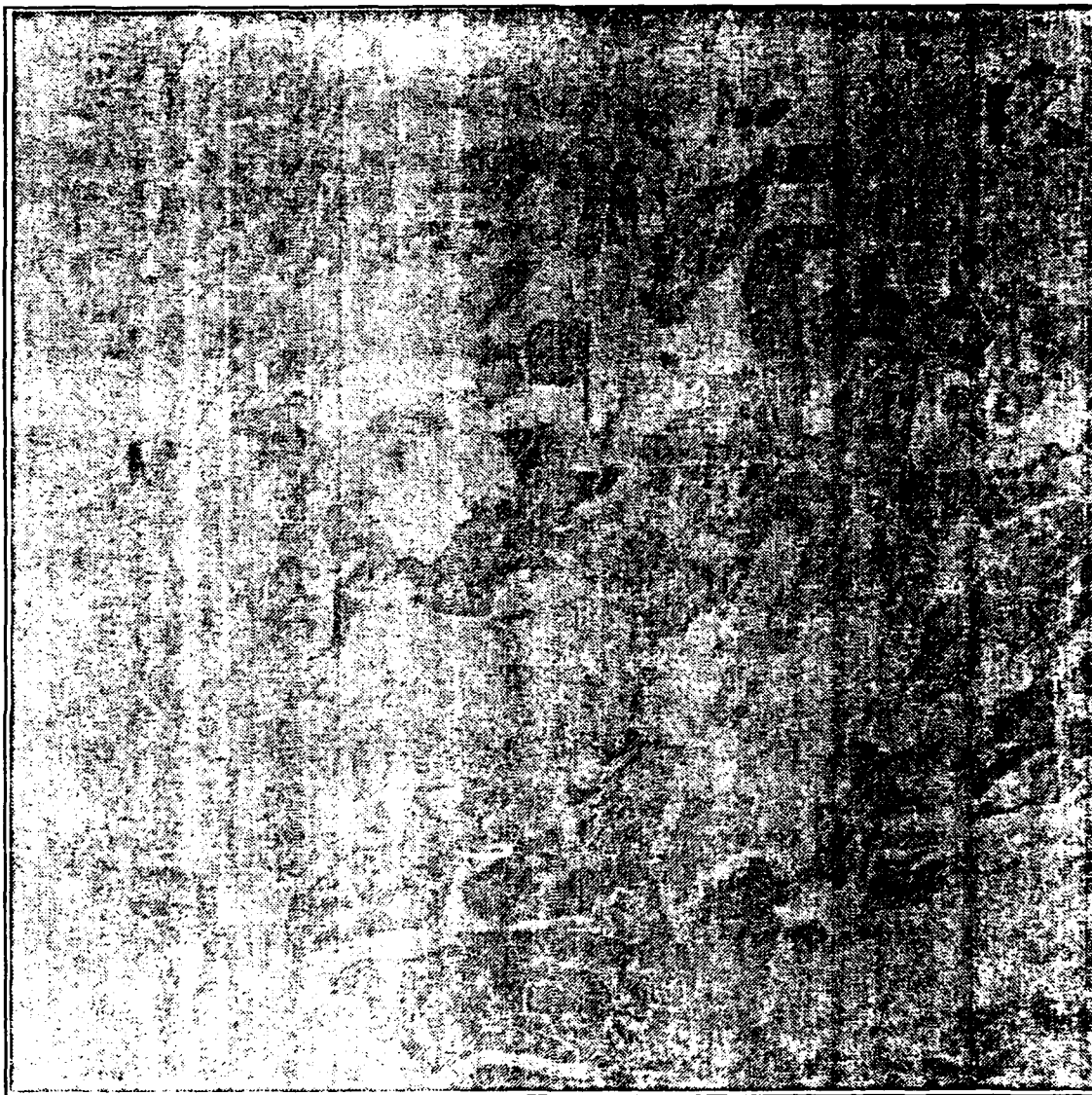
Figure 40.   CORINTO Site, Principal Component 2 Image
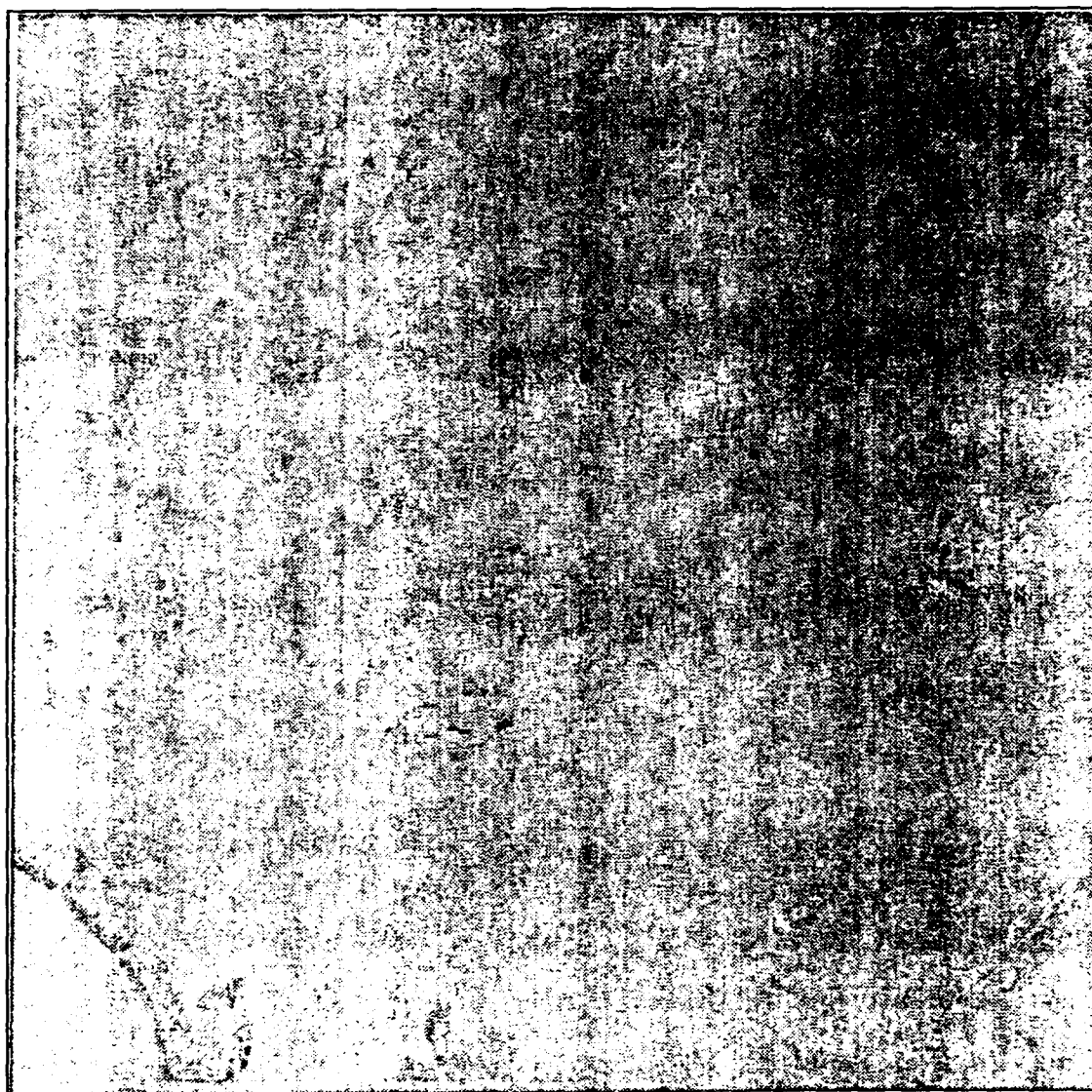
Figure 41. CORINTO Site, Principal Component 3 Image
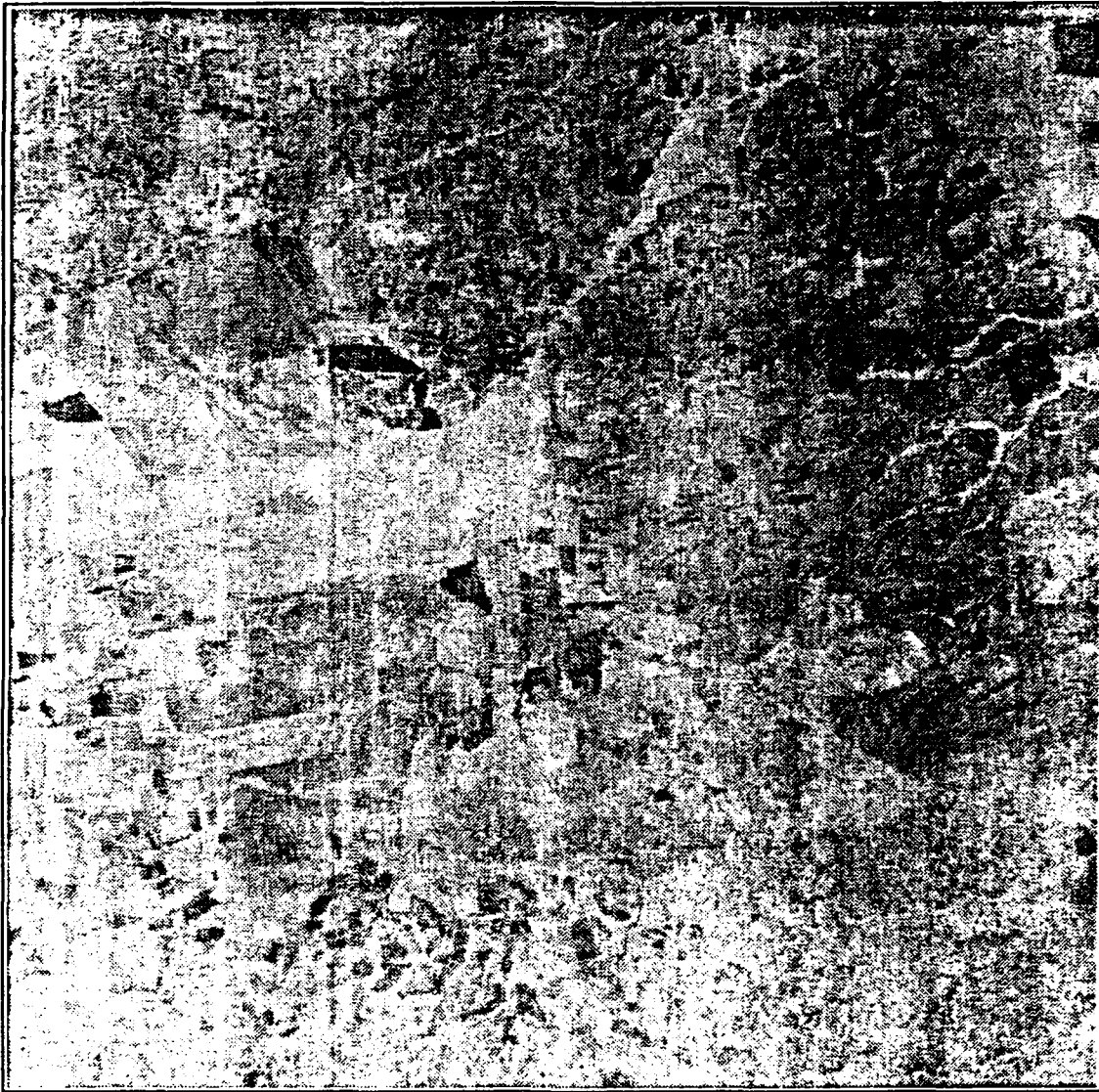
Figure 42. MALP Site, Principal Component 1 Image
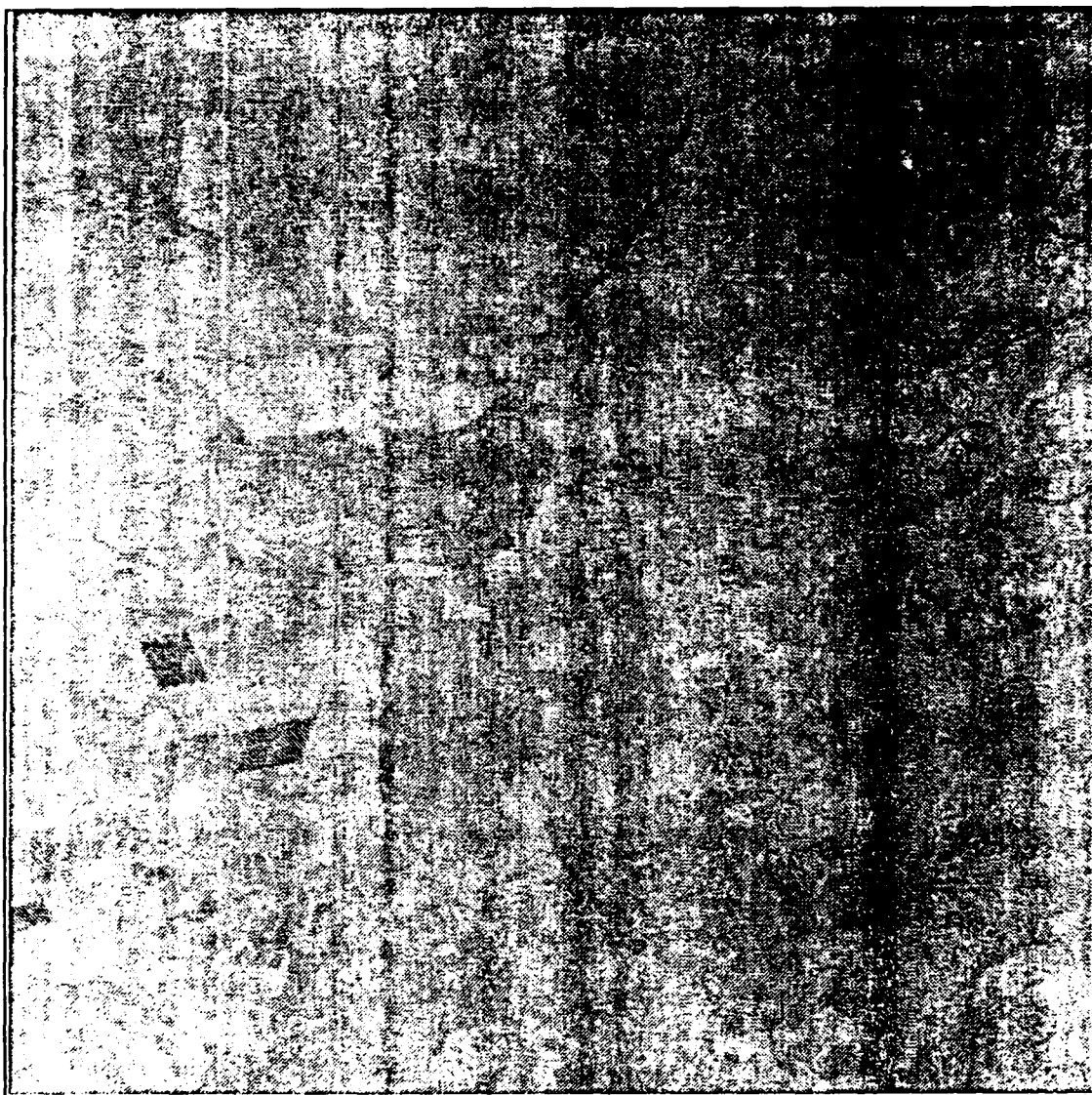
Figure 43.   MALP Site, Principal Component 2 Image
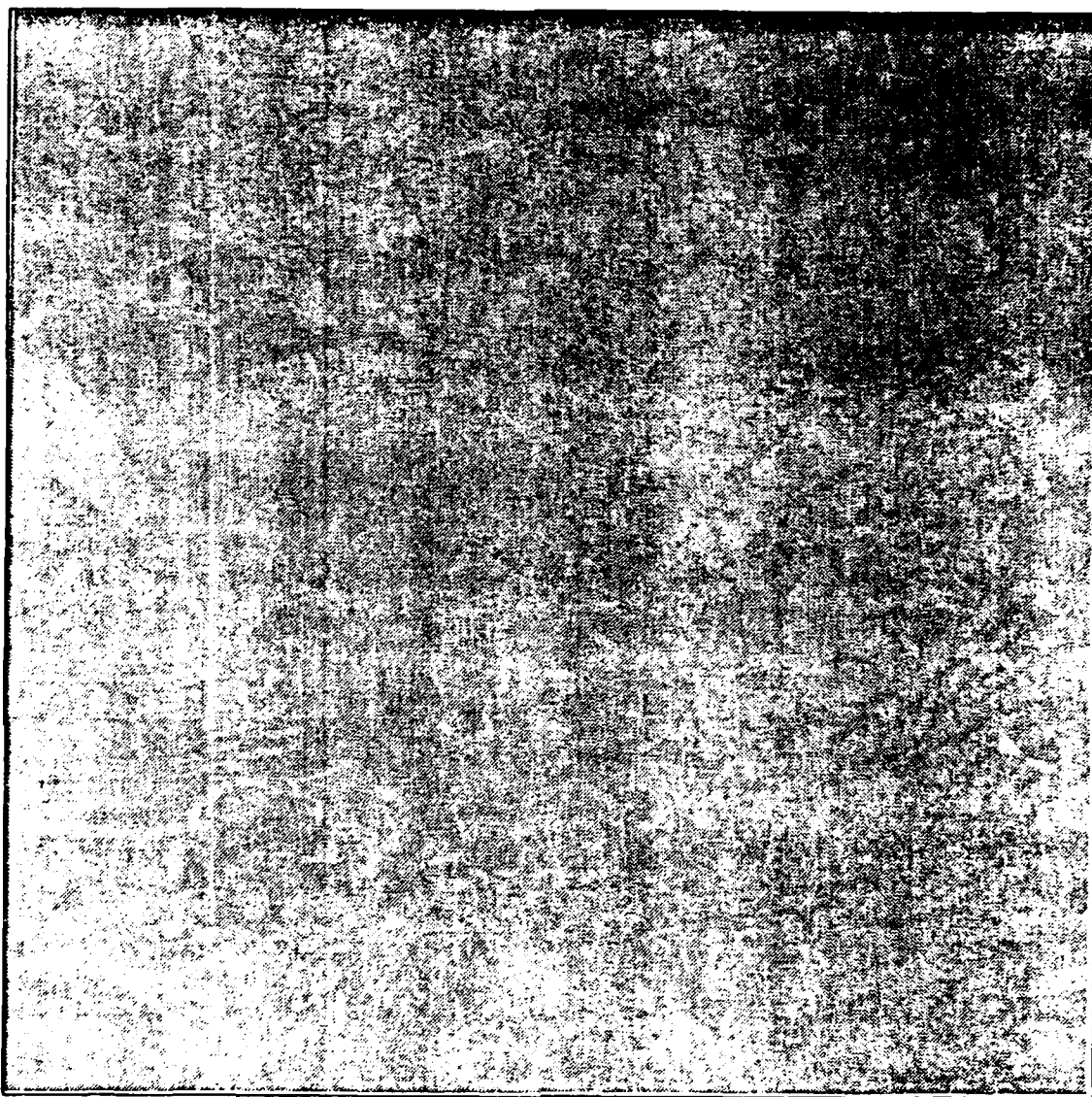
Figure 44. MALP Site, Principal Component 3 Image
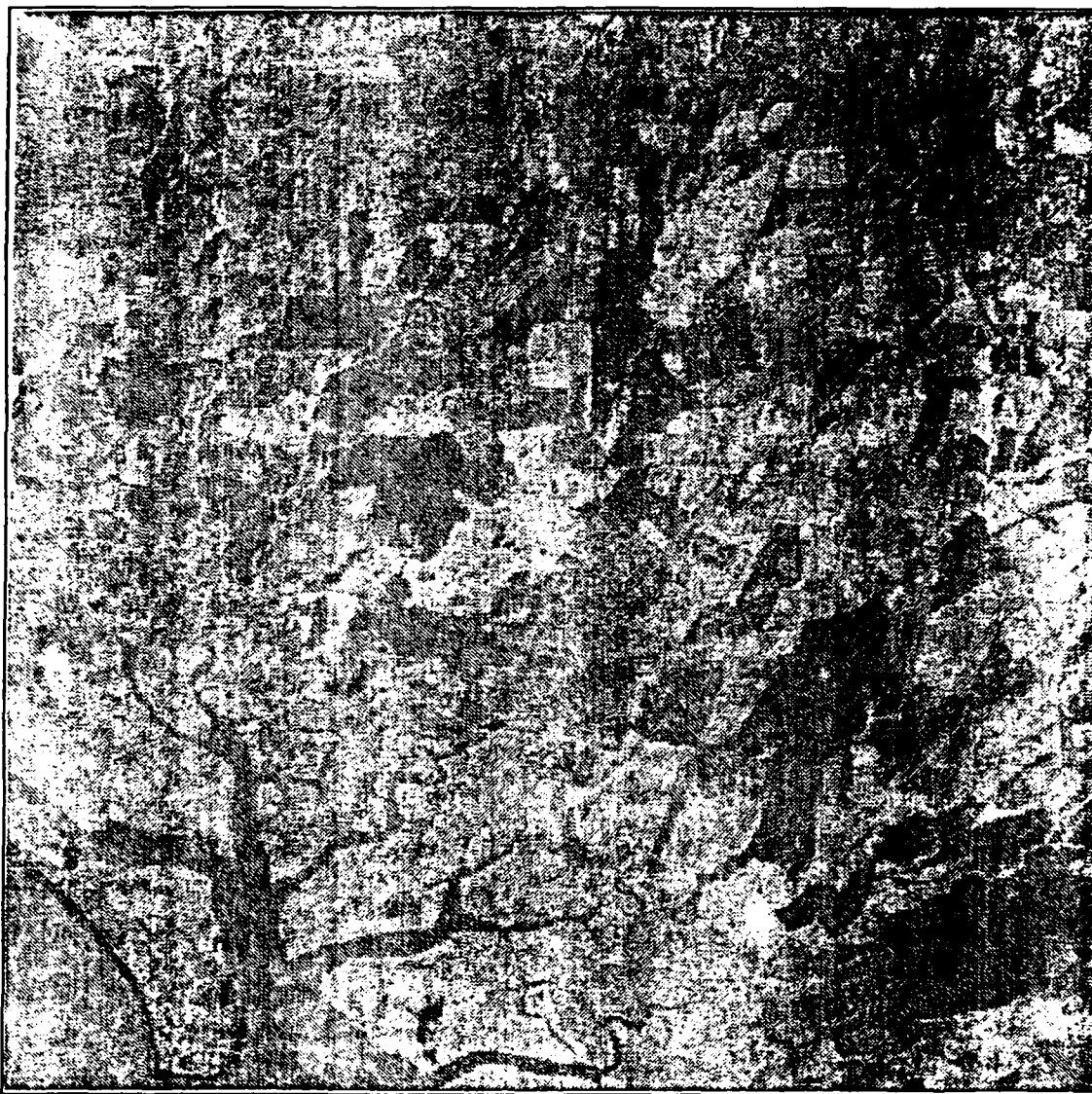
Figure 45. CORINTO Site, Tasseled Cap Greenness Image
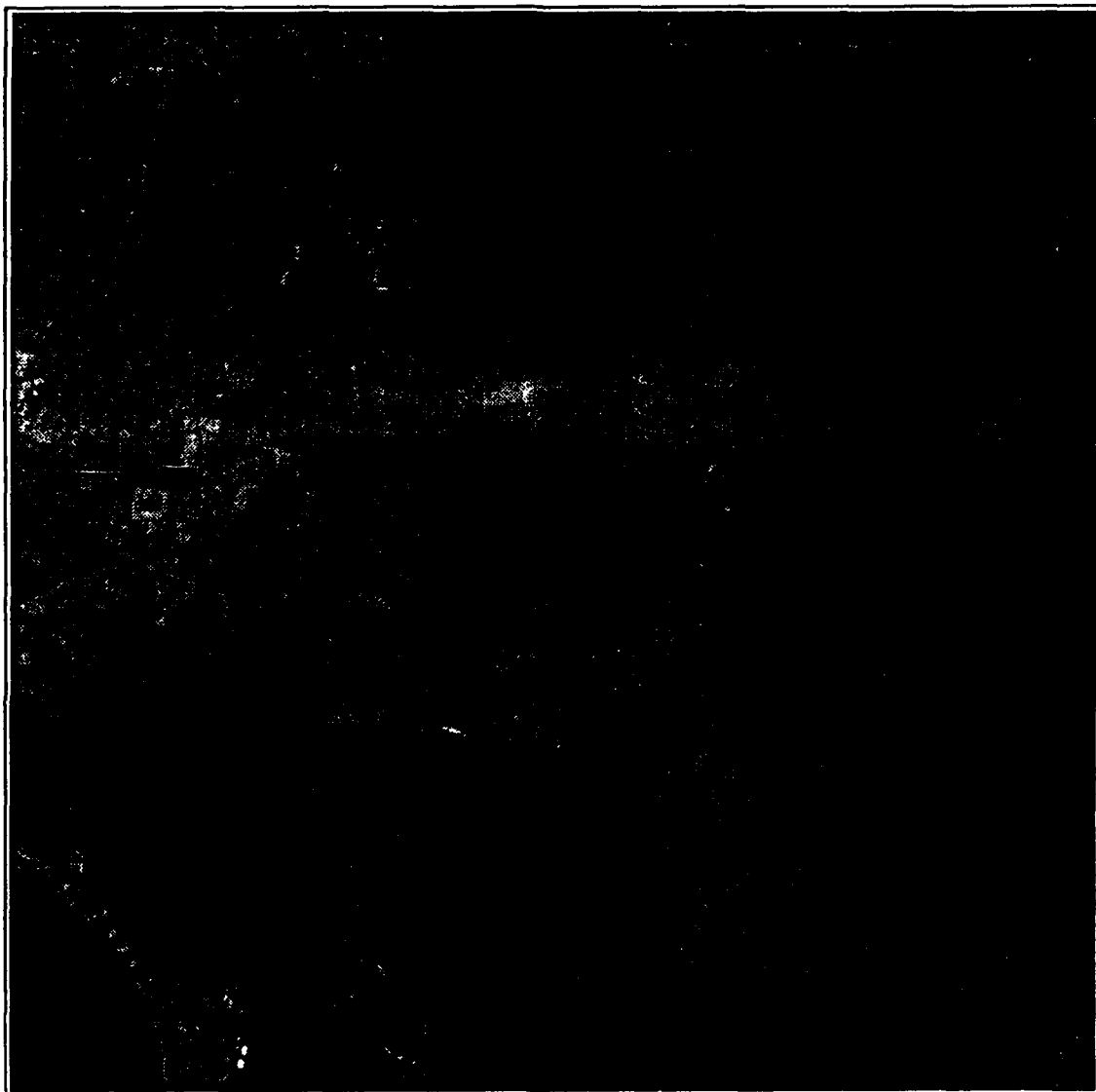
Figure 46. CORINTO Site, Tasseled Cap Brightness Image

Figure 47. CORINTO Site, Tasseled Cap Wetness Image

Figure 48.   MALP Site, Tasseled Cap Greenness Image

Figure 49. MALP Site, Tasseled Cap Brightness Image

Figure 50.   MALP Site, Tasseled Cap Wetness Image

137
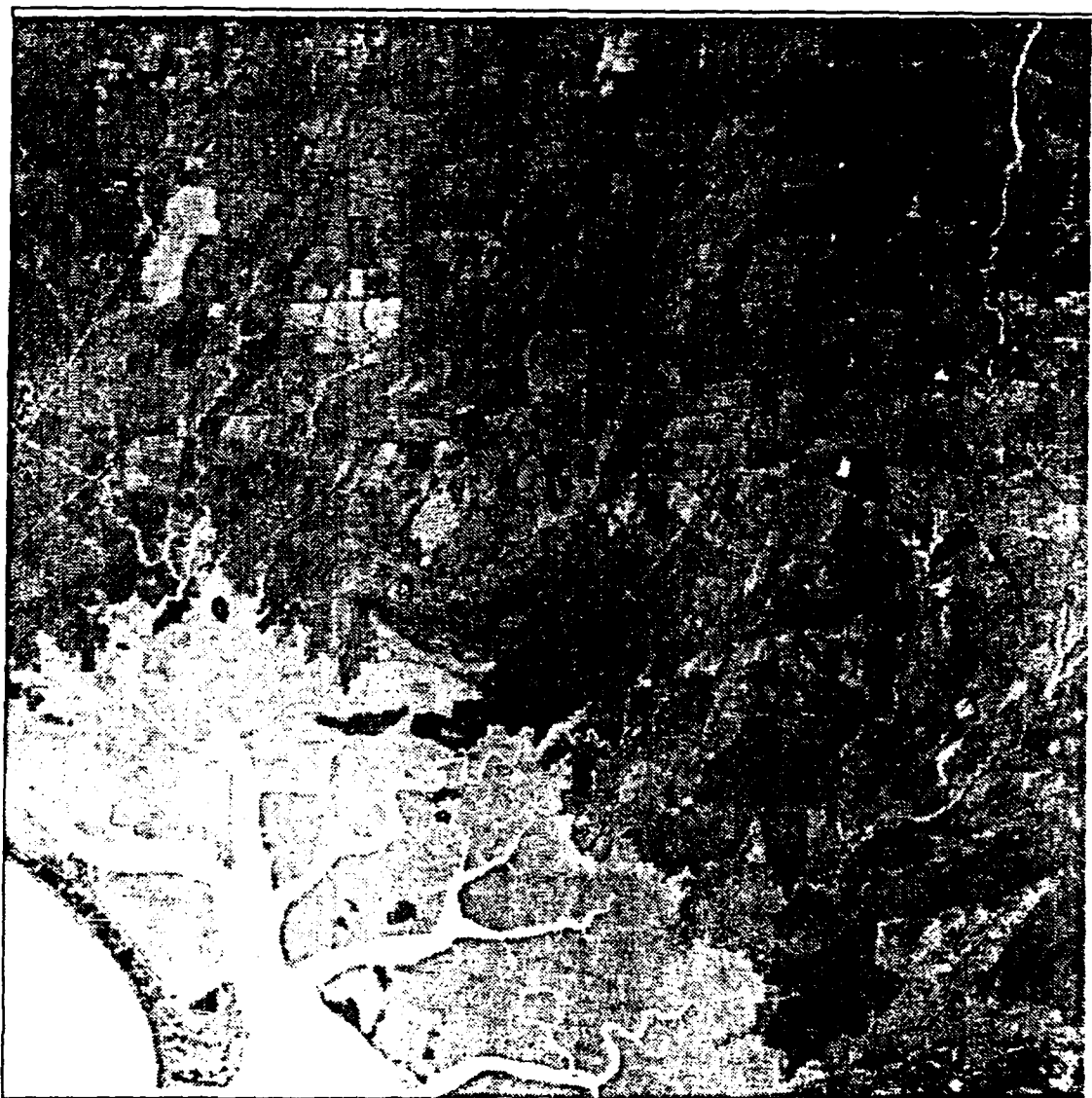
Figure 51. CORINTO Site, (Band 1)/(Band 5) Ratio Image
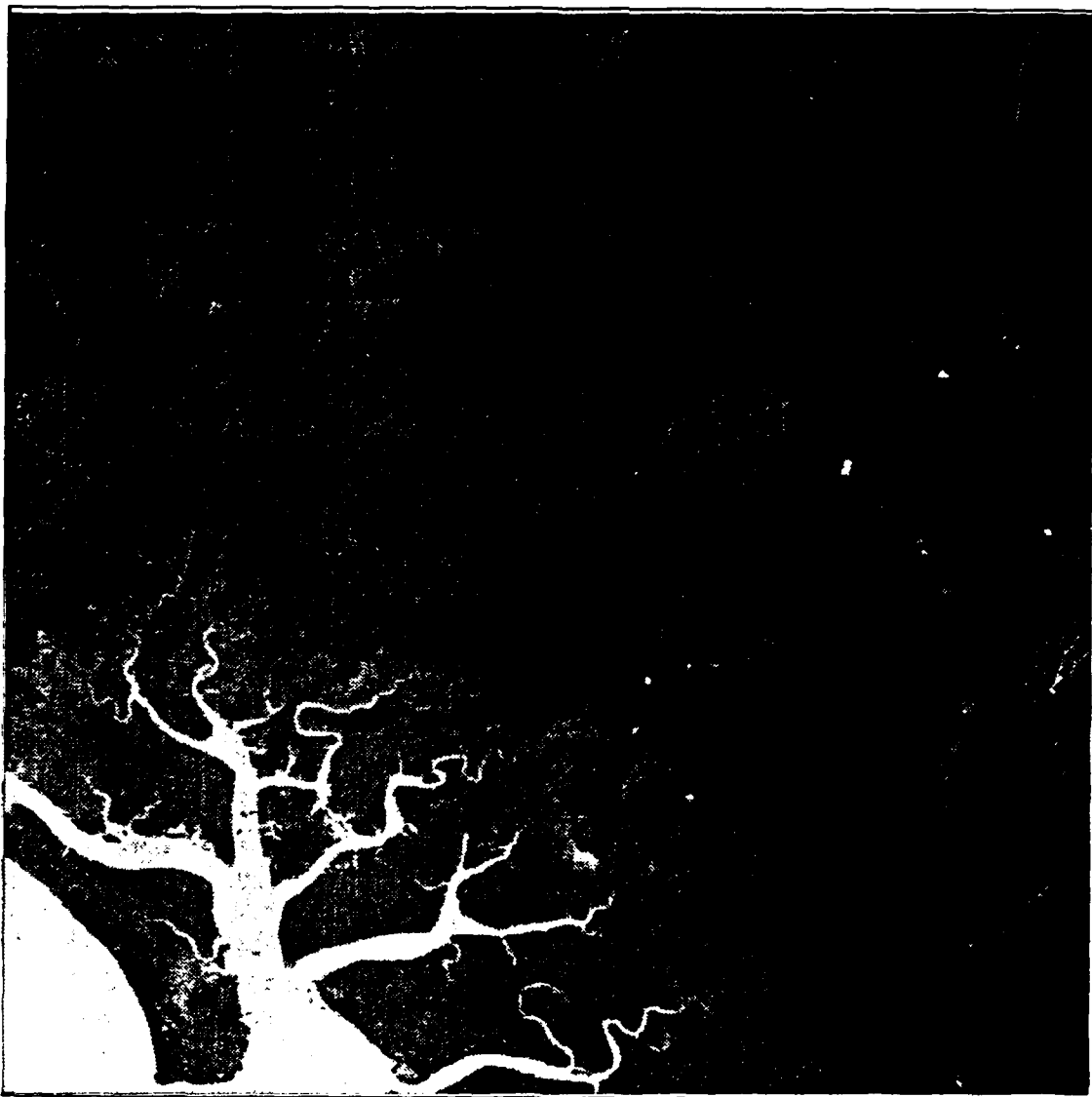
Figure 52.   CORINTO Site, (Band 2)/(Band 5) Ratio Image
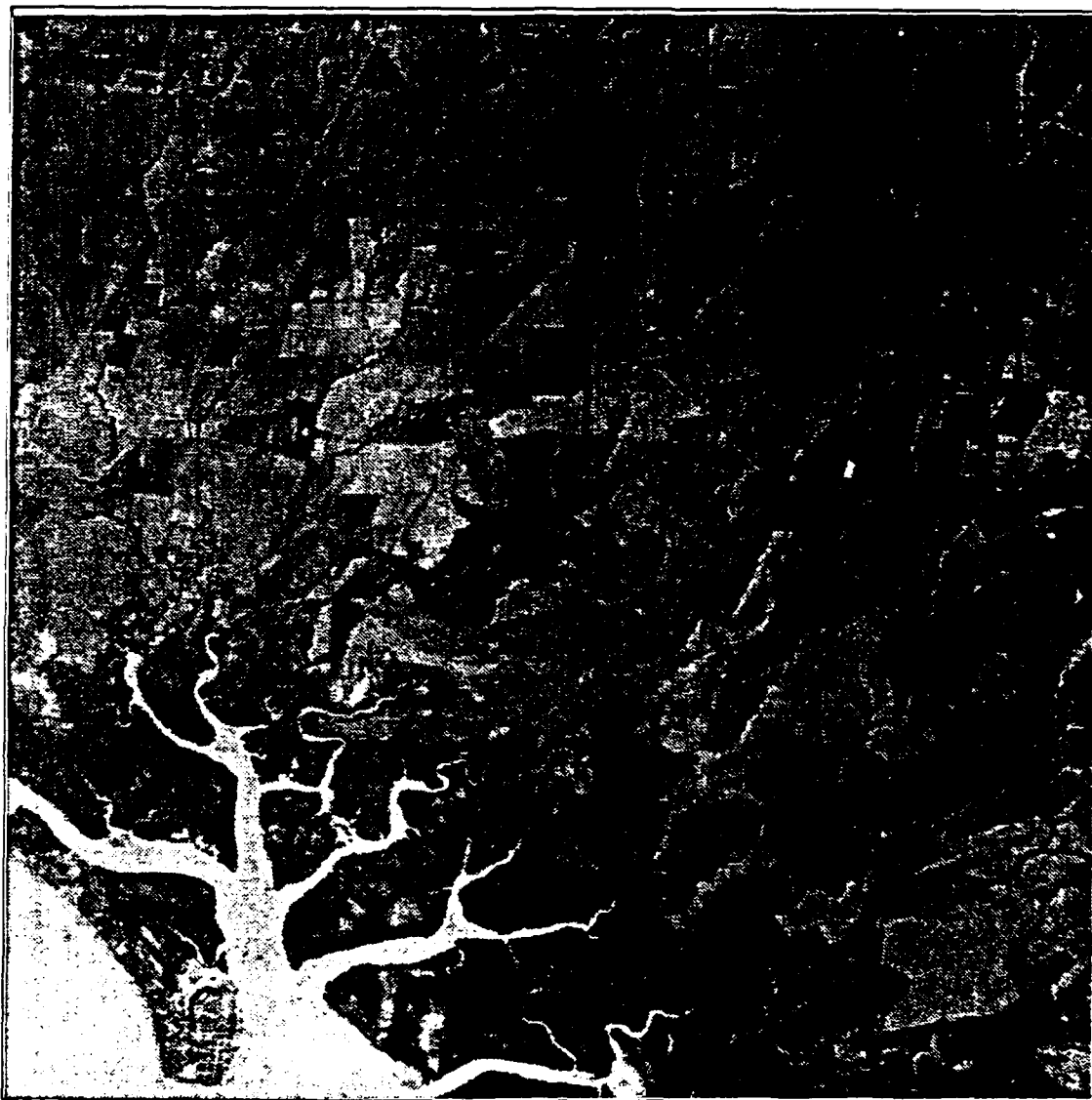
Figure 53. CORINTO Site, (Band 3)/(Band 4) Ratio Image

A. BAND RATIO PROGRAM

```
c                             ratio.for
c
c
c  purpose:
c       this program performs the band ratioing operation.
c       It operates by calculating the pixel-by-pixel
c       division of one 512 x 512 image file by another.
c       The program consists of a main program and one
c       subroutine.  The subroutine readimg reads an image
c       file.
c
c
c************************** input  ********************
c
c   this program assumes that both image files are 512 x 512
c   pixels in size, stored as BYTE (or INTEGER*1) data.
c
c   the user interactively specifies both input file names
c   and the output file name.
c
c************************** output  ********************
c
c   the output image is stored in the user specified file as
c   BYTE (or INTEGER*1) data.
c
c
c******************** main program  ******************


c       define and dimension variables

        byte   ioimg(512,512)
        integer  i,j,k,l,intimg
        real*4   numimg(512,512), denimg(512,512), scale
        character*20 imgname1, imgname2, imgname3

        parameter (scale = 162.3)

c   get filenames from user
```

```fortran
      print *, ' enter the numerator filename '
      read '(a)', imgname1
      print *, ' enter the denominator filename '
      read '(a)', imgname2
      print *, ' enter the output image filename '
      read '(a)', imgname3

c     read numerator image file

      call readimg(imgname1,numimg)

c     read denominator image file

      call readimg(imgname2,denimg)

c     divide numerator image by denominator image
c     and scale to 0-255 (real)

      do 10 i=1,512
         do 11 j=1,512
         numimg(i,j)=scale*atan2(numimg(i,j),denimg(i,j))
11       continue
10    continue

c     scale the image to 0-255 (byte)

      do 85 i=1,512
         do 86 j=1,512
            intimg = int(numimg(i,j))
            if (intimg.ge.128.0) then
               ioimg(i,j) = intimg - 256
            else
               ioimg(i,j) = intimg
            endif
86       continue
85    continue

c     write output image file

      open(unit=1,name=imgname3,type='new',access='direct',
     *recordsize=128,maxrec=512)
      do 100 i=1,512
            write(1'i) (ioimg(i,j), j=1,512)
100      continue
      close(unit=1)

      end

c                       subroutine: readimg
c
c     purpose:
```

142

```
c     subroutine to read byte input image and convert to
c     a real image

      subroutine readimg(name,image)

        byte   ioimg(512,512)
        integer  i,j
        real*4   image(512,512)
        character*20 name

        open(unit=1,name=name,type='old',access='direct',
       *recordsize=128,maxrec=512)

        do 10 i=1,512
              read(1'i) (ioimg(i,j), j=1,512)
10        continue
          close(unit=1)

      do 20 i=1,512
          do 30 j=1,512
              image(i,j)=float(jzext(ioimg(i,j)))
30        continue
20    continue

      return
      end
```

B. TASSELED CAP TRANSFORMATION PROGRAM

```
c                              tasseledcap.for
c
c
c  purpose:
c        this program performs the tasseled cap
c        transformation on six input bands and produces the
c        first three tasseled cap component images:
c        greenness, brightness, and wetness.
c        It operates by calculating the transformations one
c        at a time.
c        The program consists of a main program and two
c        subroutine.  The subroutine readimg reads an image
c        file and the subroutine scale scales the output to
c        the required 0-255 range and writes the output image
c        to disk.
c
c
c*********************** input  ***********************
c
```

143

```
c     this program assumes that all image files are 512 x 512
c     pixels in size, stored as BYTE (or INTEGER*1) data.
c
c     the user interactively specifies all six of the input
c     file names and all three of the output file names.
c
c*********************** output  *********************
c
c     the output images are stored in the user specified files
c     as BYTE (or INTEGER*1) data.
c
c
c********************** main program  ******************


c       define and dimension variables

        integer  i,j,k
        integer mindsp,maxdsp
        real*4   image(512,512), tc(512,512)
        character*20 band(6)
        character*20 green,bright,wet
           real*4 g(6)/-.2848,-.2435,-.5436,.7243,.0840,-.1800/
      real*4 b(6)/.3037,.2793,.4743,.5585,.5082,.1863/
      real*4 w(6)/.1509,.1973,.3279,.3406,-.7112,-.4572/

        parameter (mindsp=0,maxdsp=255)

c     get filenames from user

      print *, ' enter band 1 filename '
      read '(a)', band(1)
      print *, ' enter band 2 filename '
      read '(a)', band(2)
      print *, ' enter band 3 filename '
      read '(a)', band(3)
      print *, ' enter band 4 filename '
      read '(a)', band(4)
      print *, ' enter band 5 filename '
      read '(a)', band(5)
      print *, ' enter band 7 filename '
      read '(a)', band(6)
      print *, ' enter greenness (output) filename '
      read '(a)', green
      print *, ' enter brightness (output)filename '
      read '(a)', bright
      print *, ' enter wetness (output)filename '
      read '(a)', wet

c     calculate and output the greenness transformation
```

144

```fortran
      call readimg(band(1),tc)

      do 12 i=1,512
        do 13 j=1,512
          tc(i,j) = g(1)*tc(i,j)
13    continue
12  continue

      do 15 k=2,6

      call readimg(band(k),image)

      do 10 i=1,512
        do 11 j=1,512
          tc(i,j)=tc(i,j) + g(k)*image(i,j)
11    continue
10  continue
15      continue

c   scale the image to 0-255 and write to disk

      call scale(green,tc,mindsp,maxdsp)

c   calculate and output the brightness transformation

      call readimg(band(1),tc)

      do 22 i=1,512
        do 23 j=1,512
          tc(i,j) = b(1)*tc(i,j)
23    continue
22  continue

      do 25 k=2,6

      call readimg(band(k),image)

      do 20 i=1,512
        do 21 j=1,512
          tc(i,j)=tc(i,j) + b(k)*image(i,j)
21    continue
20  continue
25      continue

c   scale the image to 0-255 and write to disk

      call scale(bright,tc,mindsp,maxdsp)

c   calculate and output the wetness transformation

      call readimg(band(1),tc)
```

145

```
      do 32 i=1,512
        do 33 j=1,512
          tc(i,j) = w(1)*tc(i,j)
33      continue
32    continue

      do 35 k=2,6

      call readimg(band(k),image)

      do 30 i=1,512
        do 31 j=1,512
          tc(i,j)=tc(i,j) + w(k)*image(i,j)
31      continue
30    continue
35        continue

c     scale the image to 0-255 and write to disk

      call scale(wet,tc,mindsp,maxdsp)
      end

c
c
c                    subroutine: scale
c
c     purpose:
c     subroutine to scale image to 0-255 and write it to disk

      subroutine scale(imgname,numimg,mindsp,maxdsp)

      integer  i,j
      integer mindsp,maxdsp
      byte     ioimg(512,512)
      real*4   numimg(512,512),minmag,maxmag
      character*20 imgname

      minmag = 1.0e10
      maxmag = 0.0
      do 80 i=1,512
        do 81 j=1,512
        if (numimg(i,j).lt.minmag) then
          minmag = numimg(i,j)
        elseif (numimg(i,j).ge.maxmag) then
          maxmag = numimg(i,j)
        endif
81    continue
80    continue

      do 85 i=1,512
        do 86 j=1,512
```

```
      numimg(i,j)=(numimg(i,j)-minmag)*(maxdsp/(maxmag-minmag))
           if (numimg(i,j).gt.127) then
           ioimg(i,j) = numimg(i,j) - 256
           else
           ioimg(i,j) = numimg(i,j)
           endif
86    continue
85    continue

c     write output image file

      open(unit=1,name=imgname,type='new',access='direct',
     *recordsize=128,maxrec=512)
      do 100 i=1,512
           write(1'i) (ioimg(i,j), j=1,512)
100      continue
      close(unit=1)

      return
      end


c                      subroutine: readimg
c
c     purpose:
c     subroutine to read byte input image and convert to
c     a real image

      subroutine readimg(name,image)

      byte  ioimg(512,512)
      integer  i,j
      real*4   image(512,512)
      character*20 name

      open(unit=1,name=name,type='old',access='direct',
     *recordsize=128,maxrec=512)

      do 10 i=1,512
           read(1'i) (ioimg(i,j), j=1,512)
10       continue
      close(unit=1)

      do 20 i=1,512
        do 30 j=1,512
             image(i,j)=float(jzext(ioimg(i,j)))
30       continue
20    continue

      return
      end
```

APPENDIX D - THE LAND ANALYSIS SYSTEM

A. OVERVIEW

The Land Analysis System (LAS) is an image analysis system designed for use with satellite imagery. [Ref. 20:p. 1] It provides the capability to manipulate and analyze digital image data and includes a wide range of functions and statistical tools for image analysis. In addition to routines for extracting the study sites from a Landsat scene, image statistics calculation, and file management functions, LAS includes a variety of routines for both supervised and unsupervised classification. All three of the unsupervised classification routines (HINDU, KMEANS, and ISOCLASS) and one of the supervised classification routines (MINDIST) are described below.

B. THE HINDU CLASSIFICATION ROUTINE

HINDU classifies a multiband image based upon its multi-dimensional histogram. [Ref. 20:pp. HINDU-1 to HINDU-3] Regions in the histogram with high density are regarded as pattern clusters.

1. User Input

The user specifies the input image, the minimum and maximum acceptable number of clusters, and the number of gray levels per histogram bin [Ref. 20:p. HINDU-2].

2. Algorithm Description

Each bin or cell of the multidimensional histogram is examined for neighbors that have a higher density. [Ref. 20:p. HINDU-2] The low density cells are then assigned in proportion to their high-density neighbors. This reassignment is carried out from the lowest to the highest density cell, recalculating the density at each stage. The histogram is then searched for entries of greater than average density. These entries are considered as possible clusters. If there are too few clusters, the program aborts. If there are too many clusters, those with a lower significance are deleted to obtain the a number of clusters in the specified range. Each pixel is assigned to the nearest cluster. HINDU is suitable primarily for Landsat images.

C. KMEANS

KMEANS performs an unsupervised classification using the K-means algorithm. [Ref. 20:p. KMEANS-1] Input images can have up to 24 bands and the algorithm can produce classified images with up to 64 clusters.

1. User Input

The user specifies the input and output image names and the following parameters [Ref. 20:p. KMEANS-1]:

- NCLUST - number of clusters desired.
- MAXIT - maximum number of iterations.

- PCTCNG - threshold value of the percentage of pixels changing cluster assignment in an iteration. If the percentage of pixels changing cluster assignments between iterations falls below thing value, clustering has converged and execution is terminated.

2. Algorithm Description

KMEANS operates as follows [Ref. 20:pp. KMEANS-2 to KMEANS-3]:

- Step 1: Compute the image means and standard deviations.

- Step 2: Determine the location of initial cluster centers.

- Step 3: Assign data to clusters using the minimum Euclidean distance rule.

- Step 4: Update cluster centers using the assignments of step 3.

- Step 5: Stop if MAXIT is exceeded or if the percentage of pixels changing clusters was less than PCTCNG. Otherwise, go to step 3.

- Step 6: Compute and print statistics.

The location of initial cluster centers is given by

$$Center(cluster\ k,\ band\ i) = m_i + \sigma_i - (k-1) \times \frac{2\sigma_i}{NCLUST-1} \qquad (1)$$

where m_i is the mean value of band i, σ_i is the standard deviation of band i, and k ranges from 1 to NCLUST.

D. ISOCLASS

ICOSLASS performs unsupervised classification of a multispectral image using an isodata-type clustering algorithm. [Ref. 20:p. ISOCLASS-1] Input images can have up to 24 bands and the algorithm can produce classified images with up to 64 clusters. ISOCLASS had the capability of continuing a classification by reading an input statistics file from a previous execution.

1. User Input

The user specifies the input and output image names, the output statistics file name, and the following parameters [Ref. 20:p. ISOCLASS-1 to ISOCLASS-2]:

- MAXIT - Maximum number of iterations.

- DLMIN - Two clusters whose means are closer than DLMIN are combined.

- NMIN - Minimum number of members desired in any cluster. Clusters that have less than NMIN members are deleted.

- STDMAX - Any cluster whose standard deviation is greater than STDMAX and whose number of members is greater than 2(NMIN + 1) is split.

- MAXCLS - Maximum number of clusters.

- CHNTHS - Threshold for chaining clusters.

2. Algorithm Description

ISOCLASS operates as follows [Ref. 20:pp. ISOCLASS-2 to ISOCLASS-3]:

- Step 1: ISOCLASS reads the initial cluster centroids from the statistics file, or assumes that all of the data are a single cluster and computes the mean and standard deviation vectors. The mean vector is split (see below).

- Step 2: Data is assigned to clusters using the minimum cityblock distance rule.

- Step 3: Cluster means and standard deviations are computed.

- Step 4: If MAXIT has been reached, go to step 9.

- Step 5: All clusters with fewer than NMIN members are deleted.

- Step 6: The type of iteration, split or combine, is determined (see below).

- Step 7: Cluster centroids are split or combined (depending on the type of iteration).

- Step 8: Go to step 2.

- Step 9: Statistics are computed and a summary is printed. The statistics are stored in the output statistics file.

- Step 10: The image is chained (see below).

a. Splitting Clusters

A cluster is split in the jth band if the cluster's maximum standard deviation is in the jth band, the standard deviation in the jth band is greater than STDMAX, and the cluster has more than 2(NMIN + 1) members. [Ref. 20:pp. ISOCLASS-3 to ISOCLASS-4] On a given iteration, all clusters that meet the criteria are split, as long as the maximum number of clusters has not been reached. Once the

maximum number of clusters has been reached, classification continues without the creation of new clusters.

b. Determining the Type of Iteration

ISOCLASS begins with a sequence of split operations. [Ref. 20:p. ISOCLASS-5] This sequence ends when at least 80 percent of the clusters have standard deviations less than STDMAX. At that point, the operations alternate between combine and split operations until the last iteration, which is always a split operation. The initial sequence of split operations is to initialize the cluster centers. The sequence of initial split operations is shortened considerably if the initial cluster centers are provided in an input statistics file.

c. Chaining Clusters

The last step is to chain all clusters with intercluster distances less then CHNTHS. [Ref. 20:p. ISOCLASS-5] The chaining procedure was adopted because the minimum variance procedure used in ISOCLASS tends to form ellipsoidal clusters with Gaussian distributions. While the Gaussian distribution is natural and is normally satisfactory, there could also be natural groupings of data that are oddly shaped which cannot be approximated by a Gaussian distribution.

The statistics of the chained clusters are not calculated because the chained cluster cannot be represented

by a Gaussian distribution. [Ref. 20:p. ISOCLASS-5] The chained clusters are not combined in the classified image. Instead, a message is printed in the classification summary to indicate that clusters meet the chaining criteria.

E. MINDIST

MINDIST performs a supervised classification of a multi-band image based on minimum distance from class means. [Ref. 20:p. MINDIST-1] It has an option for specifying the maximum distance a pixel can be from the nearest cluster's center and still be assigned to that cluster (this can be used for classifying pixels as "unknown," too far from any cluster).

MINDIST can be used to improve on the results of the unsupervised clustering algorithms, either by discarding pixels that are too far from cluster centroids or by reclassifying the image using a different distance rule.

1. User Input

The user specifies the input and output image names, the output statistics file name, and the following parameters [Ref. 20:p. MINDIST-1 to MINDIST-2]:

- MAXDIST: The maximum distance a pixel can be from the nearest cluster centroid and still be assigned to that cluster. The options are for a pixel to be assigned to the nearest cluster no matter how far away, for the user to supply a value for each class, and for a single maximum distance for all classes. If the pixel is greater than MAXDIST away from the nearest cluster

centroid, it is assigned a value of 0, signifying an unclassified pixel.

- WEIGHTS: Weights to apply to each input image band.

- METRIC: Specifies the measure used to calculate distance from the cluster centers. The CITYBLOCK and the EUCLIDEAN distance measures are available.

2. Algorithm Description

Each pixel is assigned to a cluster based on the selected distance rule.

The CITYBLOCK distance rule operates as follows [Ref. 20:p. MINDIST-2 to MINDIST-3]:

$$CD_j = \sum_{i=1}^{n} W_i |x_i - \mu_{ij}| \tag{2}$$

where CD_j is the "city block" distance between pixel x and the mean of cluster j, n is the number of bands in the image, x_i is the value of pixel x in band i, μ_{ij} is the mean in band i of class j, and W_i is the weight assigned to band i.

The EUCLIDIAN distance rule operates as follows [Ref. 20:p. MINDIST-2 to MINDIST-3]:

$$ED_j = \sqrt{\sum_{i=1}^{n} W_i (x_i - \mu_{ij})^2} \tag{3}$$

155

where ED_j is the Euclidean distance between pixel x and the mean of cluster j, n is the number of bands in the image, x_i is the value of pixel x in band i, μ_{ij} is the mean in band i of class j, and W_i is the weight assigned to band i.

The output pixel is assigned to the class j which has the minimum distance as calculated using the chosen distance rule. [Ref. 20:p. MINDIST-3] If MAXDIST was selected to classify pixels as "unknown" and the minimum distance is greater than MAXDIST, then the output pixel is assigned a value of 0.

LIST OF REFERENCES

1. U.S Army Combined Arms and Services Staff School, <u>Combined Arms Operations, Volume Two of Four Volumes</u>, Fort Leavenworth, Kansas, 1985

2. Department of the Army, <u>FM 30-5: Combat Intelligence</u>, Washington, D.C., 1971

3. Andrew J. Brookes, <u>Photo Reconnaissance</u>, Ian Allen, Ltd., Shepperton, Surrey, England, 1975

4. Earth Observation Satellite Company, <u>User's Guide for Landsat Thematic Mapper Computer-Compatible Tapes</u>, Sioux Falls, South Dakota, 1985

5. John R. Jensen, <u>Introductory Digital Image Processing: A Remote Sensing Perspective</u>, Prentice-Hall, Englewood Cliffs, New Jersey, 1986

6. Floyd F. Sabins, Jr., <u>Remote Sensing: Principles and Interpretation</u>, 2d ed., W.H. Freeman, New York, 1987

7. James B. Campbell, <u>Introduction to Remote Sensing</u>, The Guilford Press, New York, 1987

8. Thomas M. Lillesand and Ralph W. Kiefer, <u>Remote Sensing and Image Interpretation</u>, 2d ed., John Wiley and Sons, New York, 1987

9. Ray Harris, "Spectral and spatial image processing for remote sensing," <u>International Journal of Remote Sensing</u>, Vol. 1, No. 4, pp. 361-375, 1980

10. E.P. Crist and R.J. Kauth, "The tasseled cap demystified," <u>Photogrammetric Engineering and Remote Sensing</u>, Vol. 52, No. 1, pp. 81-86, 1986

11. Robert M. Haralick and King-Sun Fu, "Pattern recognition and classification," in <u>The Manual of Remote Sensing</u>, Vol. 1, Robert N. Colwell, ed., pp. 793-805, American Society of Photogrammetry and Remote Sensing, Falls Church, Virginia, 1983

12. Charles W. Therrien, <u>Decision Estimation and Classification: An Introduction to Pattern Recognition and Related Topics</u>, John Wiley and Sons, New York, 1989

157

13. Philip H. Swain, "Fundamentals of pattern recognition in remote sensing," in <u>Remote Sensing: The Quantitative Approach</u>, Philip H. Swain and Shirley M. Davis, eds., pp. 136-187, McGraw-Hill, New York, 1978

14. Richard O. Duda and Peter E. Hart, <u>Pattern Classification and Scene Analysis</u>, John Wiley and Sons, New York, 1973

15. David R. Thompson and Keith E. Henderson, "Evaluation of thematic mapper for detecting soil properties under grassland vegetation," <u>IEEE Trans. on Geoscience and Remote Sensing</u>, Vol. GE-22, No. 3, pp. 319-323, 1984

16. Robert E. Crippen, "The regression intersection method of adjusting image data for band ratioing," <u>International Journal of Remote Sensing</u>, Vol. 8, No. 2, pp. 137-155, 1987

17. Mark A. Karaska, Stephen J. Walsh, and David R. Butler, "Impact of environmental variables on spectral signatures acquired by the LANDSAT thematic mapper," <u>International Journal of Remote Sensing</u>, Vol. 7, No. 12, pp. 1653-1667, 1986

18. Brent Holben and Chris Justice, "An examination of spectral band ratioing to reduce the topographic effect on remotely sensed data," <u>International Journal of Remote Sensing</u>, Vol. 2, No. 2, pp. 115-133, 1981

19. Rafael C. Gonzalez and Paul Wintz, <u>Digital Image Processing</u>, 2d ed., Addison-Wesley, Menlo Park, California, 1987

20. National Aeronautics and Space Administration, <u>LAS User's Manual, Version 4.0</u>, Goddard Space Flight Center, Greenbelt, Maryland, 1987

21. Ralph Bernstein, Jeffery B. Lotspiech, H. Joseph Myers, Harwood G. Kolsky, and Robert D. Lees, "Analysis and processing of LANDSAT-4 sensor data using advanced image processing techniques and technologies," <u>IEEE Trans. on Geoscience and Remote Sensing</u>, Vol. GE-22, No. 3, pp. 192-221, 1984

22. Eric P. Crist and Richard C. Cicone, "A physically based transformation of thematic mapper data - the TM tasseled cap," <u>IEEE Trans. on Geoscience and Remote Sensing</u>, Vol. GE-22, No. 3, pp. 256-263, 1984

23. Rosendo Arguello, "Nicaragua," in The New Encyclopedia Britannica, 15th ed., Vol 13, pp. 58-63, Encyclopedia Britannica, Inc, Chicago, Illinois, 1984

24. Mary W. Helms, "The society and its environment," in Nicaragua: A Country Study, ed. by James D. Rudolph, Headquarters, Department of the Army, Washington, D.C., 1982

25. Defense Mapping Agency, Map, edition 2-DMA, series E751, sheet 2753 I (Chinandega), scale 1:50,000, Defense Mapping Agency Hydrographic/Topographic Center, Washington, D.C., 1971

26. Defense Mapping Agency, Map, edition 2-DMA, series E751, sheet 2753 II (Corinto), scale 1:50,000, Defense Mapping Agency Hydrographic/Topographic Center, Washington, D.C., 1972

27. Defense Mapping Agency, Map, edition 2-DMA, series E751, sheet 2853 I (Malpaisillo), scale 1:50,000, Defense Mapping Agency Hydrographic/Topographic Center, Washington, D.C., 1986

28. I.L. Thomas, N.P. Ching, V.M. Benning, and J.A. d'Aguanno, "A review of multi-channel indices of class separability," International Journal of Remote Sensing, Vol. 8, No. 3, pp. 331-350, 1987

29. Stephen R. Yool, Jeffery L. Star, John E. Estes, Daniel B. Botkin, David W. Eckhardt, and Frank W. Davis, "Performance analysis of image processing algorithms for classification of natural vegetation on the mountains of Southern California," International Journal of Remote Sensing, Vol. 7, No. 5, pp. 683-702, 1986

30. B.N. Haack, "An analysis if thematic mapper simulation data for urban environments," Remote Sensing of Environment, Vol. 13, pp. 265-275, 1983

INITIAL DISTRIBUTION LIST

1. Defense Technical Information Center   2
   Cameron Station
   Alexandria, Virginia 22304-6145

2. Library, Code 0142   2
   Naval Postgraduate School
   Monterey, California 93943-5002

3. Commander   1
   Naval Space Command
   Attn: Code N155
   Dahlgren, Virginia 22448

4. United States Space Command   1
   Attn: Technical Library
   Peterson AFB, Colorado 80914

5. Director   1
   Navy Space Systems Division (OP-943)
   Washington, D.C. 20350-2000

6. U.S. Army Space Institute   1
   Attn: ATZL-SI
   Fort Leavenworth, Kansas 66027-7300

7. U.S. Army Space Program Office   1
   2810 Old Lee Highway
   Fairfax, Virginia 22031-4304

8. Space Systems Academic Group, Code SS   1
   Naval Postgraduate School
   Monterey, California 93943-5000

9. Chairman, Code EC   1
   Department of Electrical and Computer Engineering
   Naval Postgraduate School
   Monterey, California 93943-5000

10. Professor Chin-Hwa Lee, Code EC/Le   3
    Department of Electrical and Computer Engineering
    Naval Postgraduate School
    Monterey, California 93943-5000

11. Professor Jeffrey A. Nystuen, Code OC/Ny   1
    Department of Oceanography
    Naval Postgraduate School
    Monterey, California 93943-5000